NASA

National Aeronautics and
Space Administration

Lyndon B. Johnson Space Center

ARES
Astromaterials Research & Exploration Science
Biennial Report 2011-2012

Contents

Astromaterials Research and Exploration Science Directorate

Eileen K. Stansbery, Ph.D.

Since the return of the first lunar samples, what is now the Astromaterials Research and Exploration Science (ARES) Directorate has had curatorial responsibility for all NASA-held extraterrestrial materials. Originating during the Apollo Program (1960s), this capability at Johnson Space Center (JSC) included scientists who were responsible for the science planning and training of astronauts for lunar surface activities as well as experts in the analysis and preservation of the precious returned samples. Today, ARES conducts research in basic and applied space and planetary science, and its scientific staff represents a broad diversity of expertise in the physical sciences (physics, chemistry, geology, astronomy), mathematics, and engineering organized into three offices (figure 1): Astromaterials Research (KR), Astromaterials Acquisition and Curation (KT), and Human Exploration Science (KX).

Scientists within the Astromaterials Acquisition and Curation Office preserve, protect, document, and distribute samples of the current astromaterials collections. Since the return of the first lunar samples, ARES has been assigned curatorial responsibility for all NASA-held extraterrestrial materials (Apollo lunar samples, Antarctic meteorites – some of which have been confirmed to have originated on the Moon and on Mars – cosmic dust, solar wind samples, comet and interstellar dust particles, and space-exposed hardware). The responsibilities of curation consist not only of the long-term care of the samples, but also the support and planning for future sample collection missions and research and technology to enable new sample types. Curation provides the foundation for research into the samples. The Lunar Sample Facility and other curation clean rooms, the data center, laboratories, and associated instrumentation are unique NASA resources that, together with our staff's fundamental understanding of the entire collection, provide a service to the external research community, which relies on access to the samples.

The curation efforts are greatly enhanced by a strong group of planetary scientists who conduct peer-reviewed astromaterials research. Astromaterials Research Office scientists conduct peer-reviewed research as Principal or Co-Investigators in planetary science (*e.g.*, cosmochemistry, origins of solar systems, Mars fundamental research, planetary geology and geophysics) and participate as Co-Investigators or Participating Scientists in many of NASA's robotic planetary missions. Since the last report, ARES has achieved several noteworthy milestones, some of which are documented in detail in the sections that follow.

Within the Human Exploration Science Office, ARES is a world leader in orbital debris research, modeling and monitoring the debris environment, designing debris shielding, and developing policy to control and mitigate the orbital debris population. ARES has aggressively pursued refinements in knowledge of the debris environment and the hazard it presents to spacecraft. Additionally, the ARES Image Science and Analysis Group has been recognized as world class as a result of the high

quality of near-real-time analysis of ascent and on-orbit inspection imagery to identify debris shedding, anomalies, and associated potential damage during Space Shuttle missions. ARES Earth scientists manage and continuously update the database of astronaut photography that is predominantly from Shuttle and ISS missions, but also includes the results of 40 years of human spaceflight. The Crew Earth Observations Web site (http://eol.jsc.nasa.gov/Education/ESS/crew.htm) continues to receive several million hits per month. ARES scientists are also influencing decisions in the development of the next generation of human and robotic spacecraft and missions through laboratory tests on the optical qualities of materials for windows, micrometeoroid/orbital debris shielding technology, and analog activities to assess surface science operations.

ARES serves as host to numerous students and visiting scientists as part of the services provided to the research community and conducts a robust education and outreach program. ARES scientists are recognized nationally and internationally by virtue of their success in publishing in peer-reviewed journals and winning competitive research proposals. ARES scientists have won every major award presented by the Meteoritical Society, including the Leonard Medal, the most prestigious award in planetary science and cosmochemistry; the Barringer Medal, recognizing outstanding work in the field of impact cratering; the Nier Prize for outstanding research by a young scientist; and several recipients of the Nininger Meteorite Award. One of our scientists received the Department of Defense (DoD) Joint Meritorious Civilian Service Award (the highest civilian honor given by the DoD). ARES has established numerous partnerships with other NASA Centers, universities, and national laboratories. ARES scientists serve as journal editors, members of advisory panels and review committees, and society officers, and several scientists have been elected as Fellows in their professional societies.

This biennial report summarizes a subset of the accomplishments made by each of the ARES offices and highlights participation in ongoing human and robotic missions, development of new missions, and planning for future human and robotic exploration of the solar system beyond low Earth orbit.
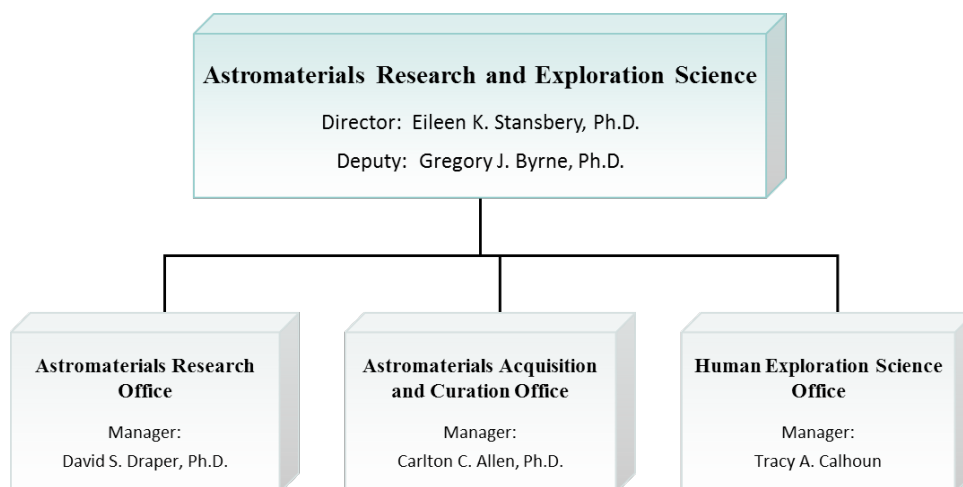
Figure 1.– ARES organization chart

David S. Draper, Ph.D., Manager
http://ares.jsc.nasa.gov/ares/indexkr.cfm

The staff of the Astromaterials Research Office conducts peer-reviewed astromaterials research. Scientists are funded through basic science disciplines of the NASA Research Opportunities in Space and Earth Sciences (ROSES) NASA Research Announcement (NRA) (link below), which include Cosmochemistry, Origins of Solar Systems, Astrobiology & Exobiology, Planetary Geology & Geophysics, Mars Fundamental Research and Mars Data Analysis, Planetary Mission Data Analysis, Lunar Advanced Science and Exploration Research, Laboratory Analysis of Returned Samples, Moon and Mars Analogue Mission Activities, Planetary Instrument Concepts for the Advancement of Solar System Observations, Near-Earth Object Observations, and Planetary Astronomy. Further funding comes from planetary missions and their allied programs.

http://nspires.nasaprs.com/external/solicitations/summary.do?method=init&solId={AEF75D0F-2272-7DE7-D52A-295B47C8F5CF}&path=open

The fundamental goal of our research is to understand the origin and evolution of the solar system, particularly the terrestrial, "rocky" bodies. Our research involves analysis of, and experiments on, astromaterials in order to understand their nature, sources, and processes of formation. Our state-of-the-art analytical laboratories include four electron microbeam laboratories for mineral analysis, four spectroscopy laboratories for chemical and mineralogical analysis, and four mass spectrometry laboratories for isotopic analysis. Other facilities include the experimental impact laboratory and both 1-atm gas mixing and high-pressure experimental petrology laboratories. Recent research has emphasized a diverse range of topics, including

- Study of the solar system's primitive materials, such as carbonaceous chondrites and interplanetary dust

- Study of early solar system chronology using short-lived radioisotopes and early nebular processes through detailed geochemical and isotopic characterizations

- Study of large-scale planetary differentiation and evolution via siderophile and incompatible trace element partitioning, magma ocean crystallization simulations, and isotopic systematics

- Study of the petrogenesis of Martian meteorites through petrographic, isotopic, chemical, and experimental melting and crystallization studies

- Interpretation of remote sensing data, especially from current robotic lunar and Mars missions, and study of terrestrial analog materials

- Study of the role of organic geochemical processes in the evolution of astromaterials and the extent to which they constrain the potential for habitability and the origin of life

The following reports give examples of astromaterials research done by members of this and other ARES offices.

Improved Measurement of Ejection Velocities From Craters Formed in Sand

Mark J. Cintala, Terry Byers, Francisco Cardenas, Roland Montes, Elliot E. Potter

A typical impact crater is formed by two major processes: compression of the target (essentially equivalent to a footprint in soil) and ejection of material. The Ejection-Velocity Measurement System (EVMS) in the Experimental Impact Laboratory has been used to study ejection velocities from impact craters formed in sand since the late 1990s. The original system used an early-generation Charge-Coupled Device (CCD) camera; custom-written software; and a complex, multicomponent optical system to direct laser light for illumination. Unfortunately, the electronic equipment was overtaken by age, and the software became obsolete in light of improved computer hardware.
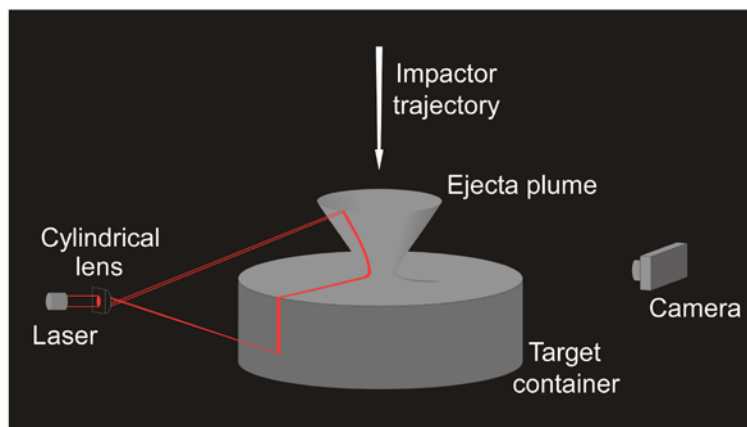
Figure 1.– *The EVMS relies on a laser that projects a "sheet" of light through the impact point and perpendicular to the target's surface. A camera, oriented to look at roughly 90° to the laser sheet, takes a time exposure of the event. The laser is programmed to flash at a known rate, providing pictures, such as the one in figure 2.*

Experience obtained from years of operating the EVMS has resulted in the design of a new, simplified, and streamlined version. The equipment has been upgraded, LabVIEW has taken the place of the custom computer code, and EVMS v.2 is now up and running. It is a much more robust system, with all of the major components integrated into a single, modular assembly, a straightforward change that greatly improves the process of aligning the optics and camera. A schematic drawing of the system that illustrates the main components is shown in figure 1.

When the button to fire the vertical gun is pressed, a signal is sent to a computer that acts as a controller. The computer sends a signal to the camera (an off-the-shelf digital single-lens reflex camera), which opens its shutter. After a short delay to allow the shutter to open completely, the computer sends a signal to the firing circuit. The gunpowder is ignited, sending the projectile (typically a sphere between 3 and 5 mm in diameter) toward the target. When the projectile interrupts a separate laser that is trained just across and above the target's surface (not shown in figure 1 for simplicity), a detector sends a signal to the illumination laser, turning it on. The illumination laser is programmed to flash at a specific rate; in some cases, a series of different illumination segments is programmed. This permits different lighting sequences to be used at different times during the crater's growth, which is very rapid initially, but much

slower toward the end. The camera's shutter remains open while the laser completes its programmed sequence, taking a time exposure. Each photograph thus includes information from every flash of the laser during the experiment.
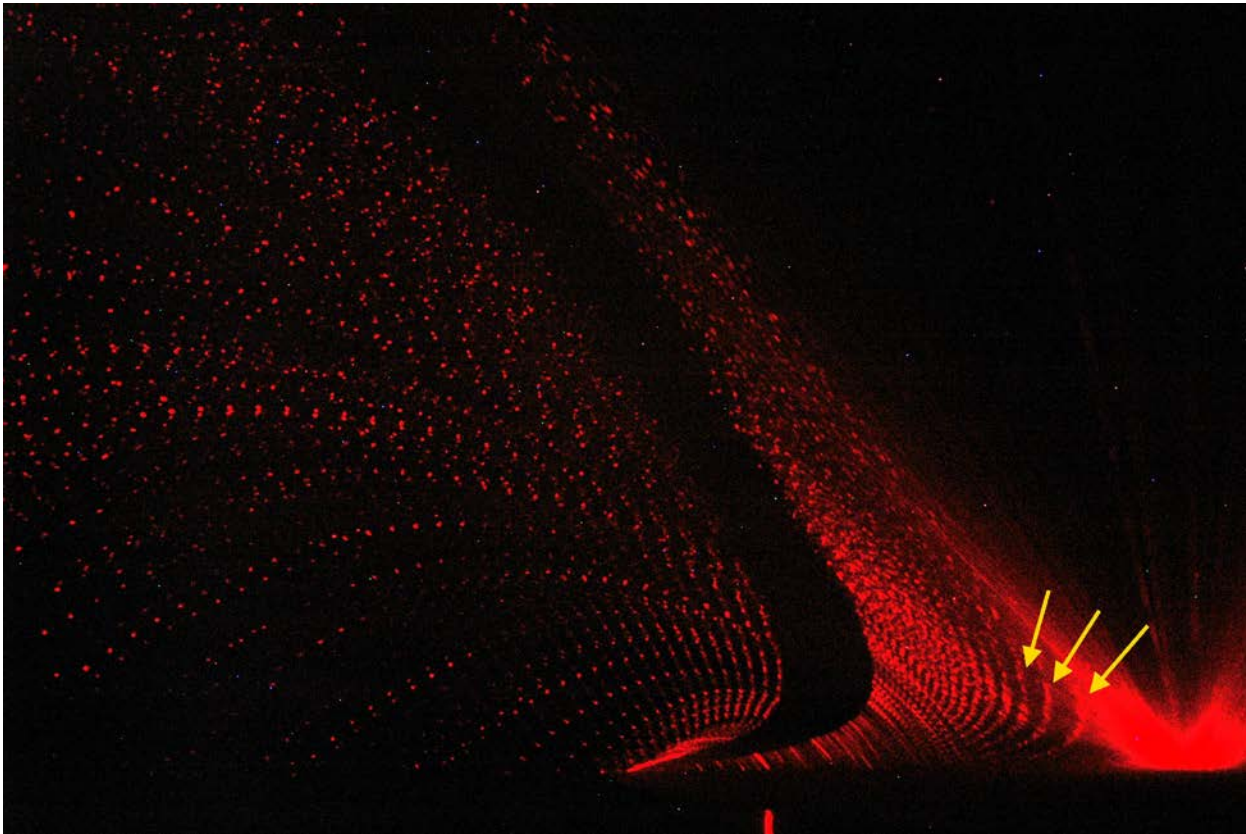
Figure 2.– Photograph of a laboratory impact taken by the newly revamped EVMS. The flash from the impact is in the lower-right corner; the crater grew, and ejecta traveled from right to left. There are two illumination segments in this picture. The one on the left was designed to show individual grains of sand in flight. Each set of dots is composed of multiple images of the same grain of sand, illuminated by the flashing laser as the grain traveled outward from the growing crater. Each set of dots thus defines a unique ballistic trajectory. The laser was flashing much faster in the illumination segment on the right and is much better at showing the shape of the ejecta plume and the rate at which the plume and crater grow. The three yellow arrows point to the profile of the ejecta plume at three different times (compare the plume's profile to that illustrated in figure 1). The black band between the two illumination segments is intentional, marking the period during which the laser was turned off (a duration of 25 ms). It delineates where the first illumination segment ends and the second begins.

An example of the kind of image that can be acquired by this system is shown in figure 2, which was recorded during the impact of a 4.76-mm stainless-steel sphere into 0.5–1-mm sand at a speed of 1.65 km/s. (It would have been very difficult, if not impossible, to image such fine-grained sand with the original EVMS.) The first segment of the illumination sequence turned the laser on once

per millisecond; that rate was constant through the first segment. The yellow arrows in figure 2 point to the illuminated profile of the ejecta plume as it grew (compare with figure 1). Because the illumination sequence was constant, the distance between the successive images of the plume's profile is directly proportional to the speed at which the plume expanded. It is readily apparent that the plume (and the crater itself) grew very rapidly just after the impact, when the impact-generated stresses in the target were highest. As time passed, however, the shock wave that initiated the ejection process expanded into the target, losing intensity in the process, much as light will decrease in intensity as the distance to its source increases. As the strength of the shock dropped, so did the motion that it imparted to the sand. Ultimately, the shock decayed to a sound wave; it became too weak to set the sand in motion, and crater growth stopped. This process is reflected in the continually decreasing gaps between the images of the plume (from right to left), until the plume was expanding so slowly that it is difficult to distinguish between the later, successive images.

The second illumination sequence was more leisurely, with 5 ms between flashes. The net effect was to separate individual images of each grain of sand in the laser sheet, allowing their trajectories to be described with very high accuracy and precision. Knowing the time between laser flashes and the scale of the picture, it is then a straightforward task to measure the distances between the successive images of the sand grains. Those data can then be used to derive the trajectories of the grains, and from there, the ejection velocities. Figure 3 illustrates the speeds of ejected grains as a function of each particle's launch position relative to the center of the crater, while figure 4 shows the corresponding ejection angles. The ejection speed drops off very rapidly with distance from the impact point, a feature that is common in all impact-cratering events. The great bulk of material is ejected at drastically lower speeds compared to that of the impactor (1.4 km/s in this case).
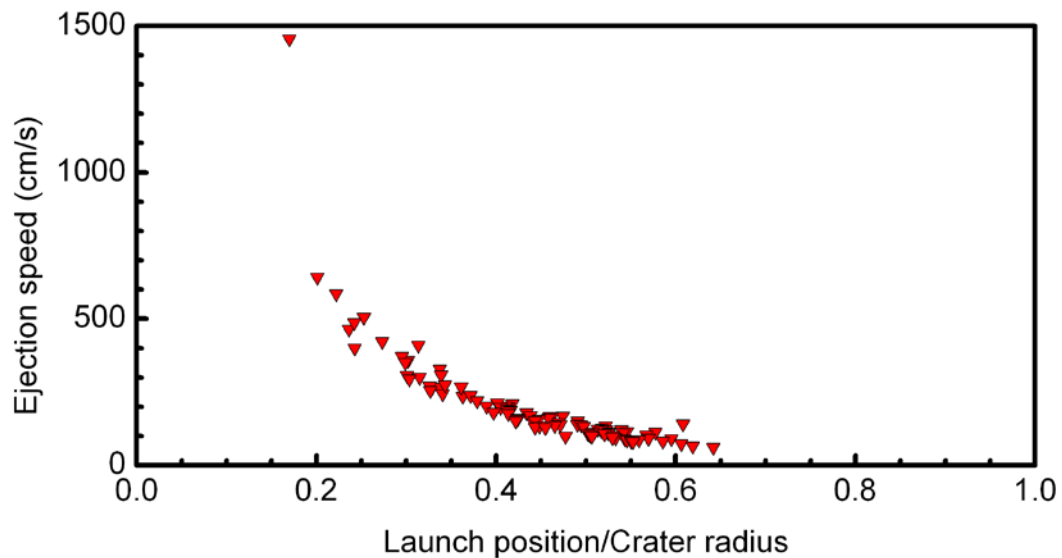
Figure 3.– Ejection speed as a function of the scaled launch position of the particle. In this figure, the center of the crater corresponds to a scaled launch position of 0, while the rim crest of the crater is at a scaled position of 1. Note the tight clustering of the data points, indicating a strong statistical correlation between the variables and the high precision of the EVMS technique.

The ejection-angle data indicate that the earliest material (closest to scaled launch position 0) left the growing crater at steeper angles than most of the material ejected later in the event. Until the advent of the EVMS, it was thought that ejection angles would be more or less constant throughout the formation of the crater. Instead, the data show that the ejection angles not only change but exhibit a more complex behavior than the ejection speeds. Not only do the angles exhibit considerably more scatter, but they also show a gradual decrease as the rim-crest location of the final crater is approached, whereupon they increase rather abruptly. This behavior has since been confirmed by other methods of measuring ejection angles, but its cause remains uncertain.
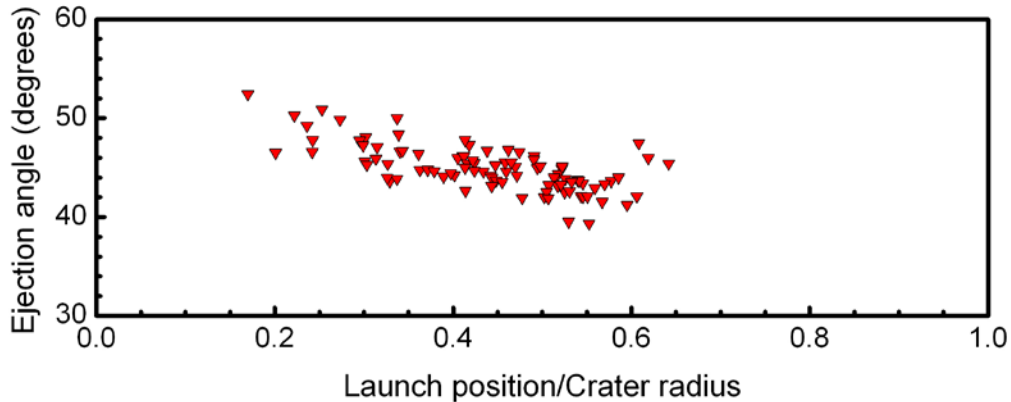
Figure 4.– Ejection angle (measured from the surface of the target) as a function of the scaled launch position. The angles scatter more than the ejection speeds (figure 3), indicating that factors not yet identified affect the geometry of the ejection process.

New Martian Meteorite Is One of the Most Oxidized Found to Date

Hejiu Hui (University of Notre Dame); Anne Peslier;
Thomas J. Lapen, John T. Shafer, Alan D. Brandon (University of Houston);
Anthony J. Irving (University of Washington)

As of 2013, about 60 meteorites from the planet Mars have been found and are being studied. Each time a new Martian meteorite is found, a wealth of new information comes forward about the red planet. The most abundant type of Martian meteorite is a shergottite; its lithologies are broadly similar to those of Earth basalts and gabbros; *i.e.*, crustal igneous rocks. The entire suite of shergottites is characterized by a range of trace element, isotopic ratio, and oxygen fugacity values that mainly reflect compositional variations of the Martian mantle from which these magmas came. A newly found shergottite, NWA 5298, was the focus of a study performed by scientists within the Astromaterials Research and Exploration Science (ARES) Directorate at the Johnson Space Center (JSC) in 2012. This sample was found in Morocco in 2008 (figure 1; NWA stands for North West Africa). Major element analyses were performed in the electron microprobe (EMP) laboratory of ARES at JSC, while the trace elements were measured at the University of Houston by laser

inductively coupled plasma mass spectrometry (ICPMS). A detailed analysis of this stone revealed that this meteorite is a crystallized magma that comes from the enriched end of the shergottite spectrum; *i.e.*, trace element enriched and oxidized (figure 2). Its oxidation comes in part from its mantle source and from oxidation during the magma ascent. It represents a pristine magma that did not mix with any other magma or see crystal accumulation or crustal contamination on its way up to the Martian surface. NWA 5298 is therefore a direct, albeit evolved, melt from the Martian mantle and, for its lithology (basaltic shergottite), it represents the oxidized end of the shergottite suite. It is thus a unique sample that has provided an end-member composition for Martian magmas.

Findings from the study of NWA 5298 were published in the journal *Meteoritics and Planetary Science*: Hui, H., Peslier, A. H., Lapen, T. J., Shafer, J. T., Brandon, A. D., Irving, A. J. (2011). Petrogenesis of basaltic shergottite Northwest Africa 5298: Closed-system crystallization of an oxidized mafic melt. *Meteor. Planet. Sci. 46* (9), pp. 1313-1328.
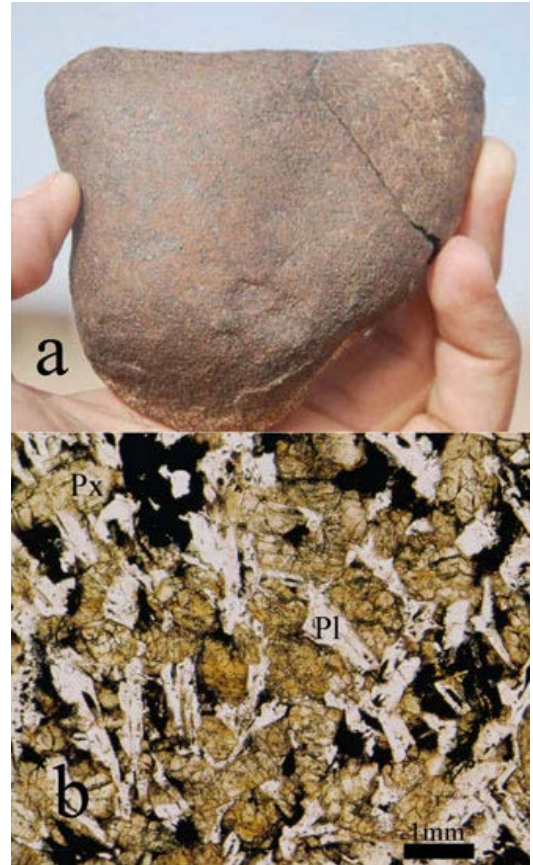
Figure 1.– (a) Photograph of the NWA 5298 meteorite showing its exterior. (b) A thin section of NWA 5298 seen under a microscope. The main minerals are pyroxene (Px) and plagioclase (Pl).
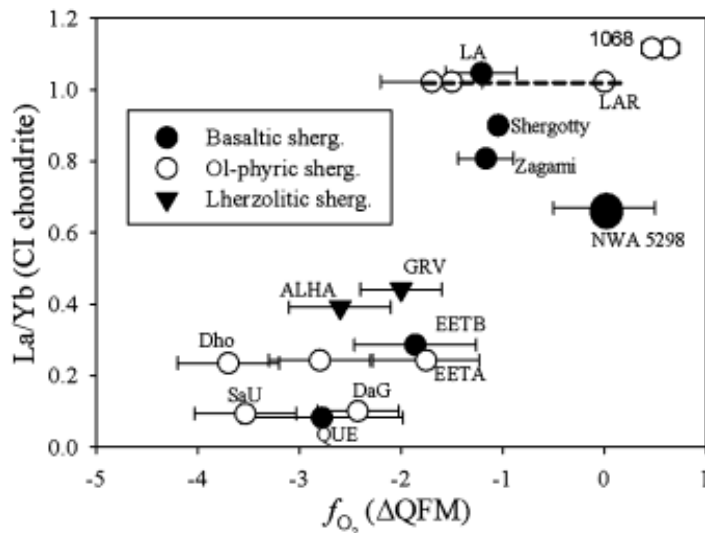
Figure 2.– Trace element (ratio of Lanthanum over Ytterbium) versus oxygen fugacity characteristics of NWA 5298 compared to those of other shergottites. NWA 5298 is enriched with trace elements and is the most oxidized basaltic shergottite that has been found to date.

Shock Effects on Cometary-Dust Simulants

Susan M. Lederer, Elizabeth Jensen (Planetary Science Institute), Diane H. Wooden (NASA Ames), Sean S. Lindsay (New Mexico State University), Douglas H. Smith (California State Univ., San Bernardino), Keiko Nakamura-Messenger, Lindsay P. Keller, Francisco Cardenas, Mark J. Cintala, Roland Montes

While comets are perhaps best known for their ability to put on spectacular celestial light shows, they are much more than that. Composed of an assortment of frozen gases mixed with a collection of dust and minerals, comets are considered to be very primitive bodies and, as such, they are thought to hold key information about the earliest chapters in the history of the solar system. (The dust and mineral grains are usually called the "refractory" component, indicating that they can survive much higher temperatures than the ices.) It has long been thought, and spacecraft photography has confirmed (figure 1), that comets suffer the effects of impacts along with every other solar system body. Comets spend most of their lifetimes in the Kuiper Belt, a region of the solar system between 30 and 50 times the average distance of the Earth from the Sun, or the Oort Cloud, which extends to ~1 light year from the Sun. Those distances are so far from the Sun that water ice is the equivalent of rock, melting or vaporizing only through the action of strong, impact-generated shock waves.

Figure 1.– The nucleus of Comet Tempel 1, which was the target of the Deep Impact mission in 2005. Craters, presumably of impact origin, are visible in a wide range of preservation states. Each of the two crisp, similar-sized craters on the bottom half of this picture has a diameter very similar to that of the Astrodome, around 220 m.

High-velocity impacts not only create craters such as those in figure 1, but the shock waves they generate also affect the refractory components of the comets' nuclei and, by inference, those of any other ice-rock body in the Kuiper Belt or Oort Cloud. With typical impact speeds of "only" around 3 km/s (~2 mi/s), the overall effects on the refractory components are not completely clear. It is known, however, that infrared (IR) spectra of dust in comets' tails are similar to IR spectra of various well-studied silicates, such as olivines and pyroxenes, but the matches are far from perfect. Furthermore, dust samples from Comet Wild 2 (figure 2) show damage to crystal structures that can be explained easily by impact-generated shock. Seeing macroscopic evidence of impact in the photography and microscopic evidence of impact in the samples, it is only natural to question what other effects impact can have on comets and their constituent materials. Characterizing the effects that relatively low-velocity impacts can have on some of the more common refractory components of comets, which is one way to attack this question, is the focus of this research.

With this in mind, scientists within the ARES Directorate are midway through a 4-year grant to investigate these effects, addressing the fundamental quest NASA has to understand planetary geophysical processes on solar system bodies. Using the vertical gun in the ARES Experimental Impact Laboratory, scientists launch 3.2-mm ceramic spheres at olivine and pyroxene crystals (figure 3), and the resulting fragments are recovered and analyzed with a Fourier-transform IR spectrometer and a transmission electron microscope (TEM).
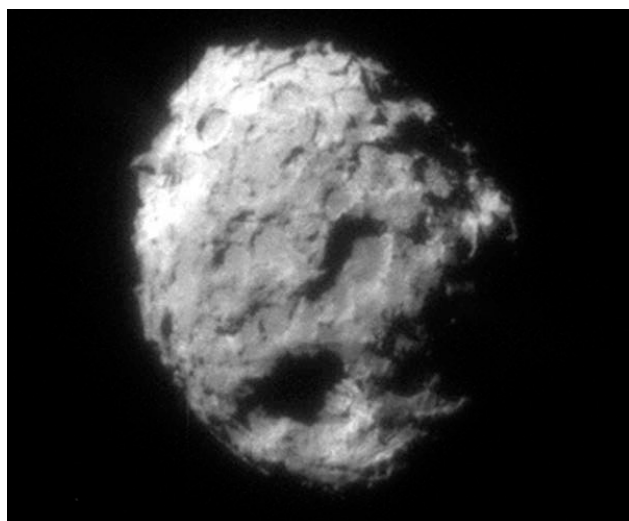
Figure 2.– The nucleus of Comet Wild 2 (about 5 km in diameter) as photographed by the Stardust spacecraft, which collected dust particles as it flew past the comet.

Aluminum-oxide ceramic was chosen as a projectile material because it is similar to rock in its density and shock behavior, and so provides a good simulation of rocky meteorites. While collisions among comets most commonly involve ice-rock mixtures colliding into ice-rock mixtures, these early experiments modeled rock colliding into ice-rock targets because such a combination would result in the greatest likelihood of damage to the rock component. Should effects be observed with the "rocky" projectiles, it would be a simple matter to use lower-density impactors to simulate ice. Pieces of pyroxene and olivine, versions of which have been found in samples from the Stardust mission and are commonly detected in spectra of comet dust, were used as targets. They were placed in a container filled with granular potassium bromide (KBr; see figure 3), which acted to absorb the residual momentum of the projectile after it collided with the target mineral. KBr has the added benefit of being soluble in water, so the shocked material could be collected after the KBr dissolved away in water, leaving the shocked mineral behind.

In this way, mineral grains were shocked at speeds up to 2.8 km/s, retrieved, and analyzed. Figure 4 shows IR spectra of shocked and unshocked forsterite grains (the gem peridot is high-quality forsterite). Note that the peaks change not only their amplitudes but their maxima, which occur at shorter wavelengths than those of the unshocked sample. Measurements of this sort provide the first indications of why the spectra of dusty comet tails do not match the spectra of pristine minerals. Furthermore, early examination of the shocked forsterite grains with the TEM shows

Figure 3.– An enstatite (a form of pyroxene) crystal before (left) and after (right) being pulverized by a ceramic projectile. The inside diameter of the target container is 34 mm (about 1.5 in.)

damage to the mineral's crystal structure that is very similar to that observed in Stardust particles. This work is continuing, and will soon involve targets cooled to very low (liquid-nitrogen) temperatures, further increasing the fidelity of the experiments.

Forsterite Solid 2.450 km/sec
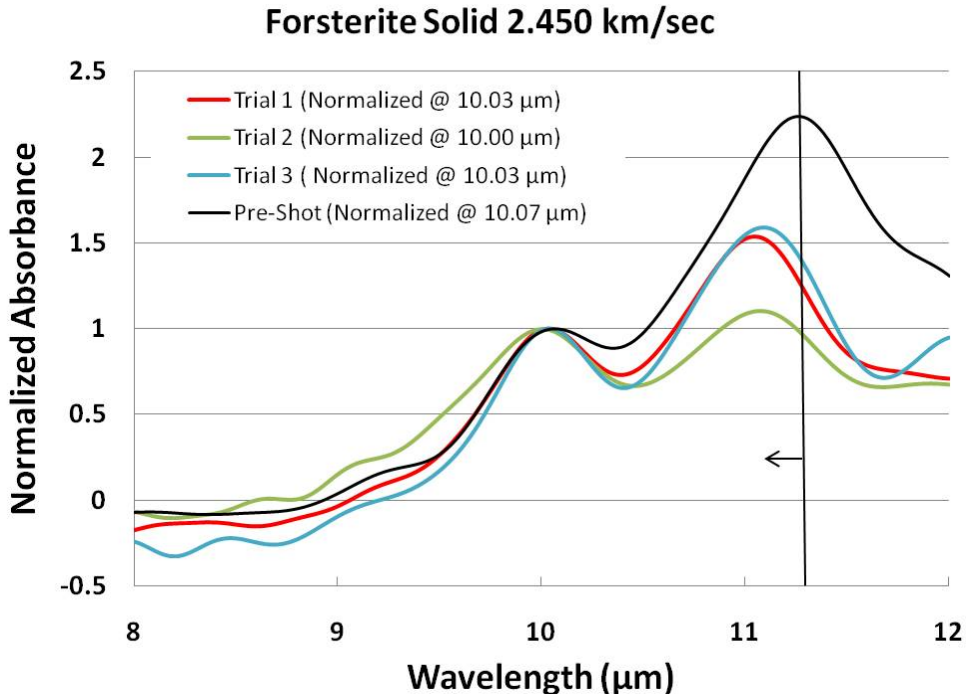
Figure 4.– Comparison of IR spectra from unshocked (black) forsterite and three samples of forsterite shocked in an impact at 2.45 km s^{-1}. The spectra of the shocked samples differ because the fragments were probably not subjected to the same shock level – a spherical projectile generates the highest shock pressure at the point of contact; the shock felt by the target at any other point depends on its location relative to the impact point.

Mars Habitability, Biosignature Preservation, and Mission Support

Dorothy Z. Oehler, Carlton C. Allen

Our work has elucidated a new analog for the formation of giant polygons on Mars, involving fluid expulsion in a subaqueous environment. That work is based on three-dimensional (3D) seismic data on Earth that illustrate the mud volcanoes and giant polygons that result from sediment compaction in offshore settings. The description of this process has been published in the journal *Icarus*, where it will be part of a special volume on Martian analogs. These ideas have been carried further to suggest that giant polygons in the Martian lowlands may be the signature of an ancient ocean and, as such, could mark a region of enhanced habitability. A paper describing this hypothesis has been published in the journal *Astrobiology*.
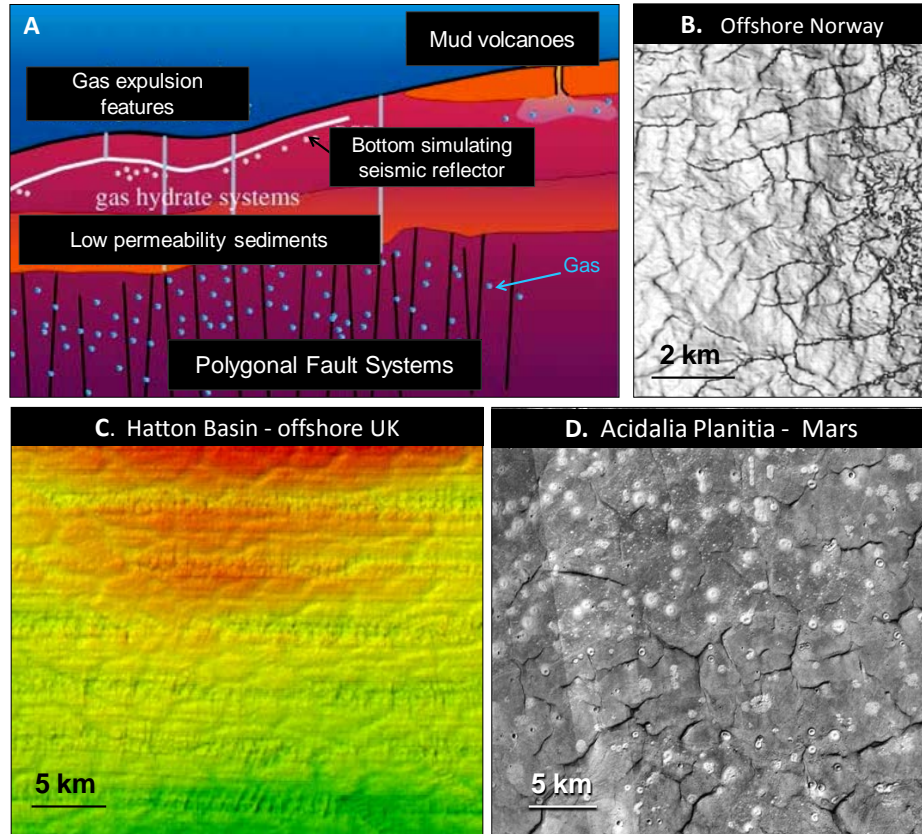
Figure 1.– Examples from Earth and Mars illustrating giant polygons and the processes that may lead to their formation. (A) Sketch showing giant polygons and mud volcanoes that can form in offshore basins (from Berndt, 2005. Phil. Trans. Royal Soc. *A). (B) A map of the Norwegian offshore, created with 3D seismic data, showing giant polygons in the subsurface (Stuevold et al., 2003.* Geol. Soc. London Sp. Publ. *216). (C) Seabed bathymetry showing giant polygons in the offshore Hatton Basin. (D) Images from the Context Camera on NASA's Mars Reconnaissance Orbiter showing giant polygons and bright mounds (interpreted as mud volcanoes) in* Acidalia Planitia*, in the Martian lowlands.*
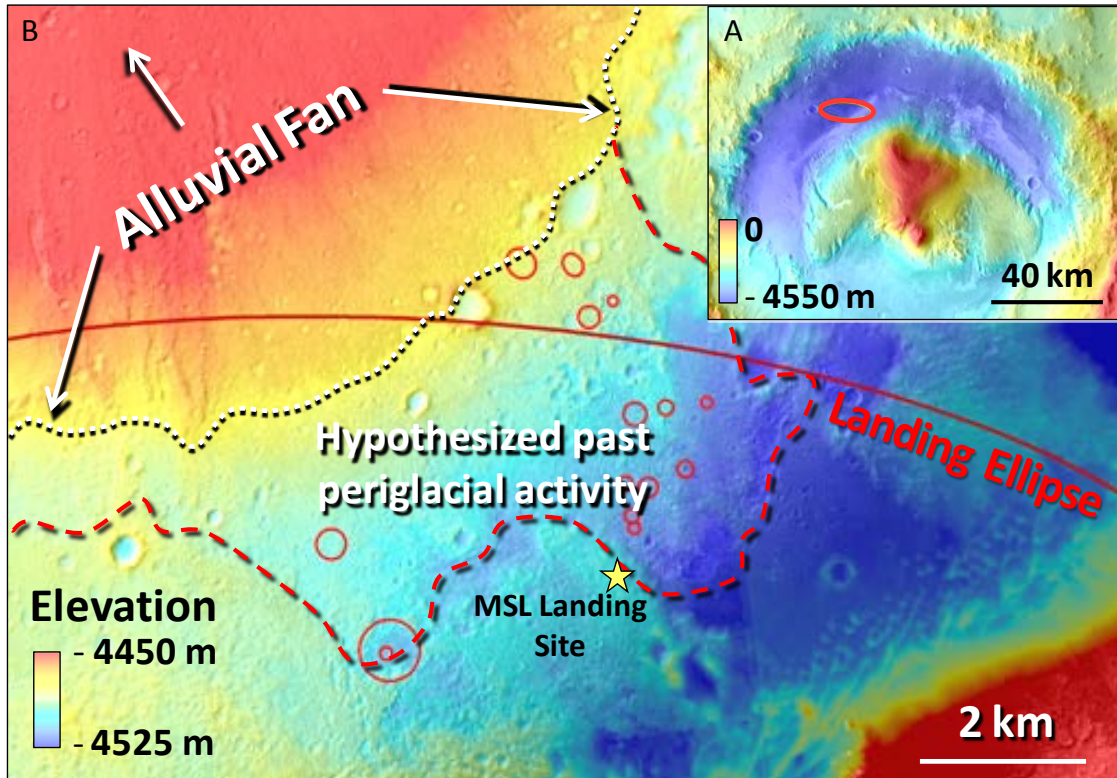
Figure 2.– Gale Crater – landing site for NASA's Mars Science Laboratory Mission. Inset (A) is an elevation map that shows Gale Crater with its central mound of sediments. The landing ellipse (red oval) is in the northwest part of the crater. (B) is a detailed elevation map showing part of the landing ellipse, the landing site (yellow star), and the unit hypothesized to have been affected by periglacial processes. This unit is bounded to the north by the white dotted line and to the east, west, and south by the red dashed line. The red circles are locations of circular patterns of polygons that resemble ice wedge features in periglacial terrain in the Arctic.

After completing work in the landing ellipse, the MSL rover (Curiosity) will traverse to Mt. Sharp, the 5-km-high central mound in Gale Crater. Curiosity is scheduled to begin its exploration of Mt. Sharp in late 2013. The mound is a massive sedimentary deposit thought to record much of the planet's early geologic history. Our preliminary investigation, with the help of Lunar and Planetary Institute summer intern Lisa Korn, supports the contention that the Mt. Sharp deposits are representative of a partially eroded sedimentary sequence covering large areas in the northern hemisphere.

Early Life on Earth and the Search for Extraterrestrial Biosignatures

Dorothy Z. Oehler, Christopher House (Penn State University)

In the last 2 years, scientists within the ARES Directorate at JSC have applied the technology of Secondary Ion Mass Spectrometry (SIMS) to individual organic structures preserved in Archean (~3 billion years old) sediments on Earth. These organic structures are among the oldest on Earth that may be microfossils – structurally preserved remnants of ancient microbes. The SIMS work was done to determine the microfossils' stable carbon isotopic composition ($\delta^{13}C$ values). This is the first time that such ancient, potential microfossils have been successfully analyzed for their individual $\delta^{13}C$ values. The results support the interpretation that these structures are remnants of early life on Earth and that they may represent planktonic organisms that were widely distributed in the Earth's earliest oceans. This study has been accepted for publication in the journal *Geology*.
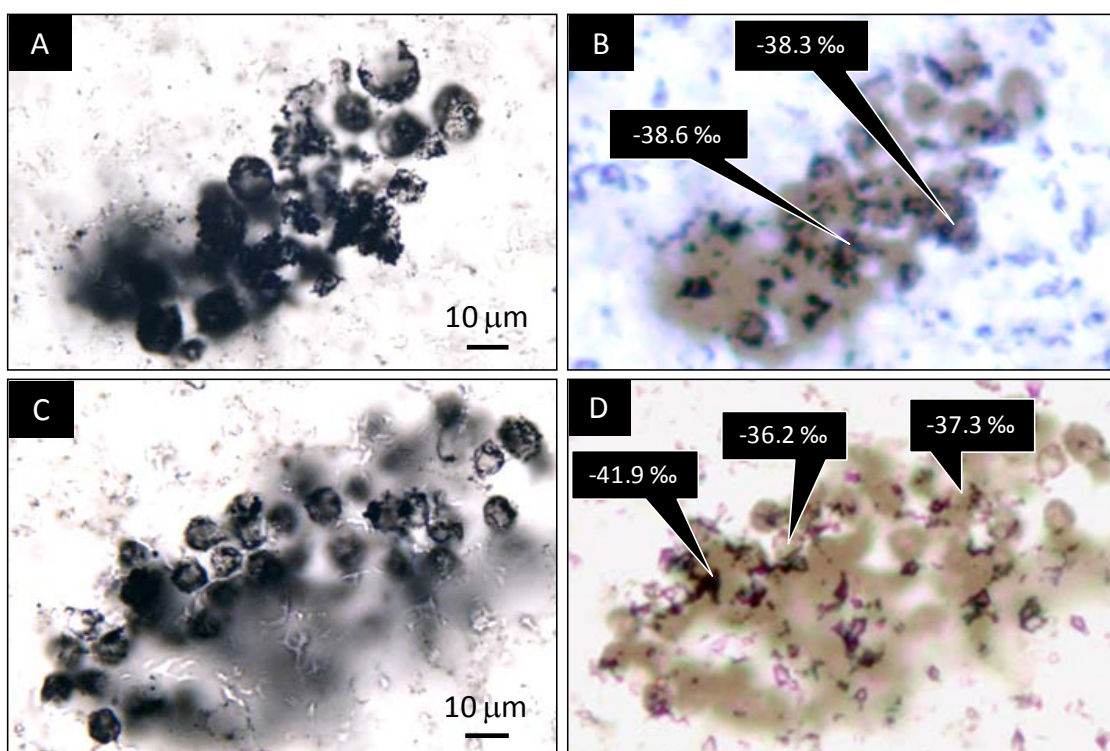
Figure. 1.– Optical photomicrographs of clusters of approximately 3-billion-year-old, spheroidal structures from the Farrel Quartzite of Australia, as seen in petrographic thin section. (A) and (C) are in transmitted light. (B) and (D) show the same structures in a combination of transmitted and reflected light with the locations of SIMS analyses and the SIMS-measured $\delta^{13}C$ values superimposed.
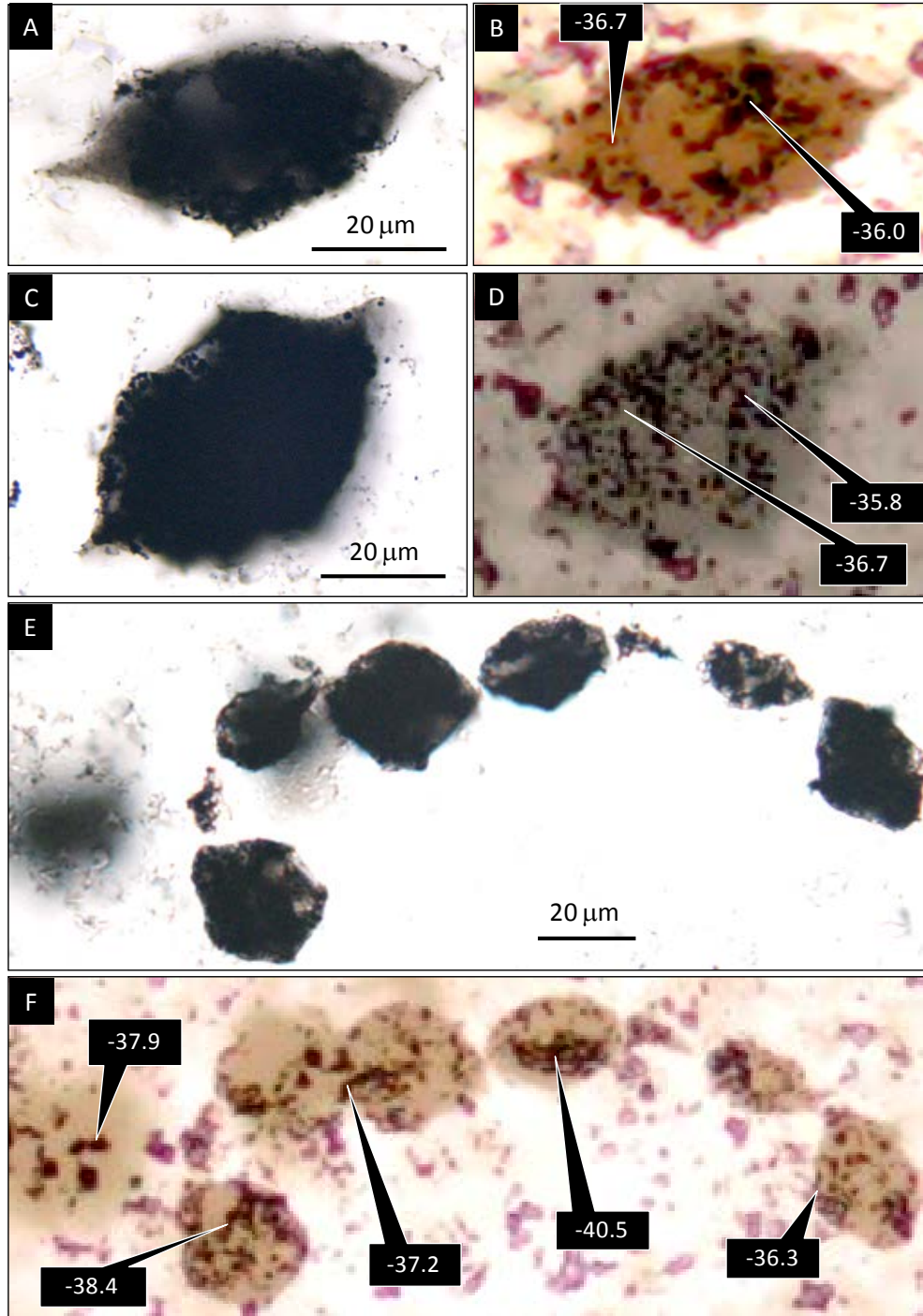
Figure 2.– Optical photomicrographs of approximately 3-billion-year-old, spindle-like microstructures from the Farrel Quartzite of Australia, as seen in petrographic thin section. (A, C, and E) are in transmitted light.
(B, D, and F) show the same structures in a combination of transmitted and reflected light, with the locations of SIMS analyses and the SIMS-measured $\delta^{13}C$ values superimposed.

Water Content of Earth's Continental Mantle Is Controlled by the Circulation of Fluids or Melts

Anne Peslier, Alan B. Woodland (University of Frankfurt),
David R. Bell (Arizona State University), Marina Lazarov (Universität Hannover),
Thomas J. Lapen (University of Houston)

A key mission of the ARES Directorate at JSC is to constrain models of the formation and geological history of terrestrial planets. Water is a crucial parameter to be measured with the aim to determine its amount and distribution in the interior of Earth, Mars, and the Moon. Most of that "water" is not liquid water *per se*, but rather hydrogen dissolved as a trace element in the minerals of the rocks at depth. Even so, the middle layer of differentiated planets, the mantle, occupies such a large volume and mass of each planet that when it is added at the planetary scale, oceans worth of water could be stored in its interior. The mantle is where magmas originate. Moreover, on Earth, the mantle is where the boundary between tectonic plates and the underlying asthenosphere is located. Even if mantle rocks in Earth typically contain less than 200 ppm H_2O, such small quantities have tremendous influence on how easily they melt (*i.e.*, the more water there is, the more magma is produced) and deform (the more water there is, the less viscous they are). These two properties alone emphasize that to understand the distribution of volcanism and the mechanism of plate tectonics, the water content of the mantle must be determined – Earth being a template to which all other terrestrial planets can be compared.

With that goal in mind, ARES scientists have studied the mantle beneath the oldest continents since 2007. These ancient continental fragments are called cratons and are underlain by a mantle keel of very old mantle rocks that have not participated in the general mantle convection (*i.e.*, the engine for plate tectonics) for more than 3 billion years (figure 1). Using Fourier transform infrared spectrometry, the water content in minerals from the Kaapvaal craton (southern Africa, figure 2) was measured and combined with other chemical tracers of mantle processes. The study shows that water in mantle rocks was brought by fluids and melts circulating through the craton keel (figure 3). The distribution of water in the continental mantle is thus heterogeneous and depends on the nature and water content of the fluid or melt and the path of the melt in the mantle. It is likely that these fluids or melts are related to subduction events in the Archean and Proterozoic Eons; *i.e.*, more than 500 million years ago. The study is being expanded with ongoing similar projects on the mantles beneath the Siberian craton and the southwestern United States.

This work was published in 2012 in *Geochimica et Cosmochimica Acta*.

Peslier A. H., Woodland A., Bell D. R., Lazarov M., and Lapen T. J. (2012); Metasomatic Control of Water Contents in the Kaapvaal Cratonic Mantle. *Geochim. Cosmochim. Acta 97*, pp. 213-246, DOI: 10.1016/j.gca.2012.08.028.
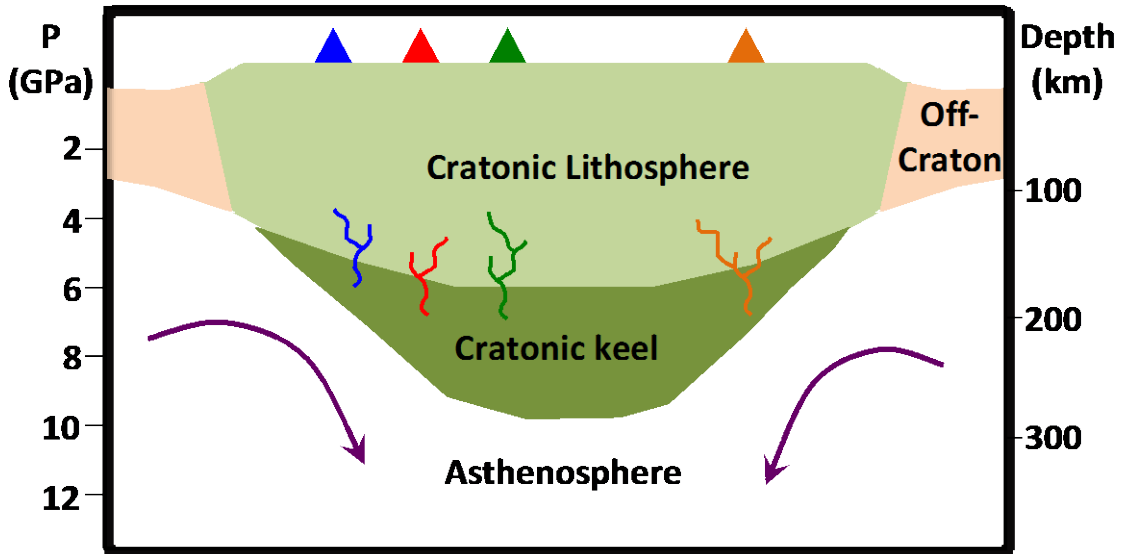
Figure 1.– Sketch of the cross-section of a craton showing the path of melts or fluids of various chemical compositions and water contents (colors) through the cratonic mantle and the corresponding xenolith locations at the surface (triangles). Purple arrows in the asthenosphere indicate mantle convection responsible for plate tectonics, from which cratonic keels appear isolated.
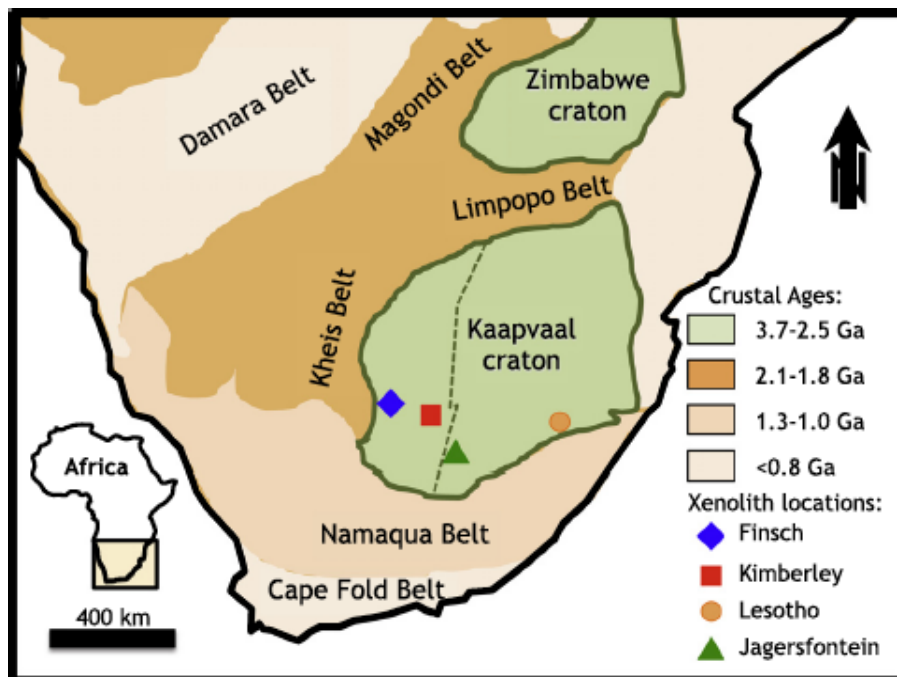
Figure 2.– Location of the Kaapvaal craton. Finsch, Kimberley, Lesotho, and Jagersfontein are diamond mines. The magma that brings up diamonds, called kimberlite, also brings up pieces of the mantle (from 100- to 200-km depth) it passes through on its way to the surface. These pieces of mantle, called xenoliths, are being analyzed for water in the present study.
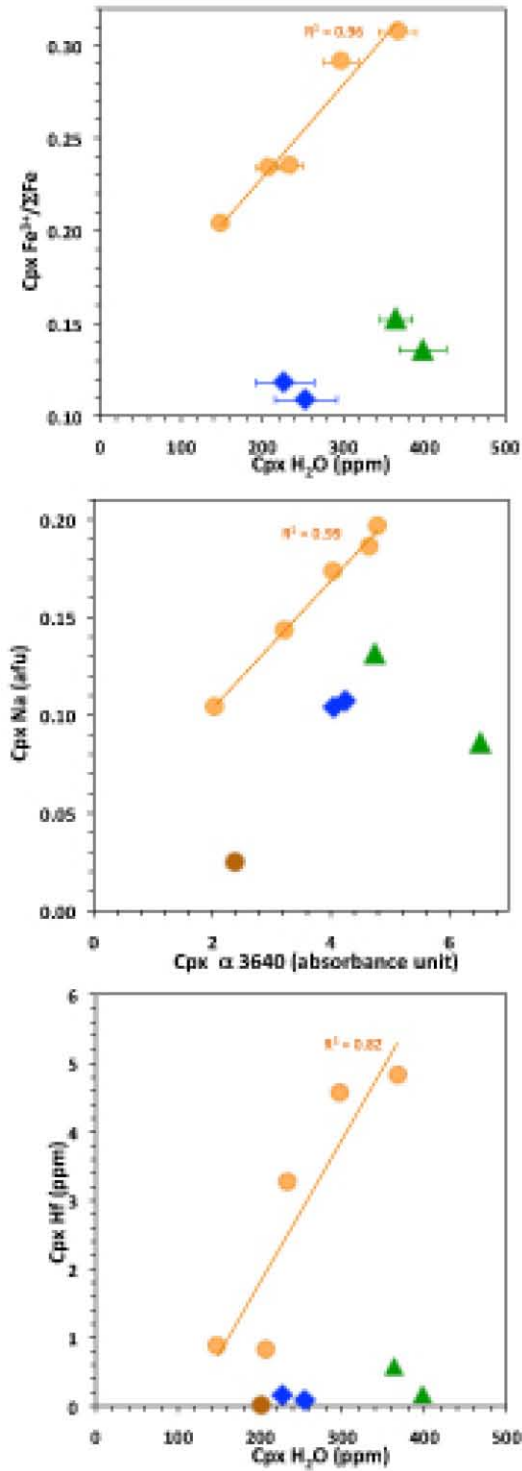
Figure 3.– Water contents of clinopyroxene minerals in Kaapvaal craton xenoliths from Lesotho (orange-filled circles) correlate with tracers of fluid or melt interaction, for example, ferric iron, sodium, and hafnium contents.

19

Water in the Oldest Lunar Rocks:
Moon is "Wetter" Than Previously Thought

Hejiu Hui (University of Notre Dame), Anne Peslier
Youxue Zhang (University of Michigan), Clive Neal (University of Notre Dame)

The recent detection of water in Mare basaltic glass beads and on the lunar surface has revolutionized our knowledge and understanding of the Moon. Until now, the Moon was thought to have lost its volatiles during the cataclysmic collision of two proto-planets that is believed to have led to its creation and during the evolution of a lunar magma ocean. In 2012, scientists in the ARES Directorate at JSC completed an analysis of the water in the oldest of the Moon rock samples collected during the Apollo Program. The rocks, which were brought back by astronauts during the Apollo 15 and 16 missions (figure 1), are pieces of the Moon's oldest crust (>4.4 x 10^9 years old) and are called ferroan anorthosites. These are thought to have crystallized from a Moon-wide magma ocean at the beginning of the Moon's history. The rocks are composed mainly of the mineral plagioclase and were analyzed for water using Fourier transform infrared (FTIR) spectrometry. These measurements were challenging because of the fragility of the samples (figure 2) and the fact that they are very precious and the water contents measured were low.

Figure 1.– Sample 15415 before it was sampled by the Apollo 15 astronauts on the lunar surface. This ferroan anorthosite is one of the best known rocks of the Apollo collection, and is popularly called the "Genesis Rock" because the astronauts thought they had a piece of the Moon's primordial crust.

Analysis of the ferroan anorthosites found about 6 ppm H_2O in the plagioclases (figure 3). Analysis also found up to 2 ppm H_2O in the plagioclases of another type of Moon rock, troctolite, that is thought to be part of the old lunar crust. Although these may seem like trivial amounts, finding water in rocks from the oldest lunar crust has profound implications. For example, there is a debate about whether the origin of the water measured in Moon rocks was brought later by impacts (of comets, for example) or was present all along from the beginning of the Moon's history. Results from the ARES analysis support the latter hypothesis.
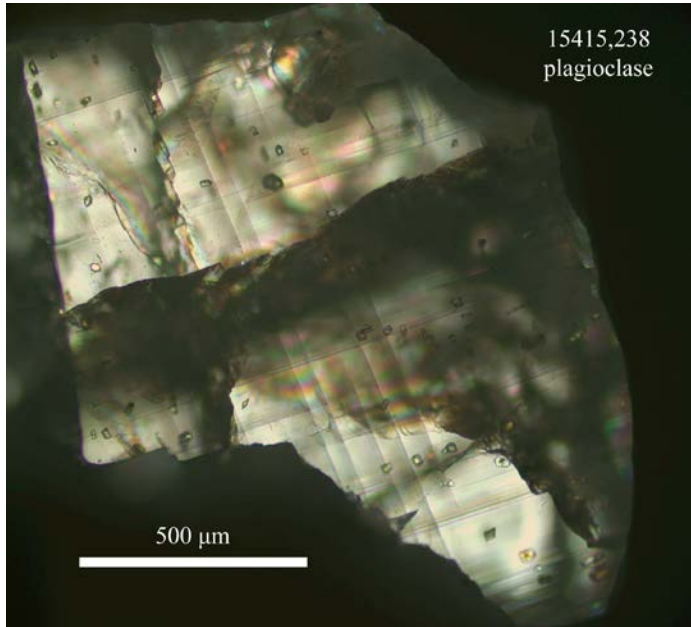
Moreover, knowing the amount of water in the earliest Moon rocks has implications for the modeling of the Moon's formation event. Finally, part of the water measured by spacecraft orbiting the Moon may be from indigenous water in crustal rocks, such as those analyzed in this study.

Figure 2.– A plagioclase grain analyzed for water in this study.
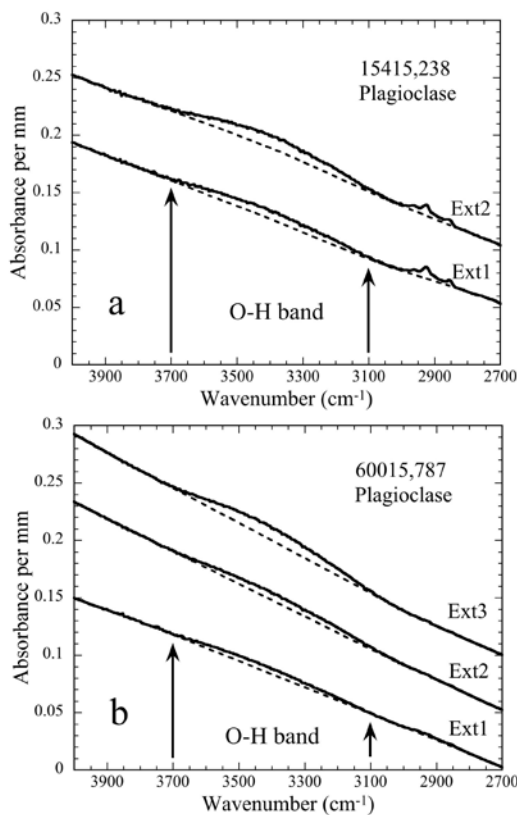
Figure 3.– An example of FTIR spectra of lunar plagioclases in the water band region. The "bump" in the spectrum above the dotted line (the baseline) is caused by absorption of the infrared light by O-H bonds in the plagioclase.

Analysis results and findings were published in the journal *Nature Geoscience* and were presented at the Lunar and Planetary Science Conference in March 2013.

Hui, H., Peslier, A. H., Zhang, Y., and Neal, C. R. (2013). Water in Lunar Anorthosites and Evidence for a Wet Early Moon. *Nature Geosci.* 6 (3), pp. 177-180, DOI: 10.1038/ngeo1735

Magnetic Nozzle Effects on Plasma Plumes

Frans H. Ebersohn, John V. Shebalin

The principal effort in this project is the computational research and development work being done by a doctoral student funded by the NASA Space Technology Research Fellowship Program and hosted by the ARES Office. An ARES astrophysicist serves as research mentor, collaborator, and theoretical advisor for the fellow, whose fellowship began in August 2011 and ends in August 2015, when the work will be completed. The work is specifically aimed at advancing the state of the art in NASA In-Space Propulsion Systems Roadmap Technical Areas 2.2.1.3.2, Magnetoplasmadynamic (MPD) Thrusters, and 2.2.1.3.3, Variable Specific Impulse Magnetoplasma Rocket (VASIMR). The goals of this research are to understand the underlying physics of plasma flow through a magnetic nozzle as well as the flow's later detachment from a plasma engine and to use this knowledge to optimize the design of both MPD rockets and VASIMR, technologies that may well prove essential for a viable program of future, long-duration solar system exploration.

Crucial aspects of MPD thruster and VASIMR performance that need to be understood are (1) how magnetic nozzle design affects an emerging plasma jet; (2) how design can be optimized to ensure plasma jet detachment with minimal plume divergence; and (3) how, at the same time, thrust and specific impulse can be optimally balanced. Research is proceeding theoretically as well as through numerical simulation of plasma flow in a magnetic nozzle, allowing a study of magnetic nozzle performance in both the single and dual jet configurations of an MPD thruster or VASIMR. This work will produce a robust design tool that may help enable long-duration space missions.

In numerical simulations performed during fiscal years 2012 and 2013, model inviscid jet expansion simulations have been seen to agree with theoretical predictions of near-vacuum jet expansion and under-expanded jet dynamics. Significant progress has also been made in modeling resistive plasma jets, and preliminary magnetic nozzle configurations have been tested as well. Example results for a case using a steady-state axisymmetric numerical plasma flow solver are shown in figure 1, where x is distance along the central plume axis, and r is distance perpendicular to the central axis. Inflow parameters similar to those of the VASIMR engine were used in this case. The top contour shows the velocity magnitude, while the bottom shows the density. The jet inlet is located at $x = 0$ and has a radius r_0 of half a meter. Several boundary and initial conditions for fluid properties, such as velocity, density, and pressure, were tested to determine which would produce the best combination of physically accurate and numerically feasible results for future magnetic nozzle test cases. Boundary and initial conditions for the diverging applied magnetic field of a magnetic nozzle were incorporated, and preliminary test cases with low magnetic field strength were studied.

Preliminary studies of the so-called "theta-pinch" problem were also conducted. Theta-pinches are characterized by a strong axial magnetic field that confines a flowing plasma. These preliminary theta-pinch studies are intended to serve as an intermediate case between the vacuum expansion and the magnetic nozzle expansion of a plasma jet. Studies of theta-pinch and resistive magnetic nozzle

plasma jet expansions will continue, and results will be compared to experiments, which will guide the evolution of the computational method. The effect of the Hall and electron pressure terms in the generalized Ohm's law will also be studied, and these terms will be incorporated as necessary in the computer program. Furthermore, the need for subgrid scale magnetohydrodynamic turbulence models will be evaluated. Periodic assessments of numerical robustness are, of course, an ongoing activity.
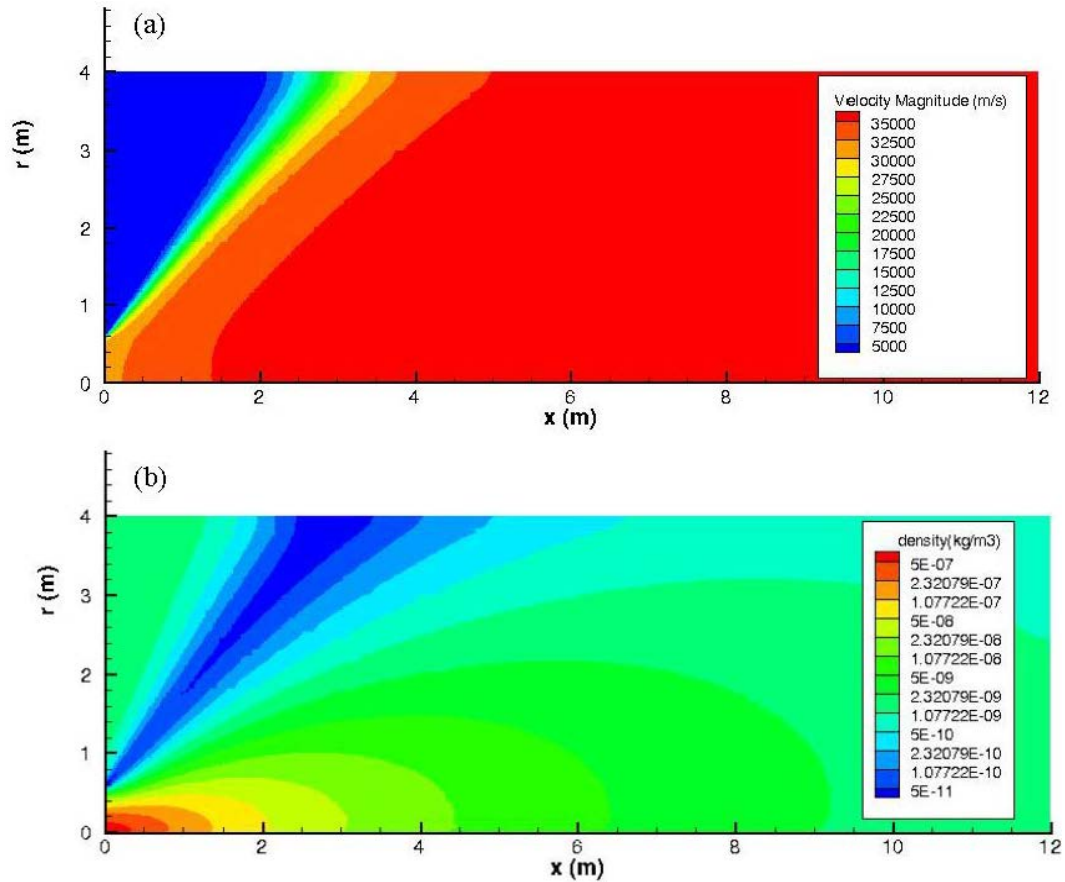
Figure 1.– (a) Velocity and (b) density contours for jet expansion with parameters near the regimes of VASIMR. No magnetic field is applied.

Magnetohydrodynamic Turbulence and the Geodynamo

John V. Shebalin

The ARES Directorate at JSC has researched the physical processes that create planetary magnetic fields through dynamo action since 2007. The "dynamo problem" has existed since 1600, when William Gilbert, physician to Queen Elizabeth I, recognized that the Earth was a giant magnet. In 1919, Joseph Larmor proposed that solar (and by implication, planetary) magnetism was due to magnetohydrodynamics (MHD), but full acceptance did not occur until Glatzmaier and Roberts solved the MHD equations numerically and simulated a geomagnetic reversal in 1995. JSC research produced a unique theoretical model in 2012 that provided a novel explanation of these physical observations and computational results as an essential manifestation of broken ergodicity in MHD turbulence. Research is ongoing, and future work is aimed at understanding quantitative details of magnetic dipole alignment in the Earth as well as in Mercury, Jupiter and its moon Ganymede, Saturn, Uranus, Neptune, and the Sun and other stars. Current computational research results showing effective dipole angle θ_D with respect to normalized rotation vector Ω_o are given in figure 1. (The dotted line is what would be expected if $\Omega_o = 0$. Also, note that saturation occurs.)
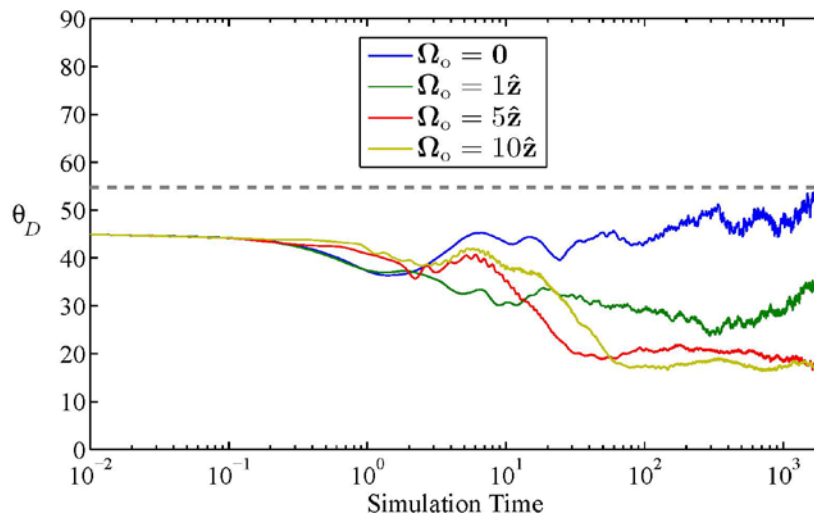
Figure 1.– Dipole angle with respect to rotation rate in a model geodynamo.

Current work focuses on the Earth because it is the planet observed most closely and the planet for which the best data exist. The geomagnetic field is of utmost importance to the growth and survival of life on Earth because it serves as a "magnetic bumper" that protects us from the solar wind, coronal mass ejection, and cosmic rays. The geomagnetic field is a primarily dipole field that allows for the existence of a stable atmosphere, without which Earth would probably look like Mars: dry, barren, and lifeless. However, the geomagnetic dipole field is not static, arising as it does from deep MHD flows, but changes over time – it has weakened about 10 percent since 1850, and its direction wanders (see figure 2) or even reverses (on average every 100,000 years). The geomagnetic field is intimately connected to the existence and location of the radiation belts, and its multipole

components cause such features as the South Atlantic Anomaly, which adversely affects low-Earth-orbit spacecraft, such as the International Space Station. A detailed knowledge of the geomagnetic field and how it changes in the short and long term is very important for understanding and predicting changes in the atmosphere (weather and climate) and for planning future near-Earth missions. Similar effects and concerns will occur in space missions that explore other planets in the solar system.

Understanding planetary magnetism is clearly important, and JSC research indicates that MHD turbulence plays a critical role. MHD processes underlie planetary magnetism and appear in the interior and exhaust plumes of plasma rocket engines, so that gaining an understanding in one area informs our efforts in the other. There is much that is still unknown, and ongoing research is expected to lead to important knowledge that can be applied to the planning and operation of future space missions and to a greater and more fundamental understanding of the origins, evolution, effects, and interactions of global magnetic fields generated within the Earth, other planets, and the Sun.
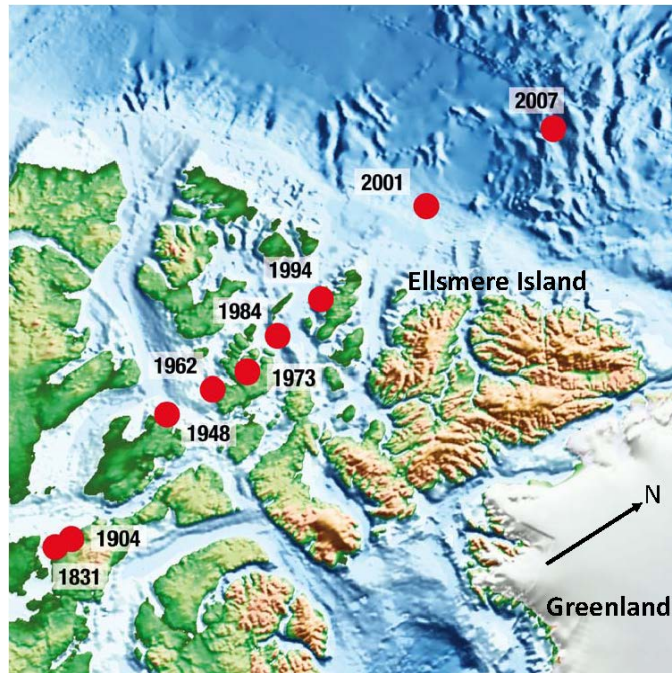
Figure 2.– Observed north dip poles from 1831–2007. (Image: Arnaud Chulliat, Institut de Physique du Globe de Paris).

Constraining Early Planetary Differentiation: The Link Between Chondrites and Achondrites Revealed From the Study of Aubrite Meteorites

David van Acken (Universität Bonn), Munir Humayun (Florida State University),
Alan D. Brandon (University of Houston), Anne Peslier

Meteorites fall into two broad categories, chondrites, which are almost pristine pieces of the early solar system before planets formed, and achondrites, which come from differentiated bodies; *i.e.*, planets or asteroids with layers of core, mantle, and crust. One type of meteorite, called aubrite or enstatite achondrite, is fascinating because it may represent a link between chondrites and achondrites. Moreover, enstatite achondrites formed very early in the solar system history, and therefore provide insight into early planetary formation.

The focus of our study was to determine the quantity of platinum group elements (PGE) in the abundant metal and sulfides of several well-known enstatite achondrites. Our sample aliquots were first characterized in the electron microprobe (EMP) laboratory of the ARES Directorate at JSC (figure 1), while the PGE were measured at Florida State University by laser inductively coupled plasma mass spectrometry (ICPMS). Our PGE measurements are consistent with samples originating from different parent bodies, and with each comes a complex history of melt extraction and differentiation, asteroid breakup and re-accretion, and infiltration by impact melts. However, the PGE patterns measured in the enstatite achondrites are similar to those of enstatite chondrites (figure 2), favoring a common origin for the two types of meteorites; *i.e.*, the origin of enstatite achondrites could be from the differentiation of enstatite chondrites.
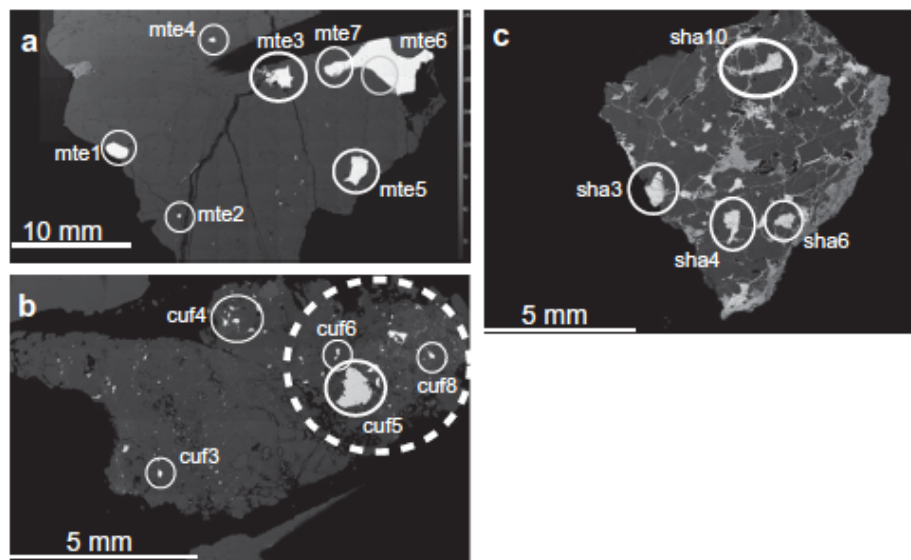
Figure 1.– Electron back-scattered maps of the aubrite thin sections – (a) Mt. Egerton, (b) Cumberland, and (c) Shallowater – showing the area targeted for PGE analysis. The brightest phases are metals and sulfides.
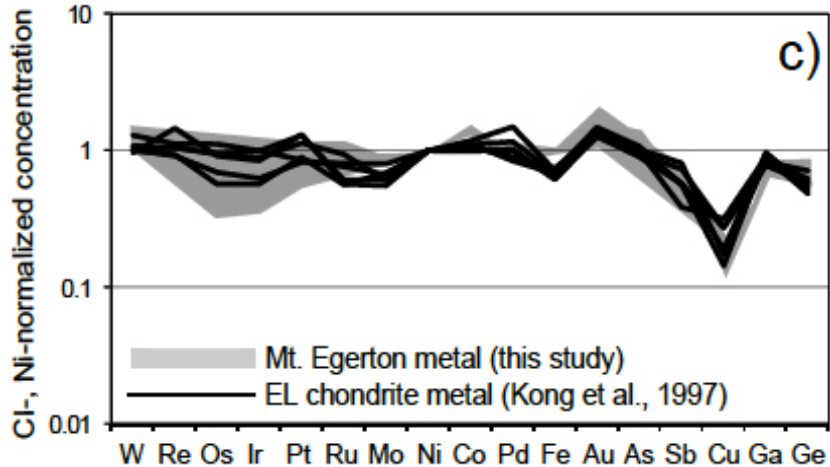
Figure 2.– PGE contents in an enstatite achondrite (Mt. Egerton in black) are similar to those of enstatite achondrites (EL in grey).

This study was published *in Geochimica et Cosmochimica Acta*:
Van Acken D., Humayun M., Brandon A.D., Peslier A.H. (2012); Siderophile Trace Elements in Metals and Sulfides in Enstatite Achondrites Record Planetary Differentiation in an Enstatite Chondritic Parent Body. *Geochim. Cosmochim. Acta* 83, pp. 272-291.

Probing Asteroid (4) Vesta, Part 1: Dawn Mission Science

David W. Mittlefehldt

A long, long time ago in a state far, far away, a young geochemistry graduate student began his research career studying a clan of igneous meteorites that were thought to have come from the asteroid (4) Vesta. Little did he know that NASA would launch a spacecraft mission to that asteroid in his "greybeard" years, or that he would be a member of the mission science team. The Dawn spacecraft was launched in September 2007 and, using the turtle's "slow and steady wins the race" methodology, arrived at Vesta in July 2011. The spacecraft spent 14 months in a series of orbits of different altitudes, studying the surface with its framing camera (FC), visible and infrared mapping spectrometer (VIR), and gamma ray and neutron detector (GRaND), and probing the interior through gravity measurements. Vesta is located in the asteroid belt between Mars and Jupiter and is the second largest asteroid, with a mean radius of 263 km.

The Dawn mission has confirmed that the mineralogy, composition, and interior structure of Vesta are fully consistent with its being the source of the howardite, eucrite, and diogenite (HED) clan of meteorites. More importantly, the wealth of data returned by the spacecraft has provided an unprecedentedly detailed look at the geology of any asteroid. Prior to Dawn's arrival, Vesta was known to have broad terrains of differing albedo and spectra, as shown by Hubble Space Telescope images (figure 1a). As Dawn orbited ever closer to the surface, geologic detail came into focus in FC images. The triplet of craters informally known as "the snowman" was discovered within a broad region of low albedo (figure 1b). The southern-most of the three, Marcia crater, is fresh and young and contains layered deposits of bright and dark materials high on the crater walls (figures 1c and d). Young craters such as Marcia have exposed rock units with differing albedos and spectral characteristics that allow the Dawn science team to investigate the detailed geologic history of Vesta.
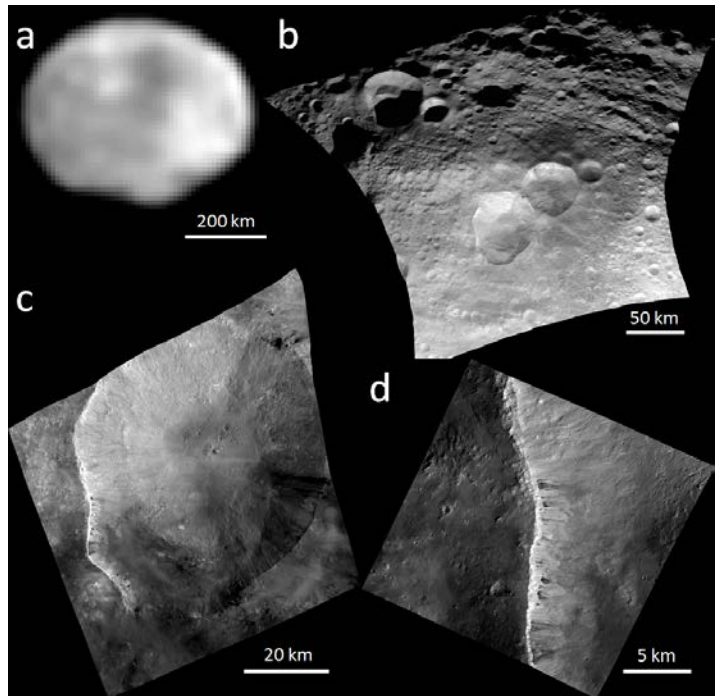
Figure 1.– (a) NASA/ESA Hubble Space Telescope image of the asteroid Vesta taken in May 1996. Image credit: Ben Zellner (Georgia Southern University), Peter Thomas (Cornell University), NASA/ESA. (b-d) Framing camera clear filter images of the Vesta "snowman" region at increasing resolution, revealing details of the geologic structure of Vesta. Images courtesy of NASA/JPL-Caltech/ UCLA/MPS/DLR/IDA.

The composition of the Vestan surface was measured by the GRaND instrument. As is the case for all airless bodies in the solar system, the surface of Vesta is covered by fragmental debris produced by a continuous bombardment of asteroids and meteoroids. The GRaND instrument collects data on this debris down to a depth of about 1 m, but at relatively coarse spatial scale. GRaND has shown that the composition of the regolith is consistent with that of meteorites of the HED clan. Laboratory studies of HED meteorites indicate that Vesta is very poor in volatile elements, such as hydrogen. Nevertheless, GRaND has detected hydrogen on the surface (figure 2) and has shown that its abundance correlates with the age of the surface estimated from the density of craters and that the maximum abundance matches predictions based on the content of carbonaceous chondrite debris found in howardite meteorites. Together with other Dawn observations, the GRaND data show that the H was delivered to the surface of Vesta by carbonaceous chondrite impactors. The distribution of iron across the Vestan surface shows that the southern hemisphere is poor in Fe compared to the northern hemisphere (figure 2). The large Rheasilvia and Veneneia basins lie in this region, and their diameters show that they excavated the lower crust. Models derived from HED meteorite

studies posit that the lower crust should be iron-poor compared to the upper crust – exactly what the GRaND instrument has determined.
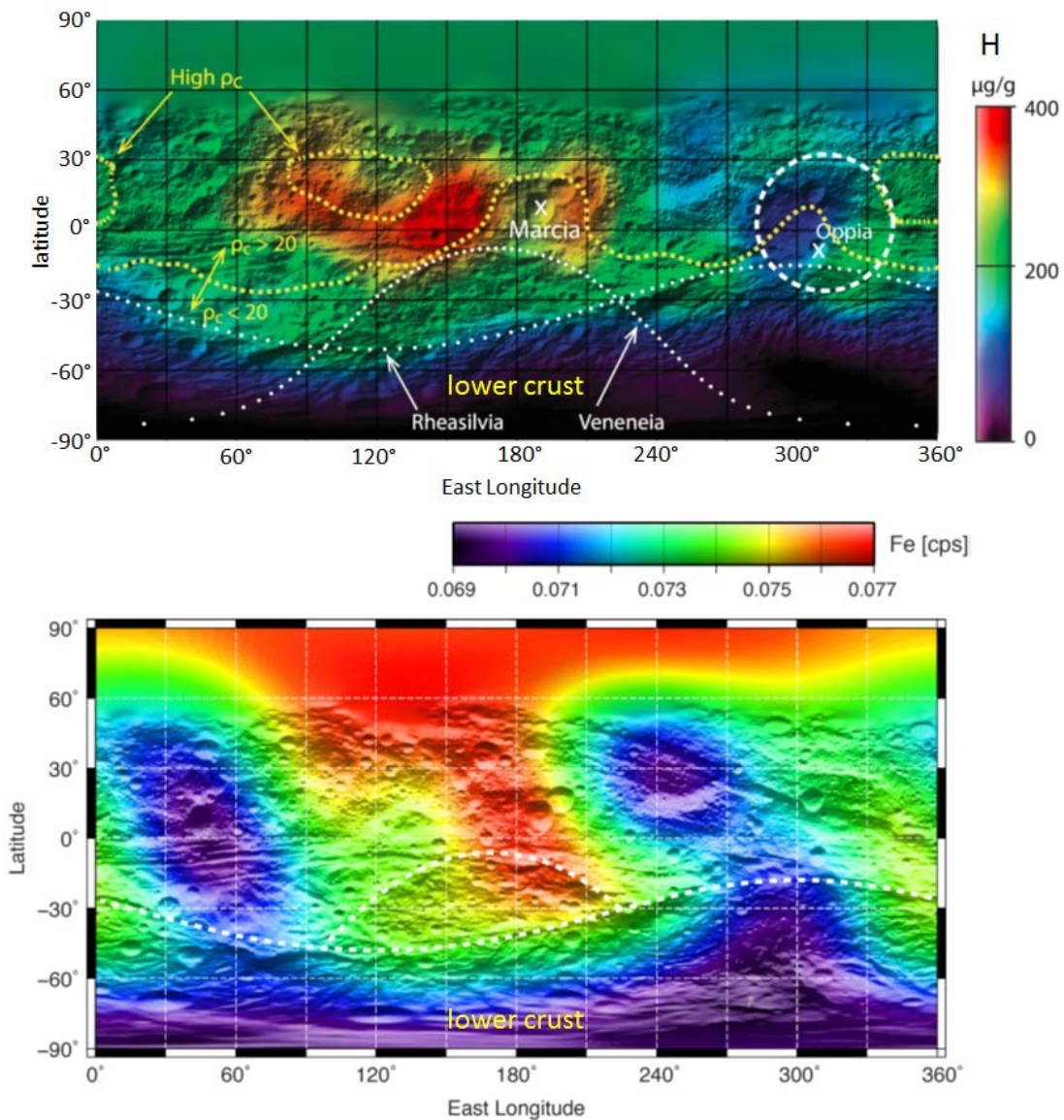
Figure 2.– Compositional maps of Vesta derived from the GRaND instrument. Upper panel: Hydrogen distribution in relation to geological feature; the rims of the large Rheasilvia and Veneneia basins and regions of high crater density (ρ_c), which indicate terrains with greater age. Map modified from Prettyman et al. (2012). Lower panel: Iron distribution in relation to the Rheasilvia and Veneneia basin rims. Map modified from Yamashita et al. (2013).

Dawn is now speeding toward its final destination, asteroid (1) Ceres. The Dawn science team continues working through the wealth of data returned from Vesta, and additional revelations on Vesta's geologic history will undoubtedly result.

Early results of the Dawn mission were published as collected papers in issues of *Science* and *Nature*, as listed below:

Science vol. **336**, no. 6082, 11 May 2012; six papers on the geology, lithologic diversity, mineralogy and cratering history of Vesta.

Science vol. **338**, no. 6104, 12 October 2012; two papers on the composition of the Vestan surface and the geology of an unusual terrain.

Nature vol. **491**, no. 7422, 01 November 2012; two papers on an unusual lithology on Vesta and on alteration of the surface characteristics by space weathering.

The GRaND element maps shown in figure 2 are from
Prettyman, T.H., Mittlefehldt, D.W., Yamashita, N., Lawrence, D.J., Beck, A.W., Feldman, W.C., McCoy, T.J., McSween, H.Y., Toplis, M.J., Titus, T.N., Tricarico, P., Reedy, R.C., Hendricks, J.S., Forni, O., Le Corre, L., Li, J.-Y., Mizzon, H., Reddy, V., Raymond, C.A., Russell, C.T., 2012. Elemental Mapping by Dawn Reveals Exogenic H in Vesta's Regolith. *Science* **338,** 242-246.

Yamashita, N., Prettyman, T.H., Mittlefehldt, D.W., Toplis, M.J., McCoy, T.J., Beck, A.W., Reedy, R.C., Feldman, W.C., Lawrence, D.J., Peplowski, P.N., Forni, O., Mizzon, H., Raymond, C.A., Russell, C.T., 2013. Distribution of Iron on Vesta. *Meteoritics & Planetary Science*, in press.

Probing Asteroid (4) Vesta, Part 2: Meteorites From Vesta

David W. Mittlefehldt

In the early 1970s, asteroid (4) Vesta was shown to have a unique reflectance spectra in the visible to infrared wavelength range and to be similar to the laboratory spectra of a clan of igneous meteorites composed of the groups howardites, eucrites, and diogenites (HEDs). With continued astronomical study, the hypothesis that Vesta is the parent asteroid of the HED clan gained widespread support in the scientific community. At the same time, laboratory studies of the HED meteorites resulted in increasingly detailed models for the geologic evolution of their parent asteroid. In anticipation of the arrival of the Dawn spacecraft at Vesta, I began synergistic studies of two types of HED meteorites, diogenites and howardites.

The consensus view is that Vesta differentiated as a global magma ocean that crystallized upon cooling. This model is derived primarily through matching the compositions of basaltic eucrites with chemical models. Diogenites are igneous rocks that were formed by accumulation of minerals from an intrusive magma body. The major minerals of diogenites are magnesium-rich orthopyroxene and olivine. In the consensus view of Vestan geologic evolution, the diogenites formed prior to basaltic eucrites, and thus diogenite compositions should indicate an earlier stage of magma-ocean crystallization. Curiously, the mineralogies (figure 1) and compositions of diogenites do not easily fit into the consensus model. Diogenites show a wide range of trace element

compositions that are difficult to reconcile with an origin in a single, large-scale magma ocean. Studies performed with colleagues from the University of Tennessee, Rice University, and Kilgore College showed that the compositions of diogenites are more consistent with formation in a series of magmas with different trace element contents. The conundrum raised by this result remains to be resolved and continues to be an area of active research.
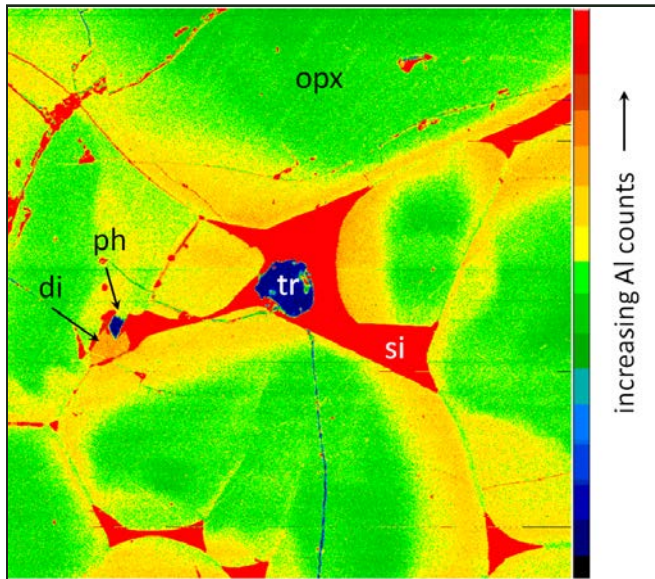
Figure 1.– Aluminum X-ray map of a portion of the diogenite Miller Range 07001. Orthopyroxene (opx) grains have low-Al cores (green) zoned to more Al-rich rims (yellow). Minor phases are the high-Ca pyroxene diopside (di), Ca-phosphate (ph), the iron sulfide troilite (tr), and a silica phase (si) filling the interstices between orthopyroxene grains. The width of the map is 0.5 mm.

Howardites are not igneous rocks. Rather, they are fragmental breccias formed from the debris derived from igneous rocks. All airless bodies in the solar system are covered by fragmental debris engendered by the constant pummeling by meteoroids and asteroids; Vesta is no exception. The fragmental debris layer, or regolith, from Vesta is represented by the howardites. Studies of howardites performed in collaboration with scientists from Franklin and Marshall College; the Max-Planck-Institut für Chemie in Mainz, Germany; and the contractor workforce at JSC should improve understanding of the processes behind the formation and mixing of the Vesta regolith. Through petrologic studies done here, chemical analyses done here and at Franklin and Marshall College, and noble gas analyses done at the Max-Planck-Institut für Chemie, we have identified a subset of howardites that were formed from material from the topmost layer of the regolith that was exposed to the solar wind. We also identified a unique howardite that is composed of roughly equal parts howarditic rock and debris from a carbonaceous chondrite impactor (figure 2). Such rocks inform us of the mixing process acting on Vesta, and understanding their history will help in interpreting data returned by the Dawn spacecraft.
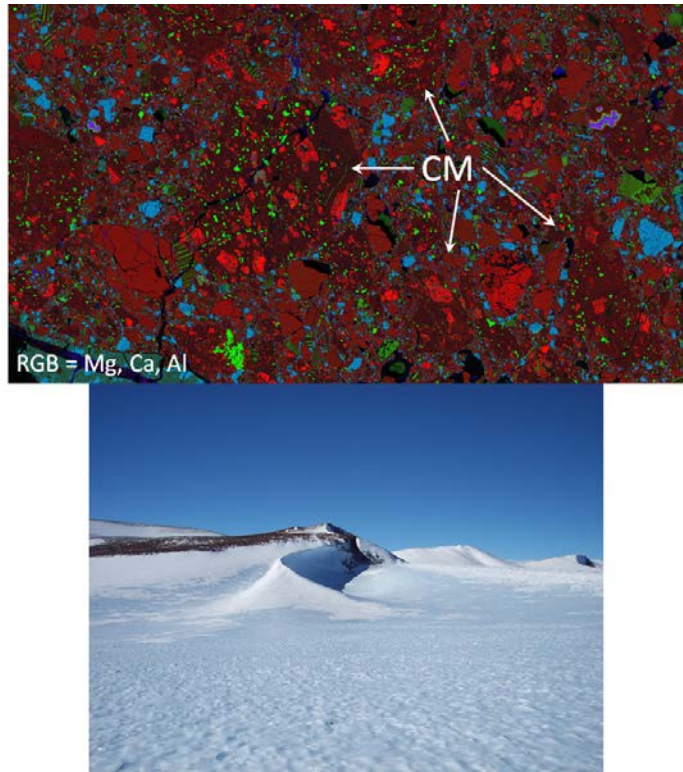
Figure 2.– Upper panel: Elemental X-ray mosaic of howardite Mount Pratt (PRA) 04401 colored using Mg = red, Ca = green, and Al = blue. Roughly 60 percent of the area consists of carbonaceous chondrite clasts (CM), which may be identified by their reddish/brownish-purple matrix. Bright red grains are olivine in CM clasts; the bright green in CM clasts are calcite grains. Light blue grains in the host are HED plagioclase grains. Green-striped grains are HED pyroxenes. The image is 9 mm across. Image acquired and mosaicked by D. K. Ross of Jacobs. Lower panel: Mount Pratt, Antarctica, the find location of PRA 04401. Image by the author, a member of the 2004–2005 Antarctic Search for Meteorites field team that discovered PRA 04401.

Small-Scale Impact Processes on Stony Asteroids

Mark J. Cintala, Fredrich Hörz, David W. Mittlefehldt, Francisco Cardenas

Asteroids are a very diverse group of small objects (when compared to the much larger planets) orbiting the Sun. Most known asteroids are located between the orbits of Mars and Jupiter (in the "asteroid belt"), but large numbers are in orbits that cross that of the Earth. While scientific curiosity historically has driven investigations of asteroids, it is becoming intensely apparent that detailed information about asteroids could someday be critical in dealing with a potentially disastrous impact. Some asteroid types are believed to be sources of one of the most common types of meteorite, the "ordinary chondrites." In fact, the large meteoroid that exploded over Chelyabinsk in Russia in February 2013 was an ordinary chondrite, and evidence suggests that ordinary-chondrite asteroids constitute a large fraction of the "Earth crossers."

Earth-based astronomical observations have long implied and recent spacecraft missions have shown that even small asteroids (figure 1) are covered with unconsolidated debris (as is the Moon), which is generically termed "regolith." The regolith on any typical airless body in the solar system is generated primarily through the breaking up (or "comminution") of surface rock by impacting meteoroids. This is a process that, while it cannot be duplicated exactly on Earth for a variety of reasons, is amenable to simulation in the laboratory. All that is needed is an accelerator that can launch projectiles accurately at speeds of at least 2 km/s, a vacuum chamber, a piece of ordinary chondrite, a container to keep it confined, and people obsessed enough to shoot it 59 separate times, sieving it after every few shots and removing samples for later analysis. Amazingly, all of those requirements can be met in one place: the Experimental Impact Laboratory. (Actually, the ordinary chondrite is a piece from a larger meteorite that was found in Antarctica in 1985, brought to Houston, and kept in the Antarctic meteorite curatorial facility until it was allocated to us for the experiments.)

Figure 1.– The asteroid Itokawa, as photographed by the Japan Aerospace Exploration Agency's Hayabusa spacecraft in 2005. The maximum dimension of the asteroid in this view is about 535 m (about a third of a mile). This asteroid is almost pathological in its regolith configuration, with textures ranging from patches of fine material to enormous blocks, such as the 50-m example at the extreme right, named Yoshinodai.

The 464-g (just over 1 lb) meteorite was subjected to 2 km/s impacts with 3.2-mm (1/8-in.) ceramic spheres. The largest fragment remaining after each shot was used as the target for the next impact, until the biggest surviving fragment was less than half the weight of the impacted piece. The meteorite required nine separate shots before it met that criterion, which means that it was a surprisingly tough rock. By comparison, similar experiments using terrestrial gabbro targets (a coarse-grained, strong, igneous rock fairly common on Earth and the Moon) required only about half of that energy to reach the same level of destruction. Given this, it is possible that, had the Chelyabinsk meteoroid been a large block of gabbro instead of ordinary chondrite, it might well have broken up at a higher altitude, doing less damage on the ground.

All of the debris from those nine shots was collected, put in a container, and impacted repeatedly. Regular breaks were taken to sieve the results, which allowed us to follow the "evolution" of this artificial regolith. Identical experiments using gabbro and basalt (a very fine-grained equivalent of the gabbro) were also performed, but they stopped at 25 shots, by which time enough information was in hand for comparison (figure 2). The larger pieces of the chondrite, again surprisingly, disrupted sooner than those of the gabbro and basalt, and when the pieces of the chondrite broke apart, they did so more thoroughly. It is entirely possible that, when the meteorite was disrupted initially, it suffered more internal fracturing than was apparent.

Work is underway to investigate possible chemical and mineralogical effects that might have occurred when the meteorite changed from rock to "regolith." It is already obvious, however, that the formation of regoliths on asteroids could be very different in detail from the equivalent process on a larger body like the Moon.
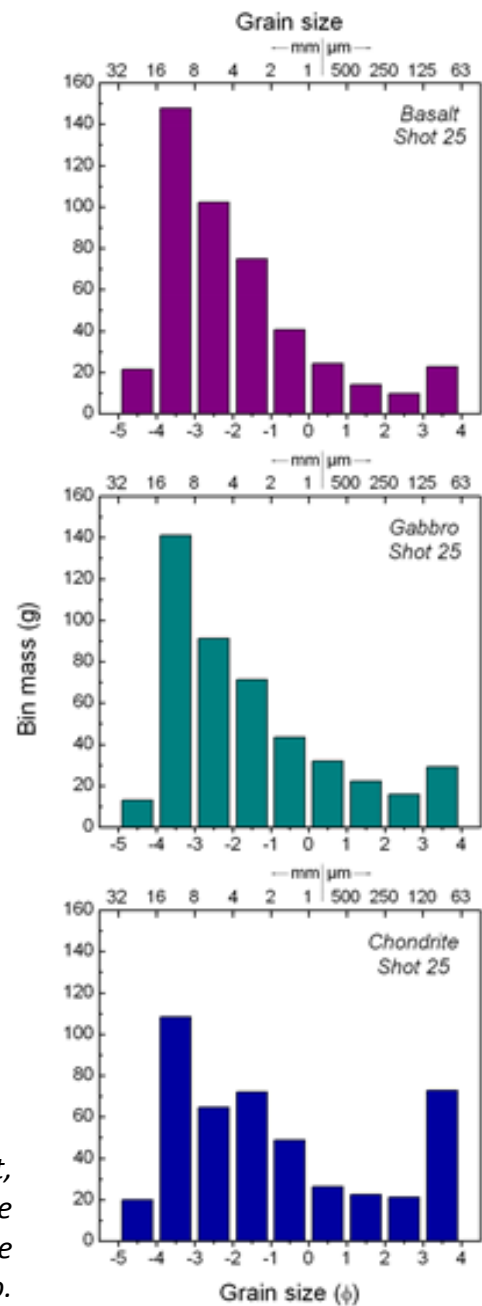
Figure 2.– Comparison between size distributions of basalt, gabbro, and chondrite after 25 impacts each. Note the similarity between the two terrestrial rocks and the difference between them and the gabbro.

Astromaterials Acquisition and Curation Office (KT)
Overview

Carlton Allen, Ph.D., Astromaterials Curator, Manager
http://curator.jsc.nasa.gov/index.cfm

The Astromaterials Acquisition and Curation Office has the unique responsibility to curate NASA's extraterrestrial samples – from past and forthcoming missions – into the indefinite future. Currently, curation includes documentation, preservation, physical security, preparation, and distribution of samples from the Moon, asteroids, comets, the solar wind, and the planet Mars. Each of these sample sets has a unique history and comes from a unique environment. The curation laboratories and procedures developed over 40 years have proven both necessary and sufficient to serve the evolving needs of a worldwide research community. A new generation of sample return missions to destinations across the solar system is being planned and proposed. The curators are developing the tools and techniques to meet the challenges of these new samples.

Extraterrestrial samples pose unique curation requirements. These samples were formed and exist under conditions strikingly different from those on the Earth's surface. Terrestrial contamination would destroy much of the scientific significance of extraterrestrial materials. To preserve the research value of these precious samples, contamination must be minimized, understood, and documented. In addition, the samples must be preserved – as far as possible – from physical and chemical alteration. The elaborate curation facilities at JSC were designed and constructed, and have been operated for many years, to keep sample contamination and alteration to a minimum.

Currently, JSC curates seven collections of extraterrestrial samples:

- Lunar rocks and soils collected by the Apollo astronauts
- Meteorites collected on dedicated expeditions to Antarctica
- Cosmic dust collected by high-altitude NASA aircraft
- Solar wind atoms collected by the Genesis spacecraft
- Comet particles collected by the Stardust spacecraft
- Interstellar dust particles collected by the Stardust spacecraft
- Asteroid soil particles collected by the Japan Aerospace Exploration Agency (JAXA) Hayabusa spacecraft

Each of these sample sets has a unique history and comes from a unique environment. We have developed specialized laboratories and practices over many years to preserve and protect the samples, not only for current research but for studies that may be carried out in the indefinite future.

Catalogs, images, compendia of research results, and instructions for requesting samples from each collection are published online at http://curator.jsc.nasa.gov/.

Space agencies and researchers around the world have recognized the value of sample return missions to further scientific understanding and support exploration of planetary bodies. The U.S. National Research Council's Planetary Decadal Survey listed the first lander in a Mars sample return campaign as the highest priority for a flagship-class mission, and sample return missions to the lunar South Pole-Aitken basin, the surface of a comet, and the surface of an asteroid are among its highest priority missions for the New Frontiers program. In 2011, NASA selected the Origins Spectral Interpretation Resource Identification Security – Regolith Explorer (OSIRIS-Rex), designed to return samples from a C-class asteroid in 2023, as its next New Frontiers mission. JAXA is preparing to launch Hayabusa 2, a second asteroid sampling mission, in 2014. President Obama has announced the goal of a human visit to a near-Earth asteroid, and the eventual goal of a human mission to Mars. Samples from any of these destinations would be invaluable for scientific research and for enabling human exploration across the solar system.

Lessons learned for the future from 40+ years of curating NASA's extraterrestrial samples

- The main point of any sample return mission is laboratory analysis.
  - Everything must be designed, built, and operated to get the highest quality samples to the best laboratories.
- Curation starts with mission design.
  - Samples will never be cleaner than the tools and containers used to collect, transport, and store them.
- We must be ready for contingencies.
  - Really bad things can, and do, happen – careful planning and dedicated people can sometimes save the day.
- Every sample set is unique.
  - Laboratories and operations must respond to the diversity and special requirements of the samples.
- We are in it for the long haul.
  - Samples collected years or decades ago are yielding new discoveries that totally change our understanding of planets, moons, and solar system history. These discoveries will inspire new generations of scientists and research questions, and will drive new exploration missions by robots and humans.

The following reports provide insight into the curation team's work and research in 2011 and 2012.

Collecting Comet Samples by ER-2 Aircraft: Cosmic Dust Collection During the Draconid Meteor Shower in October 2012

Ron Bastien, P.J. Burkett, M. Rodriguez, D. Frank, C. Gonzalez, G.-A. Robinson, M. Zolensky
P. Brown, M. Campbell-Brown (University of Western Ontario)
S. Broce (Computer Sciences Corporation)
M. Kapitzke, T. Moes, D. Steel, T. Williams (Dryden Flight Research Center)
D. Gearheart (University of California Santa Cruz)

Introduction. Many tons of dust grains, including samples of asteroids and comets, fall from space into the Earth's atmosphere each day. NASA periodically collects some of these particles from the Earth's stratosphere using sticky collectors mounted on NASA's high-flying aircraft (figure 1).
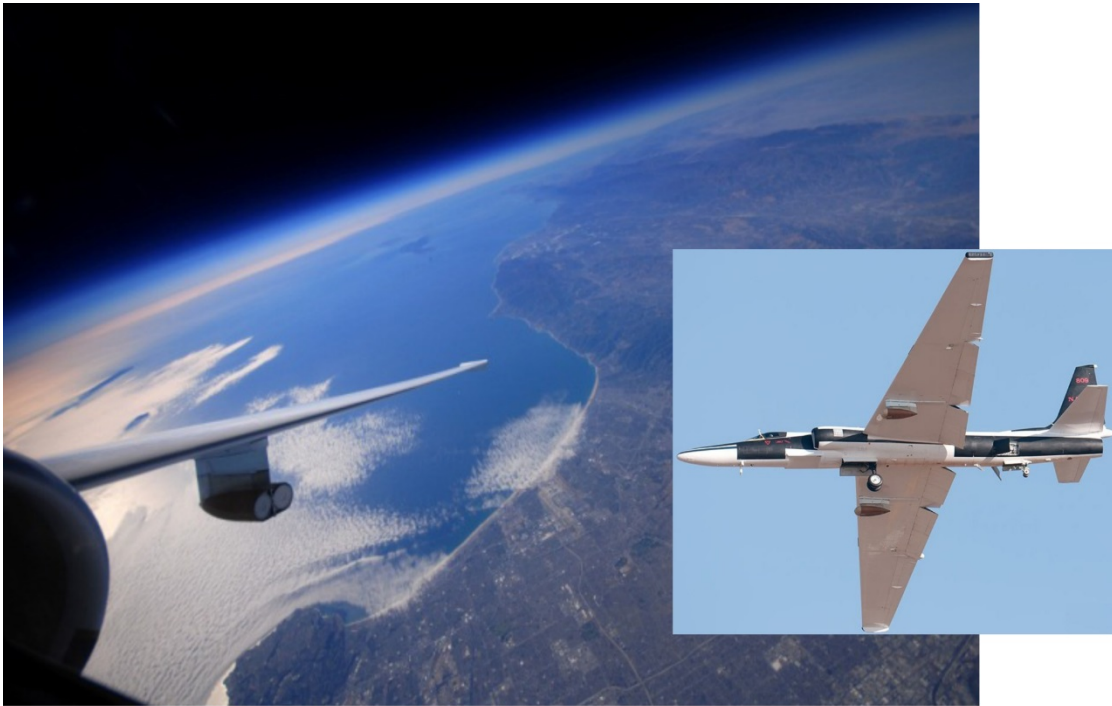
Figure 1.– The ER-2 (right) and a photo from the flight of October 16, 2012, taken over Los Angeles, CA, at 70,000 ft., looking west toward Santa Barbara and the Channel Islands.

Sometimes, especially when the Earth experiences a known meteor shower, a special opportunity is presented to associate cosmic dust particles with a known source. NASA JSC's Cosmic Dust Collection Program has made special attempts to collect dust from particular meteor showers and asteroid families when flights can be planned well in advance. However, it has rarely been possible to make collections on very short notice. In 2012, the Draconid meteor shower presented that opportunity (figure 2). The Draconid meteor shower, originating from Comet 21P/Giacobini-Zinner, has produced both outbursts and storms several times during the last century, but the 2012 event was not predicted to be much of a show. Because of these predictions, the Cosmic Dust team had not

targeted a stratospheric collection effort for the Draconids, despite the fact that they have one of the slowest atmospheric entry velocities (23 km/s) of any comet shower, and thus offer significant possibilities of successful dust capture. However, radar measurements obtained by the Canadian Meteor Orbit Radar during the 2012 Draconids shower indicated a meteor storm did occur October 8 with a peak at 16:38 (±5 min) UTC for a total duration of ~2 hours.
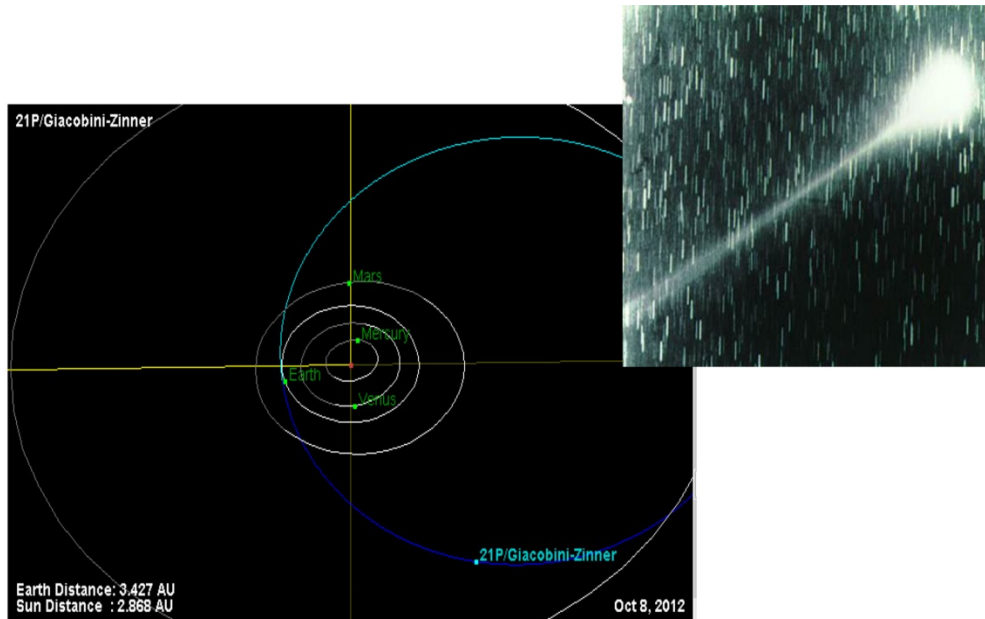
Figure 2.– Orbit of Giacobani-Zinner (upper right), showing where the Earth crossed the orbital path October 8, 2012. This image is from the Jet Propulsion Laboratory's (JPL's) Small-Body Database Browser.

Meteor Observations. The Canadian Meteor Orbit Radar (CMOR) is an automated radar meteor echo detection and orbital measurement system operating at 29.85 MHz. CMOR records ~5000 orbits per day for meteoroids with mass $>10^{-7}$ kg on average. At Draconids entry speeds (23 km/s), the radar typically detects particles with diameters >500 μm. The Draconids shower flux measured by CMOR in 2012 was the highest shower flux measured during the entire operational lifetime of CMOR (1999–present). The CMOR team reported that the peak flux was more than an order of magnitude higher than that measured by CMOR in the 2005 or 2011 Draconids outbursts. The equivalent Zenithal Hourly Rate (ZHR) (for 5-min bins) was in excess of 5000 at the peak. Data from the radar also allowed the team to calculate a variety of the shower's attributes, including that the storm appears to have been particularly rich in smaller meteoroids.

Collection Efforts. The large and small area collectors L2094, L2095, L2096, L2097, U2153, and U2154, were flown from October 15 to 17, 2012. Each flight accumulated between 7 and 8 hours of collection time (figure 3). The small collectors (U2153 and U2154) received an additional 5.7 hours October 11.
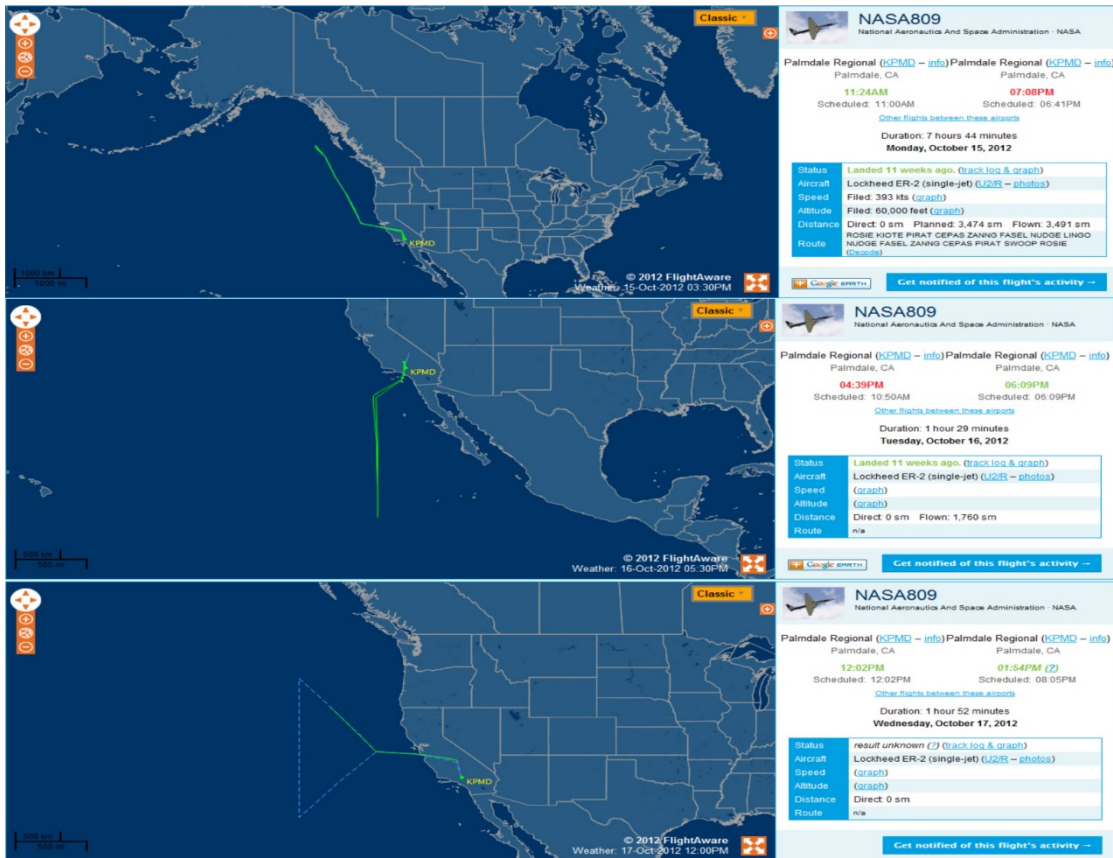
Figure 3.– Flight data from FlightAware data for aircraft ER-2 NASA809 October 15–17, 2012, showing the aircraft flight path during sample collection.

Preliminary Examination. JSC's Cosmic Dust Laboratory received the ER-2 flight collectors in late October 2012. Upon first review, we noted that one pair of large collectors (L2096 and L2097) had suffered an O-ring failure and possible ground contamination; collection was stopped after 15.1 hours. Preliminary examination of L2094 and L2095 revealed a low concentration of particulate matter on the surface of the collectors due to the short collection period (approximately 23 hours).

The harvest of likely particles from the various collection surfaces has begun. An example of each cluster particle is examined as well as a subset of all interesting individual grains. Using a scanning electron microscope (SEM), energy-dispersive X-ray spectra (EDX) are collected for each grain. Several examples of *potential* Giacobini-Zinner grains are shown in figure 4. If successful, this collection effort will essentially be a comet coma sample return mission accomplished at a tiny fraction of the cost of a spacecraft mission.
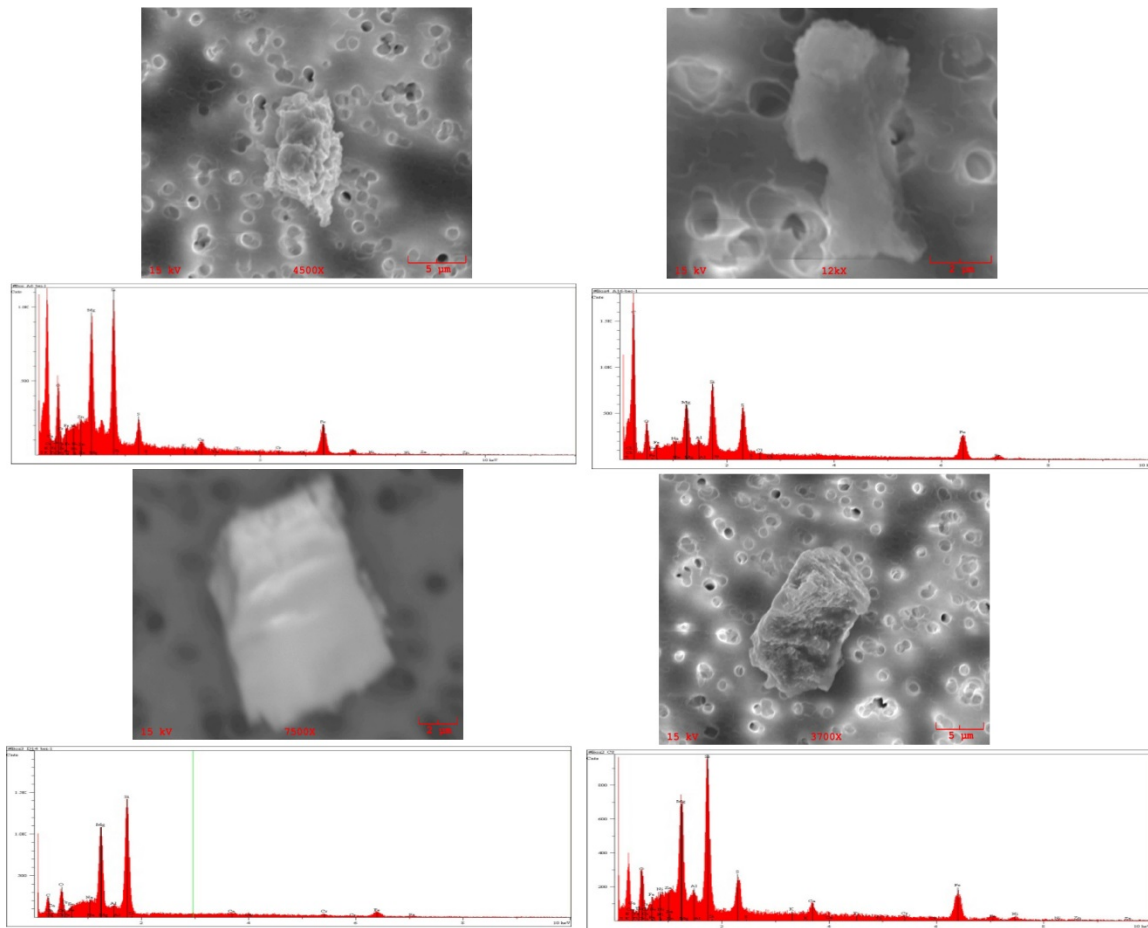
Figure 4.– SEM images and EDX spectra for four particles harvested from collector L2094. These EDX spectra are consistent with an extraterrestrial origin.

GeoLab: A Geological Workstation for Future Missions

Cynthia Evans, Michael Calaway, Mary Sue Bell
Zheng Li, Shuo Tong, Ye Zhong, Ravi Dahiwala (University of Bridgeport)

The GeoLab glovebox was, until November 2012, fully integrated into NASA's Deep Space Habitat (DSH) Analog Testbed (figure 1). The conceptual design for GeoLab came from several sources, including current research instruments (Microgravity Science Glovebox) used on the International Space Station, existing Astromaterials Curation Laboratory hardware and clean room procedures, and mission scenarios developed for earlier programs.

GeoLab allowed NASA scientists to test science operations related to contained sample examination during simulated exploration missions. The team demonstrated science operations that enhance the

early scientific returns from future missions and ensure that the best samples are selected for Earth return. The facility was also designed to foster the development of instrument technology.

Figure 1.– GeoLab glovebox (left) inside NASA's DSH (right).

Since 2009, when GeoLab design and construction began, the GeoLab team [a group of scientists from the Astromaterials Acquisition and Curation Office within the Astromaterials Research and Exploration Science (ARES) Directorate at JSC] has progressively developed and reconfigured the GeoLab hardware and software interfaces and developed test objectives, which were to 1) determine requirements and strategies for sample handling and prioritization for geological operations on other planetary surfaces, 2) assess the scientific contribution of selective in-situ sample characterization for mission planning, operations, and sample prioritization, 3) evaluate analytical instruments and tools for providing efficient and meaningful data in advance of sample return and 4) identify science operations that leverage human presence with robotic tools.

In the first year of tests (2010), GeoLab examined basic glovebox operations performed by one and two crewmembers and science operations performed by a remote science team. The 2010 tests also examined the efficacy of basic sample characterization [descriptions, microscopic imagery, X-ray fluorescence (XRF) analyses] and feedback to the science team. In year 2 (2011), the GeoLab team tested enhanced software and interfaces for the crew and science team (including Web-based and mobile device displays) and demonstrated laboratory configurability with a new diagnostic instrument (the Multispectral Microscopic Imager from the JPL and Arizona State University). In year 3 (2012), the GeoLab team installed and tested a robotic sample manipulator and evaluated robotic-human interfaces for science operations.

GeoLab Robotic Sample Manipulator. Sample-return missions have strict protocols to reduce potential contamination of samples, and sample handling in microgravity presents special challenges. To begin to address these challenges in the GeoLab, scientists at JSC joined engineering students from the University of Bridgeport in Bridgeport, CT. The students were awarded one of the 2012 National Space Grant Foundation Exploration Habitat (XHab) Academic Challenges (see

) to develop an engineering design for tools to handle geological samples for analysis in a microgravity glovebox environment. The Bridgeport XHab team designed and built a robotic arm system with a three-finger gripper that could manipulate geologic samples within the existing GeoLab glovebox (figure 2). An innovation developed by the Bridgeport team was the large curvature of each finger, a design that reduced contact with the irregular surfaces of a rock sample, thus minimizing contamination risk while still allowing a significant capture force to be applied to the uneven surfaces of a rock (figure 3).
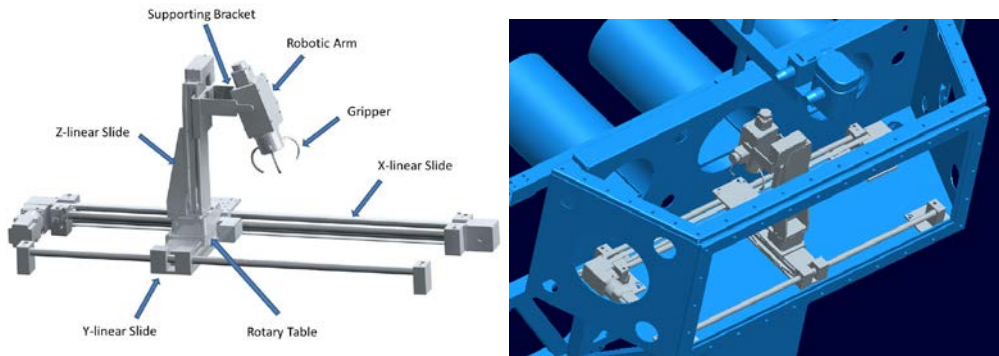
Figure 2.– GeoLab Robotic Sample Manipulator computer-aided design (CAD) design and CAD rendering of the robotic arm inside a glovebox, created by the University of Bridgeport XHab 2012 team.
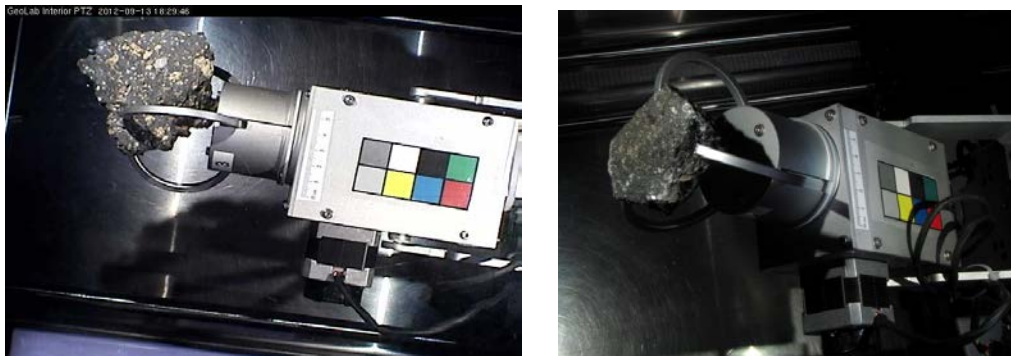
Figure 3.– Views of the robotic sample manipulator three-fingered end effector holding and positioning rock samples.

The robotic manipulator was required to be able to capture and release samples, translate the full volume of the glovebox, and precisely manipulate samples for imaging, microscopic examination, and positioning for XRF analyses. The full range of motion (translation in the X, Y, and Z directions, up and down pivot motion, and rotating end effector) was accomplished with a linear slide for the length of the glovebox (X-direction) and precision linear stages or motion along the Y and Z axes. The Z-axis linear stage was mounted on a motorized rotary stage.

All four (X, Y, Z, and rotation) stages were enabled by a motion controller. The robotic arm pitch used a series of enclosed gears attached to a motor. The three-fingered grasper enabled 360° rotation with two additional motors; all three motors were controlled by one controller. Both controllers were Ethernet enabled and connected to the DSH avionics network switches. The software interface for the controllers was a touch-screen display, mounted above the glovebox, designed by the DSH software team.

The tests of the robotic arm provided insight into technologies that will be required for higher readiness levels. The ultimate goal is to build a robotic system that can autonomously conduct the preliminary examination of returned samples and downlink this data to Earth-based mission scientists. The team's current goal for sample science in the context of planetary exploration is to have autonomous robotic systems, assisted by human crewmembers when required, that can 1) collect and stow samples in an archival manner, 2) conduct preliminary examination of samples, 3) downlink the data to mission scientists for sample return prioritization, and 4) maintain rigorous curation protocols that preserve the scientific integrity of the samples.

Three Years of GeoLab Tests. Over the 3 years that GeoLab was integrated into the DSH, GeoLab participated in 19 days of simulated mission testing and monitored operations with 18 different test subjects. The GeoLab team also conducted standalone tests with nearly 20 other operators. While complete compilation and assessment of test results are still underway, the GeoLab team can confidently report the following:

1) *The GeoLab design supports autonomous crew operations of the basic glovebox functions.* The trained crew enhances science returns by providing spontaneous observations; this is especially important when time delays preclude real-time science team involvement.

2) *Good sample imagery is key for preliminary characterization.* Imagery collected at a range of scales forms the basis for additional characterization. The earliest tests indicated that basic microscopy provided invaluable data for rapid assessment of samples.

3) *Robotic assists for sample handling are critical in microgravity.* Robotics aid crew and enable precision sample handling for data collection. The 2012 tests validated the quantity and quality of microscopy that could be achieved with a robotic sample holder. The sample holder made possible one-person operations (crew efficiency), provided flexibility in sample positioning (see figure 3), and enabled systematic sample positioning, allowing for mapping of the sample for future analyses. Finally, proper robotic sample handling can result in less sample handling and therefore present less risk of damaging or compromising a sample.

4) *A combination of imaging tools and robotic tools provides significant flexibility for designing facilities and operations related to sample characterization and sample handling.* Progressive tests using robotic interfaces will help develop requirements, instruments, and procedures for different exploration scenarios.

5) *Preliminary sample characterization provides data that supports smart decisions during mission operations.* Data supports sample prioritization, enables a better understanding of the regional geology being explored, highlights details on samples, and is useful for future exploration plans. The types of data that were collected in the GeoLab during the analog tests allow for wide dissemination and broad participation by scientists and students on Earth.

Dividing the Concentrator Target From the Genesis Mission

H. V. Lauer, Jr., P. J. Burkett, S. J. Clemett, C. P. Gonzales,
K. Nakamura-Messenger, M. C. Rodriguez, T. H. See, B. Sutter

The Genesis spacecraft, launched in 2001, traveled to a Lagrangian point between the Earth and Sun to collect particles from the solar wind and return them to Earth. However, during the return of the spacecraft in 2004, the parachute failed to open during descent, and the Genesis spacecraft crashed into the Utah desert. Many of the solar wind collectors were broken into smaller pieces, and the field team rapidly collected the capsule and collector pieces for later assessment. On each of the next few days, the team discovered that various collectors had survived intact, including three of four concentrator targets. Within a month, the team had imaged more than 10,000 fragments and packed them for transport to the Astromaterials Acquisition and Curation Office within the ARES Directorate at JSC. Currently, the Genesis samples are curated along with the other extraterrestrial sample collections within ARES.

Although they were broken and dirty, the Genesis solar wind collectors still offered the science community the opportunity to better understand our Sun and the solar system as a whole. One of the more highly prized concentrator collectors survived the crash almost completely intact (figure 1). The Genesis Concentrator was designed to concentrate the solar wind by a factor of at least 20 so that solar oxygen and nitrogen isotopes could be measured.

One of these materials was the Diamond-on-Silicon (DoS) concentrator target. Unfortunately, the DoS concentrator broke on impact (figure 1). Nevertheless, the scientific value of the DoS concentrator target was high. The Genesis Allocation Committee received a request for ~1 cm^2 of the DoS specimen taken near the focal point of the concentrator for the analysis of solar wind nitrogen isotopes. The largest fragment, Genesis sample 60000, was designated for this allocation and needed to be precisely cut. The requirement was to subdivide the designated sample in a manner that prevented contamination of the sample and minimized the risk of losing or breaking the precious requested sample fragment.

The Genesis curator determined that the use of laser scribing techniques to "cut" a precise line and subsequently cleave the sample (in a controlled break of the sample along that line) was the best method for accomplishing the sample subdivision. However, there were risks, including excess heating of the sample, that could cause some of the implanted solar wind to be lost via thermal

diffusion. Accidentally breaking the sample during the handling and cleaving process was an additional risk. Early in fiscal year 2013, to address this delicate, complicated task, the ARES Directorate assembled its top scientists to develop a cutting plan that would ensure success when applied to the actual concentrator target wafer; *i.e.*, to produce an approximately 1 cm^2 piece from the requested area of the wafer. The team, subsequently referred to as the JSC Genesis Tiger Team, spent months researching and testing parameters and techniques related to scribing, cleaving, transporting, handling, and holding (*i.e.*, mounting) the specimen. The investigation required considerable "thinking outside the box," and many, many trials using nonflight wafer analogs.
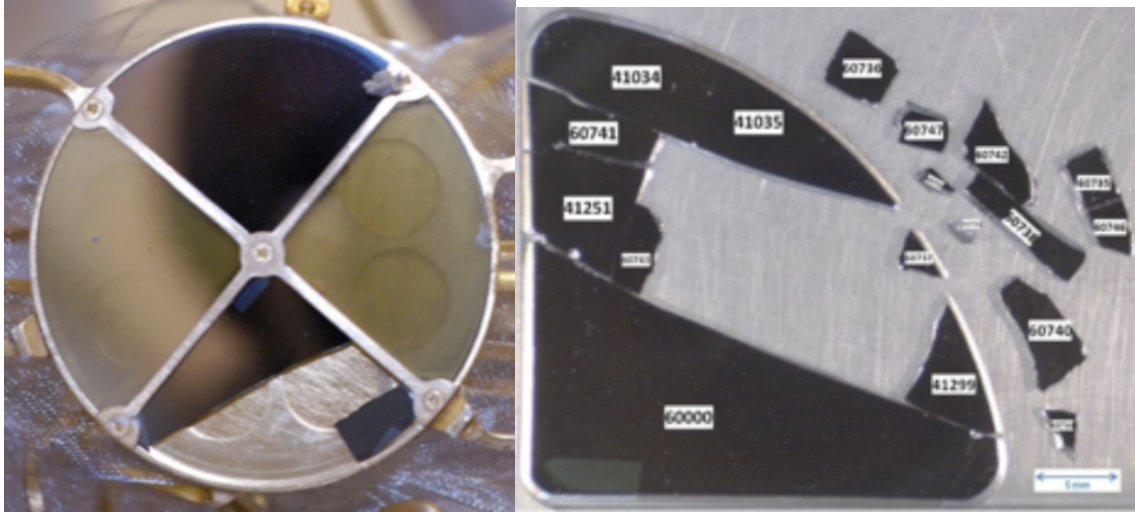
Figure 1.– Genesis Concentrator target (left) and the recovered DoS fragments (right).

After all preliminary testing, the following method was adopted as the final cutting plan. It was used in two final end-to-end practice runs before being used on the actual flight target wafer. The wafer was oriented on the laser cutting stage with the 100 and 010 directions of the wafer parallel to the corresponding X and Y directions of the cutting stage. The laser was programed to scribe 31 lines of the appropriate length along the Y stage direction. The programed scribe lines were separated by 5 µm in the X direction. The laser parameters were set as follows: (1) The laser power was 0.5 watts; (2) each line consisted of 50 passes, with the Z position being advanced 5 µm per pass; and (3) 30 s would elapse before the next line was scribed to allow for wafer cool down from any possible heating via the laser.

The ablated material that "stuck" in the "scribe-cut" was removed from the "cut" using an ultrasonic micro-tool. After all the ablated silicon was removed from the wafer, the wafer was repositioned in exactly the same orientation on the laser stage. The laser was focused using the bottom of the wafer channel, and the 31-line scribing pattern described above was reprogrammed using the Z position of the groove bottom as the starting Z value instead of the top wafer surface, which was used previously. Upon completion of the second set of scribes, the ultrasonic micro-tool was again used to clean out the cut. The wafer was remounted on the stage in exactly the same orientation as before. The laser was again focused on the bottom of the groove. This time, however, the laser was

programed to scribe only one line down the exact center of the channel. The final scribe line consisted of 100 passes with a Z advance of 5 µm per pass and with the laser power set at 0.5 watts. As mentioned above, the final cutting plan was practiced in two end-to-end trials using nonflight, triangular-shaped silicon wafers similar in size and orientation to the actual DOS 60000 target sample. The actual scribing of the triangular-shaped wafers required scribing two lines and cleaving (*i.e.* scribe-cleave, then scribe-cleave) to obtain the piece requested for allocation.

Early in December 2012, after many months of experiments and practicing and perfecting the techniques and procedures, the team successfully subdivided the Genesis DoS 60000 target sample, one of the most scientifically important samples from the Genesis mission (figure 2). On December 17, 2012, the allocated piece of concentrator target sample was delivered to the requesting principal investigator.

Figure 2.– Left – Image of the back side of the DoS 60000 wafer with the location of the two proposed scribing lines projected onto the surface. Right – The actual flight specimen following successful processing by the JSC Genesis Tiger Team.

The cutting plan developed for the subdivision of this sample will be used as the model for subdividing future requested Genesis flight wafers (appropriately modified for different wafer types).

The Apollo Lunar Sample Image Collection: Digital Archiving and Online Access

Nancy S. Todd, Gary E. Lofgren, William L. Stefanov, Patricia A. Garcia (U.S. Geological Survey)

The primary goal of the Apollo Program was to land human beings on the Moon and bring them safely back to Earth. This goal was achieved during six missions – Apollo 11, 12, 14, 15, 16, and 17 – that took place between 1969 and 1972. Among the many noteworthy engineering and scientific accomplishments of these missions, perhaps the most important in terms of scientific impact was the return of 382 kg (842 lb) of lunar rocks, core samples, pebbles, sand, and dust from the lunar surface to Earth. Returned samples were curated at JSC (then known as the Manned Spacecraft Center) and,

as part of the original processing, high-quality photographs were taken of each sample (figure 1). The top, bottom, and sides of each rock sample were photographed, along with 16 stereo image pairs taken at 45-degree intervals. Photographs were also taken whenever a sample was subdivided and when thin sections were made. This collection of lunar sample images consists of roughly 36,000 photographs; all six Apollo missions are represented.
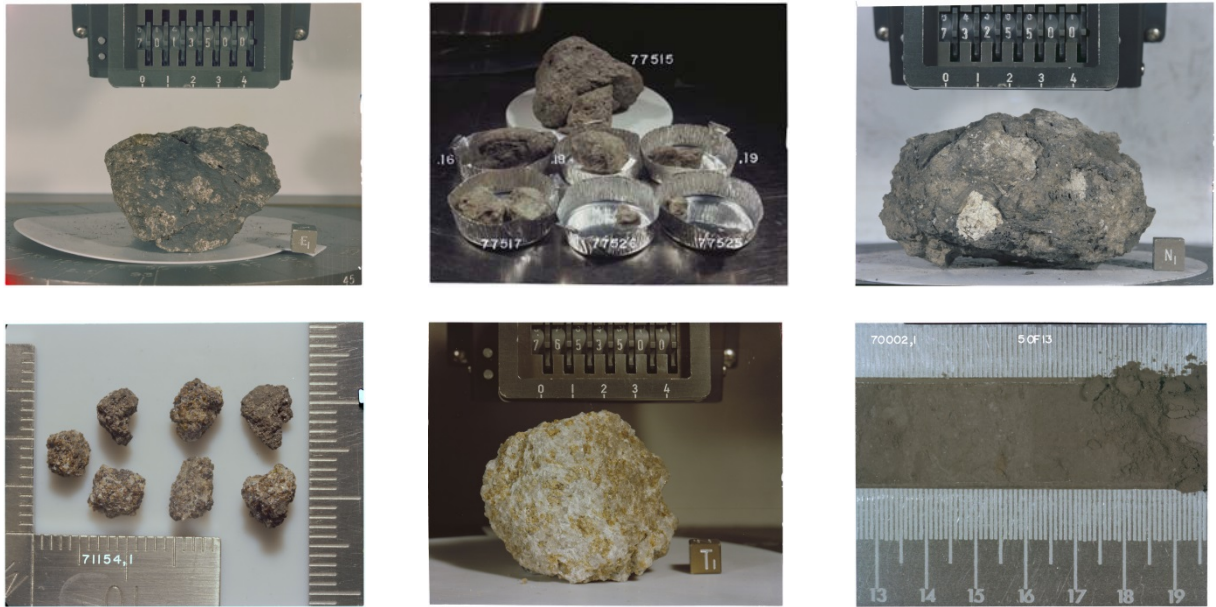
Figure 1.– Representative images of lunar samples from the JSC archive. Clockwise from top left: Ilmenite Basalt 70135, orthophoto; Rake Sample 77515, processing group photo; Impact Melt Breccia 73255, orthophoto; Core 70002, processing photo; Troctolite 76535, orthophoto; 4–10 mm Fines 71154, processing photo.

Project Objective

Throughout much of its history, the lunar sample image data set has been available only to researchers – and the public – in hardcopy at JSC or, more recently, as relatively low-resolution scanned images in Joint Photographic Experts Group (JPEG) format. Grant funding to the ARES Directorate's Astromaterials Acquisition and Curation Office at JSC was received through the NASA Lunar Advanced Science and Exploration Research (LASER) Program in 2008 to support digital scanning of the original film negatives to preserve the information contained within the aging (and degrading) film media and to develop an online database of the imagery to increase public access to the data. In many cases, these images are the only remaining record of what the samples looked like prior to subdivision, and they contain valuable information about the samples' original geologic characteristics – thus, preservation of this information in high-quality, digital form is imperative.

Creation of Digital Master Images from Original Photo Negatives
Each lunar sample image has been rescanned at 2040 pixels per inch (PPI), or 80 pixels/mm, to allow a spatial resolution of 12.5 microns and 16-bit color depth to capture the full dynamic range of the original film. Scanned images were reviewed for quality and saved in a lossless Tagged Image File Format (TIFF) format as the primary archive product. From the TIFF files, JPEG format versions of various sizes have been generated for browsing, print, and Web use.

The bulk of the work scanning the photo negatives to create the digital master images was done between 2008 and 2011; more than 27,000 photos were scanned in this period. In 2012 and 2013, another 7,000 photos were completed. The remaining photos are expected to be complete by the end of fiscal year 2013. All photo scanning work was performed by the JSC Photo Operations Multimedia Services Group.

Online Access to Lunar Sample Data
The Lunar Sample Catalog & Photo Database (http://curator.jsc.nasa.gov/lunar/samplecatalog/) was first published on the JSC ARES Astromaterials Curation Web site in November 2010, and it has been extensively reworked over the past few years to improve and extend its functionality. A completely updated interface, which incorporates additional search options, expanded references, and user-requested enhancements, was launched in the spring of 2012 and announced during the 43rd Lunar and Planetary Science Conference. The searchable database interface provides the ability to search for lunar sample information using a variety of criteria: sample generic number, mission, collection station or landmark, rock classification, and public displays that include the sample. Query results (figure 2) include sample details, photographs, listings of all reference catalogs that include the sample, and, where available, links to the petrographic and geochemical data for the sample in the Lunar Sample Compendium. Users may also search for sample images using photo numbers, type of photo, and related sample information. Image query results can be displayed in tabular or gallery format and can be downloaded as print-quality high-resolution JPEG files.

Digital Archiving of the Lunar Sample Images
As the online database is being developed, the lunar sample image collection is being archived within the NASA Planetary Data System (PDS; http://pds.nasa.gov/). The PDS archives and distributes scientific data from NASA planetary missions, astronomical observations, and laboratory measurements. The PDS also periodically conducts restoration work related to past NASA missions to migrate data from outdated media or mission-specific formats to current archive media and formats. The Apollo 17 lunar sample archive structure was developed in 2012 and 2013 by both JSC ARES and NASA PDS personnel, and the final version was released by PDS in March 2013. The archives for Apollo 11 and 12 are in the final development stages and will be released over the remainder of 2013.
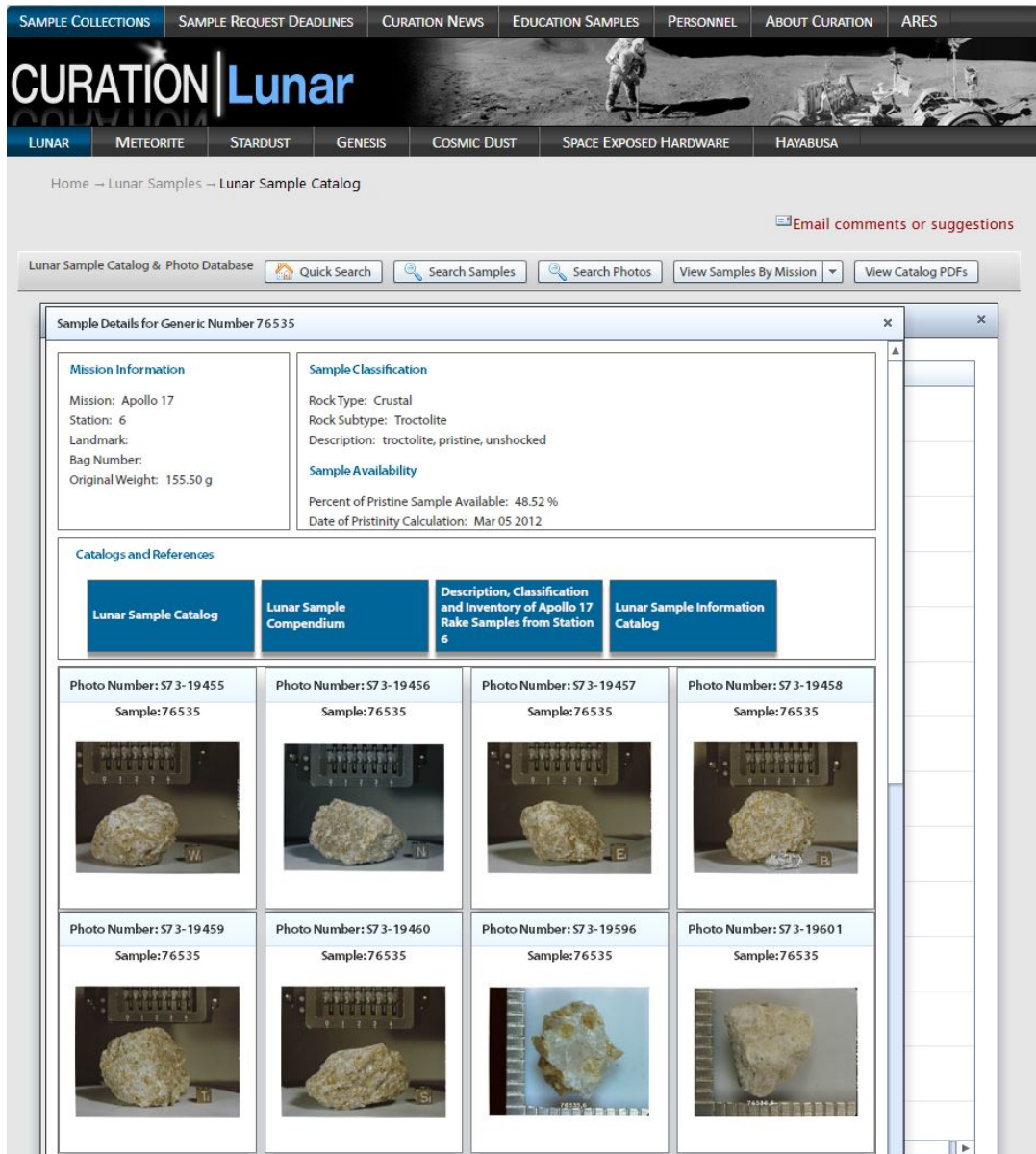
Figure 2.– Screen capture of the Lunar Sample Catalog & Photo Database interface.

For the Apollo mission archives, each sample image (a full-resolution TIFF) has a corresponding data product label. The data product label contains extensive metadata to allow ingestion into databases; query searches by sample number, mission, rock type, and descriptive mineralogical and petrographic term; and cross-mission searches by lunar landmark or collection station. Scan parameters for each image are also included in the metadata. Ancillary information provided with each mission archive includes a mission summary, references relevant to the photographs themselves (*e.g.*, film types and photographic technique), and lunar sample catalogs that correspond to the sample images.

Each archive is organized according to the geologic classification and subclassification of the samples as well as by photo type (figure 3). An Extras subdirectory contains JPEG images generated from each primary TIFF file, and a Document subdirectory contains the sample catalogs and other reference material.

Index of /Missions/Apollo/Rock_Sample_Images/A17VIS_0001 /DATA/BRECCIA

Name	Last modified	Size	Description
Parent Directory		-	
FRAGMENTAL/	27-Nov-2012 00:59	-	
IMPACT_MELT/	28-Nov-2012 22:26	-	
REGOLITH/	28-Nov-2012 22:27	-	
UNCLASSIFIED/	27-Nov-2012 01:23	-	

Figure 3.– Partial file directory for the Apollo 17 archive available from the NASA PDS (http://pdsimage.wr.usgs.gov/Missions/Apollo/Rock_Sample_Images/).

Future Plans

Film-negative scanning is expected to be complete by the end of fiscal year 2013. The remaining photos will be available in the online JSC Lunar Sample Catalog & Photo Database by spring 2014. The archives of the lunar rock sample images associated with the Apollo 14, 15, and 16 flights will be generated and delivered to the NASA PDS during the same period. Together, these efforts will preserve the unique photographic record of the original rock samples returned from the Moon and provide greater access to the images, increasing scientific use and public awareness of the Apollo missions' legacy.

Tracy A. Calhoun, Manager
http://ares.jsc.nasa.gov/ares/exploration/index.cfm

The Human Exploration Science Office supports human spaceflight, conducts research, and develops technology in the areas of space orbital debris, hypervelocity impact technology, image science and analysis, remote sensing, imagery integration, and human and robotic exploration science.

NASA's Orbital Debris Program Office (ODPO) resides in the Human Exploration Science Office. ODPO provides leadership in orbital debris research and the development of national and international space policy on orbital debris. The office is recognized internationally for its measurement and modeling of the debris environment. It takes the lead in developing technical consensus across U.S. agencies and other space agencies on debris mitigation measures to protect users of the orbital environment.

The Hypervelocity Impact Technology (HVIT) project evaluates the risks to spacecraft posed by micrometeoroid and orbital debris (MMOD). HVIT facilities at JSC and White Sands Test Facility (WSTF) use light gas guns, diagnostic tools, and high-speed imagery to quantify the response of spacecraft materials to MMOD impacts. Impact tests, with debris environment data provided by ODPO, are used by HVIT to predict risks to NASA and commercial spacecraft. HVIT directly serves NASA crew safety with MMOD risk assessments for each crewed mission and research into advanced shielding design for future missions.

The Image Science and Analysis Group (ISAG) supports the International Space Station (ISS) and commercial spaceflight through the design of imagery acquisition schemes (ground- and vehicle-based) and imagery analyses for vehicle performance assessments and mission anomaly resolution. ISAG assists the Multi-Purpose Crew Vehicle (MPCV) Program in the development of camera systems for the Orion spacecraft that will serve as data sources for flight test objectives that lead to crewed missions.

The multi-center Imagery Integration Team is led by the Human Exploration Science Office and provides expertise in the application of engineering imagery to spaceflight. The team links NASA programs and private industry with imagery capabilities developed and honed through decades of human spaceflight, including imagery integration, imaging assets, imagery data management, and photogrammetric analysis. The team is currently supporting several NASA programs, including commercial demonstration missions.

The Earth Science and Remote Sensing Team is responsible for integrating the scientific use of Earth-observation assets onboard the ISS, which consist of externally mounted sensors and crew photography capabilities. This team facilitates collaboration on remote sensing and participates in research with academic organizations and other Government agencies, not only in conjunction with ISS science, but also for planetary exploration and regional environmental/geological studies.

Human exploration science focuses on science strategies for future human exploration missions to the Moon, Mars, asteroids, and beyond. This function provides communication and coordination between the science community and mission planners. ARES scientists support the operation of robotic missions (*i.e.*, Mars Exploration Rovers and the Mars Science Laboratory), contribute to the interpretation of returned mission data, and translate robotic mission technologies and techniques to human spaceflight.

Reports on several projects are given in the following pages.

Imagery Integration Team

Tracy Calhoun, Dave Melendrez

The Human Exploration Science Office (KX) provides leadership for NASA's Imagery Integration (I^2) Team, an affiliation of experts in the use of engineering-class imagery intended to monitor the performance of launch vehicles and crewed spacecraft in flight. Typical engineering imagery assessments include studying and characterizing the liftoff and ascent debris environments; launch vehicle and propulsion element performance; in-flight activities; and entry, landing, and recovery operations. I^2 support has been provided not only for U.S. Government spaceflight (*e.g.*, Space Shuttle, Ares I-X) but also for commercial launch providers, such as Space Exploration Technologies Corporation (SpaceX) and Orbital Sciences Corporation, servicing the International Space Station.
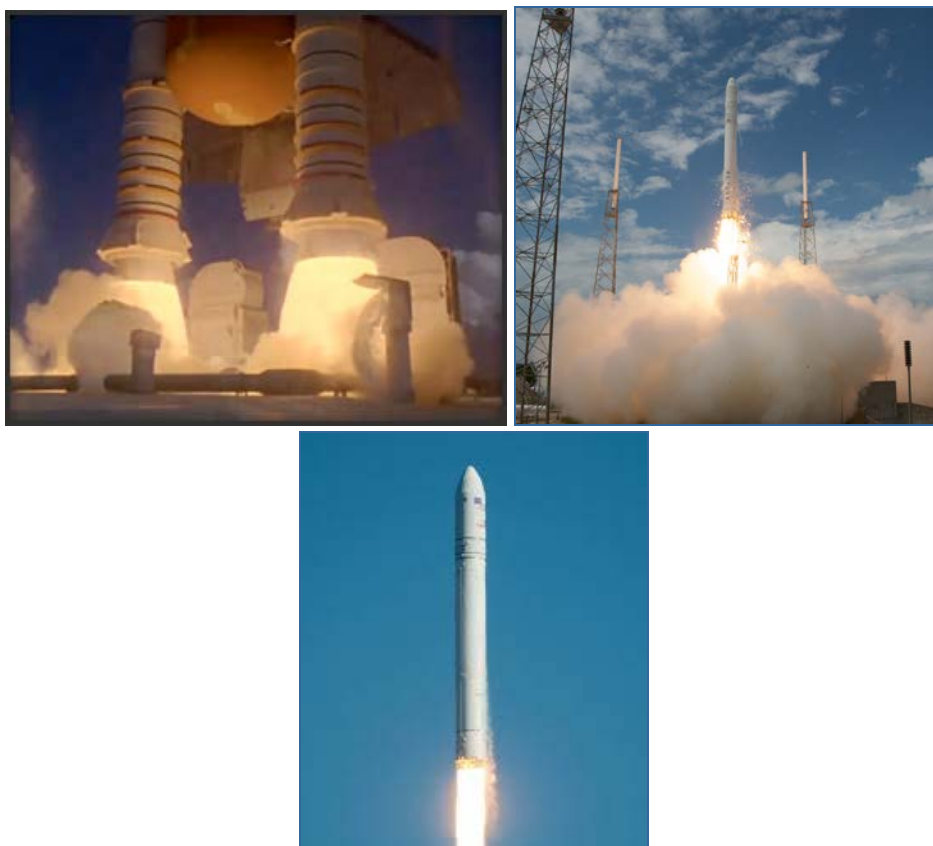
Figure 1.– Examples of launch imagery for (clockwise from top left) the Space Shuttle, SpaceX Falcon 9, and Orbital Antares.

The NASA I^2 Team is composed of imagery integration specialists from JSC, the Marshall Space Flight Center (MSFC), and the Kennedy Space Center (KSC), who have access to a vast pool of experience and capabilities related to program integration, deployment and management of imagery assets, imagery data management, and photogrammetric analysis. The I^2 team is currently providing

integration services to commercial demonstration flights, Exploration Flight Test-1 (EFT-1), and the Space Launch System (SLS)–based Exploration Missions (EM)-1 and EM-2. EM-2 will be the first attempt to fly a piloted mission with the Orion spacecraft.
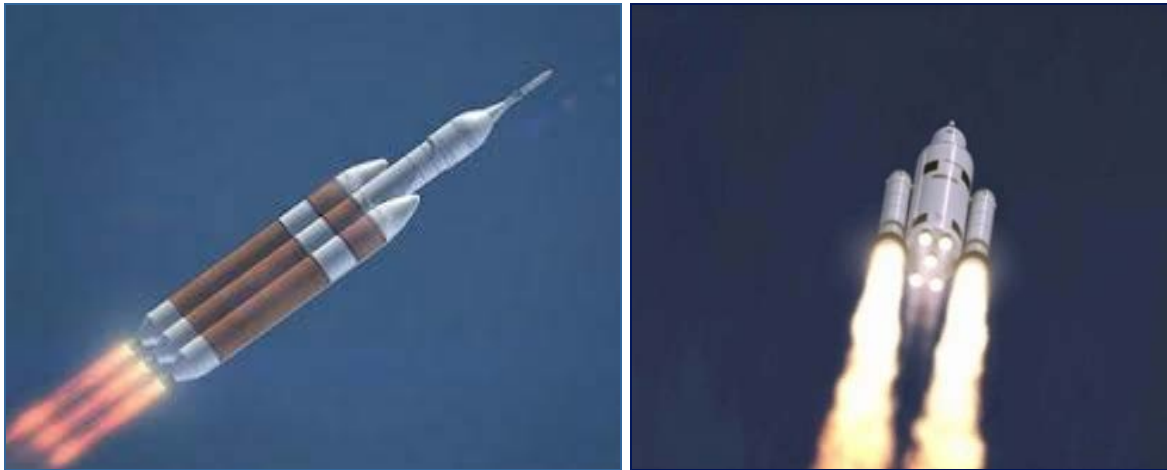
Figure 2.– (Left to right) Notional views of the EFT-1 launch vehicle and SLS.

The I^2 Team provides the customer (both commercial and Government) with access to a wide array of imagery options – ground-based, airborne, seaborne, or vehicle-based – that are available through the Government and commercial vendors. The team guides the customer in assembling the appropriate complement of imagery acquisition assets at the customer's facilities, minimizing costs associated with market research and the risk of purchasing inadequate assets. The NASA I^2 capability simplifies the process of securing one-of-a-kind imagery assets and skill sets, such as ground-based fixed and tracking cameras, crew-in the-loop imaging applications, and the integration of custom or commercial-off-the-shelf sensors onboard spacecraft.

*Figure 3.– (Left) Tracking cameras monitor ascent performance and separation events.
(Right) The Ares 1-X test launch in October 2009.*

For spaceflight applications, the I^2 Team leverages modeling, analytical, and scientific resources along with decades of experience and lessons learned to assist the customer in optimizing engineering imagery acquisition and management schemes for any phase of flight – launch, ascent, on-orbit, descent, and landing.
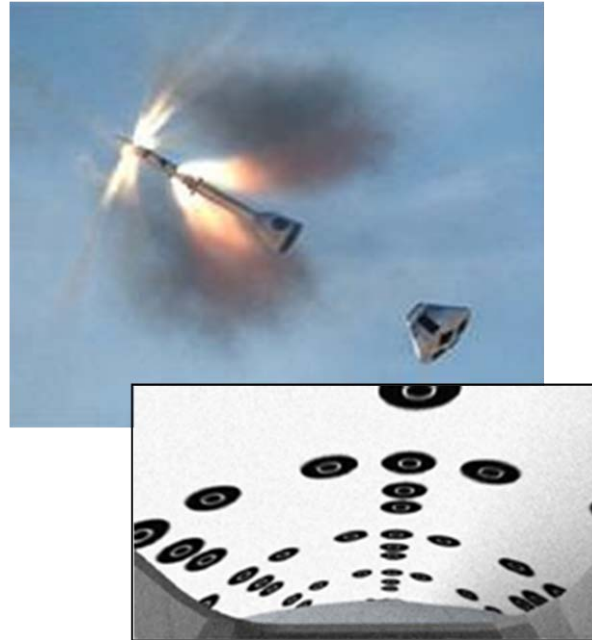
Figure 4.– Modeling of separation event to evaluate the locations of photogrammetric targets.

The I^2 Team guides the customer in using NASA's world-class imagery analysis teams, which specialize in overcoming inherent challenges associated with spaceflight imagery sets. Precision motion tracking, two-dimensional (2D) and three-dimensional (3D) photogrammetry, image stabilization, 3D modeling of imagery data, lighting assessment, and vehicle fiducial marking assessments are available.
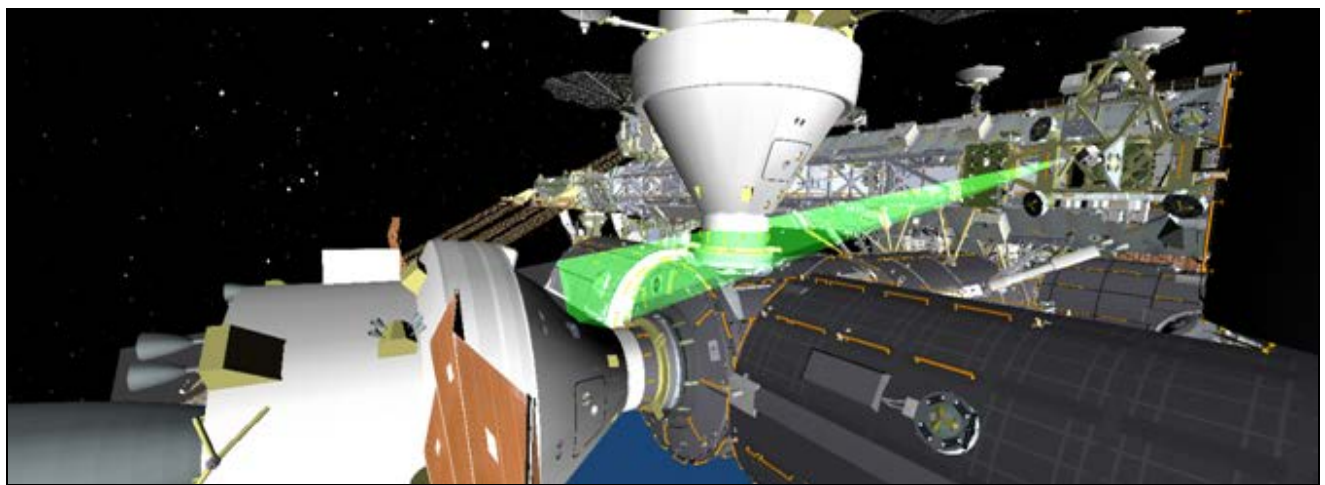
Figure 5.– Modeling of spacecraft on-orbit inspections prior to entry.

During a mission or test, the I^2 Team provides oversight of imagery operations to verify fulfillment of imagery requirements. The team oversees the collection, screening, and analysis of imagery to build a set of imagery findings. It integrates and corroborates the imagery findings with other mission data sets, generating executive summaries to support time-critical mission decisions.
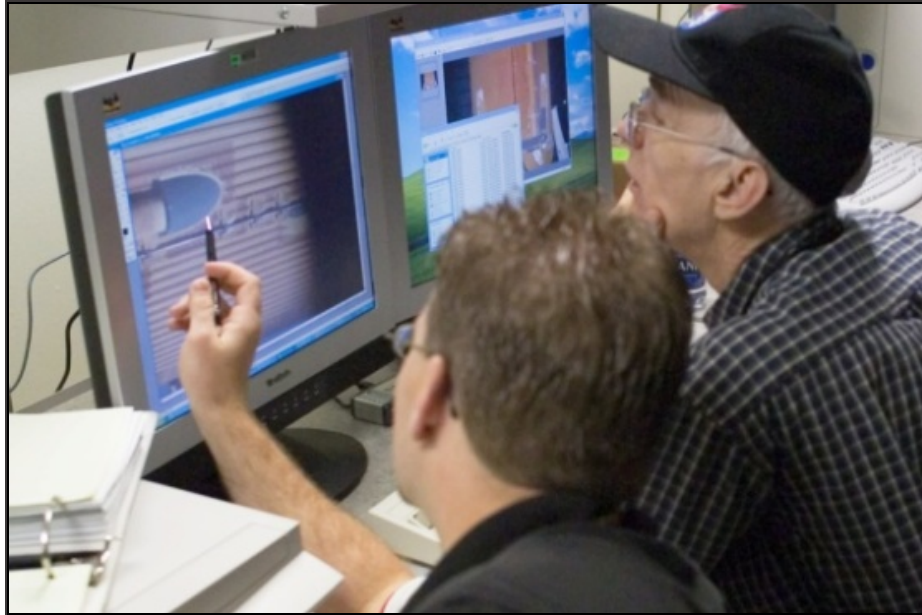
Figure 6.– Screening and analysis.

Advancements in Capsule Parachute Analysis

David Bretz

The Image Science and Analysis Group (ISAG), a subgroup within the ARES Directorate, has provided image analysis support of the Capsule Parachute Assembly System (CPAS) testing being conducted at the Yuma Proving Grounds by JSC Engineering. The work being done by ISAG is a continuation of photogrammetric analysis that began in 2010, which is expected to extend through 2014 with the development and analysis of parachutes for the Multi-Purpose Crew Vehicle (MPCV) being developed at JSC.

At the request of the engineers, ISAG developed methods for converting video imagery into parachute flight performance parameters, such as fly-out angles, parachute skirt diameters, and drogue mortar deployment speeds. This information (along with many other parameters measured with a variety of instruments) is used by engineers to understand and accurately model parachute behavior, drag coefficient, and rate of descent. Good models will improve the fidelity of MPCV simulations of roll control and splashdown impacts.

In the last 2 years, the tests have evolved to use more realistic drop test vehicles, such as the Parachute Compartment Drop Test Vehicle (PCDTV), which has a realistic parachute compartment but a long body and dart-shaped nose, and the Parachute Test Vehicle (PTV), which has a capsule shape to mimic the dynamics of the true MPCV (figure 1).

Figure 1.– (Left to Right) Images showing the PCDTV and the PTV.

The cameras installed on these vehicles have been upgraded from early testing and have expanded the role of photogrammetry. They now provide 60 frames per second (progressive) high-definition quality (1280 x 720 pixel) imagery of the main parachute during all phases of activity as well as 300 frames per second high-speed imagery of very dynamic events, such as the drogue mortar deployment, drogue inflation, main parachute deployment, and main parachute reefing stages. Characterization of the optical properties of these cameras, such as focal length and lens distortions, and the fine-tuning of the exposure settings have been important aspects of ISAG support during this period.

The methods of photogrammetric analysis have also evolved in technique and in the variety of investigations. Determination of the fly-out angles (angle between parachute center and centroid of the parachute cluster) and the main parachute skirt diameters has improved. Previous methods used features at the top of the canopy to provide direct scaling of image features, and while these methods corrected for lens distortion, they did not account for image distortions caused by the change in perspective as the parachutes fly out from the center of the cluster, tilting to the side in the wide field of view. A new method was developed to account for this wide perspective. The method, which requires no additional camera, assumes the parachutes move on the surface of a sphere of constant radius surrounding the camera because they are tethered to the vehicle (figure 2). The points on the video image that track the edge of the parachute are used to define vectors in space that intersect this sphere. This allows the points on the actual skirt to be located in 3D space relative to the camera, and these points can then be analyzed to determine the inlet area and diameter of each parachute canopy over time (figure 3).
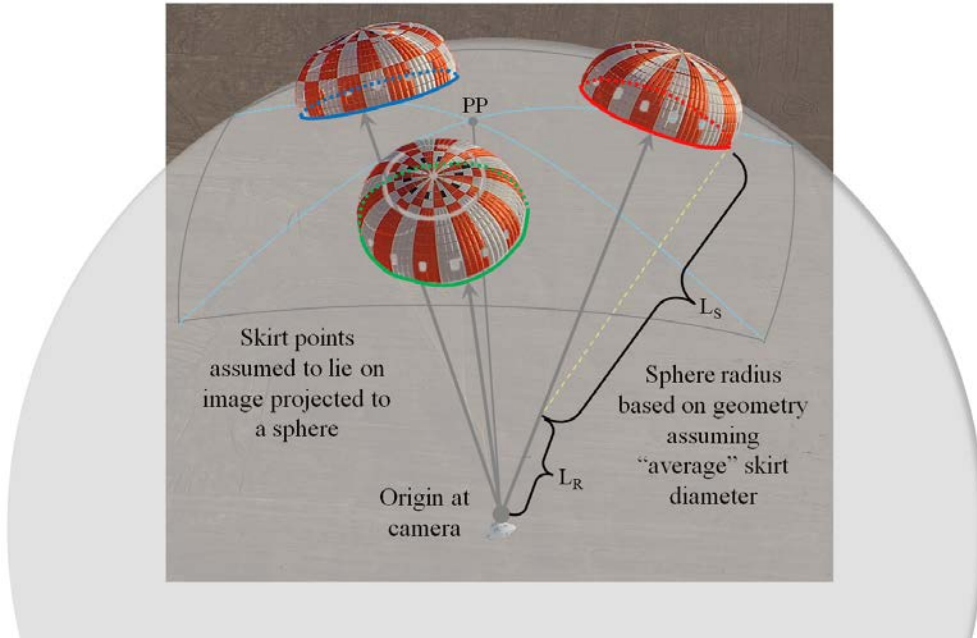
Figure 2.– Diagram illustrating how points on the main parachute skirts can be assumed to lie on the surface of a sphere centered on the vehicle. L_R and L_S are the lengths of the parachute riser line and suspension lines, respectively, which define the radius of the sphere when an average skirt diameter is assumed.
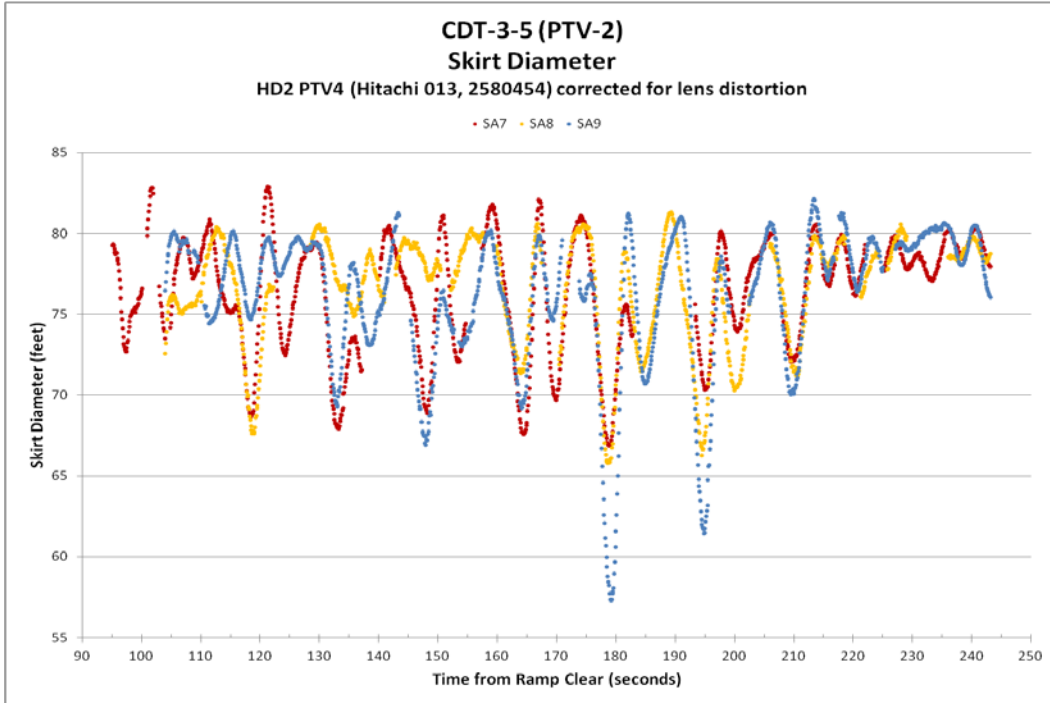
Figure 3.– Parachute diameters versus time for Cluster Development Test 3-5 (CDT-3-5).

A high-speed camera with a view of one of the two drogue mortars on each test has allowed measurement of the velocity of the drogue mortar as it exits and travels away from the camera. Figure 4 shows the early moments in the deploy sequence. The deployment bag containing the parachute is fixed to a rigid and circular mortar lid at the front. (A circular shaped sabot attached to the back of the bag falls away soon after ejection.) Points on the front lid are tracked, and the apparent diameter of the lid is calculated. Knowing the diameter of the lid and the camera's focal length allows the distance to the deployment bag to be calculated. The measurement method was verified by recording and analyzing similar images during a ground test at General Dynamics in early 2012. Figure 5 shows the mortar speeds measured for five tests.
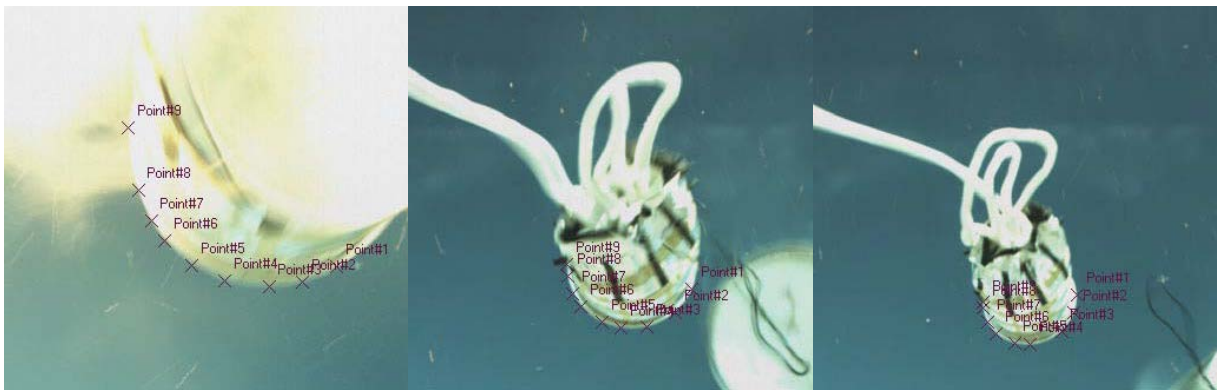
Figure 4.– High-speed camera images showing drogue mortar deployment on CDT-3-1. The rigid lid affixed to the front of the drogue deployment bag is used to measure distance while the sabot (back-facing lid) comes free and falls to the right.

Drop Test	Vehicle	Mortar Speed (feet/sec)	Distance Range for Speed Calculation (feet)
CDT-3-1	PCDTV	140	7-28
CDT-3-2	PCDTV	148	2.5-24
CDT-3-3	PTV	123	2.5-27
CDT-3-4	PCDTV	144	7-93
CDT-3-5	PTV	140	2.5-32

Figure 5.– Mortar speeds calculated using high-speed imagery recorded during drogue parachute deployment.

Current and future parachute tests (through 2014) will involve an analysis of parachute fly-out angles and diameters. Additional analysis of the dynamics of the main parachute bag deployment also will be performed.

Solving Problems Caused by Small Micrometeoroid and Orbital Debris Impacts for Space-Walking Astronauts

E. L. Christiansen, D. M. Lear

The external handrails used by the International Space Station (ISS) crew during extravehicular activity (EVA) are exposed to MMOD impacts that cause craters with raised edges, called "crater lips" (figure 1). These crater lips are often very sharp and represent an EVA cut-glove hazard. There have been several cases of craters reported to the ISS handrail team. For instance, the ARES HVIT group identified six craters on a single 13.7-in.-long handrail from an ISS pump module (PM) returned on the last Space Shuttle mission, STS-135. This PM handrail was exposed to MMOD impacts for 8.7 years. The largest crater on the PM handrail measured 1.85-mm diameter (outside) with a 0.33-mm lip height (figure 2). The size of the other five craters ranged from 0.12 mm to 0.56 mm in diameter, with crater lips that ranged from 0.01 mm to 0.08 mm high. Other MMOD craters have been observed on ISS handrails and EVA tools (figure 3).
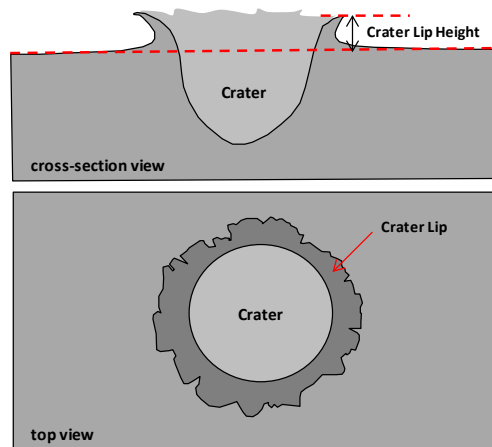
Figure 1.– MMOD impact craters into metals typically exhibit raised sharp-edged "crater lips."

If the crater lips from hypervelocity impacts are large enough, they can tear or cut into the materials used in the EVA gloves. Crater lip heights of 0.01 in. (0.25 mm) were found to be sufficient to cut EVA glove materials in ground experiments coordinated by the NASA EVA engineering community. These experiments were performed after there were several incidents of cut gloves reported on EVAs during STS-109, STS-110, STS-116, STS-118, STS-120, STS-125, and other missions. Some of these glove cuts were large enough to result in early termination of the EVA. For instance, on STS-118, during a routine glove inspection, one of the EVA crew members noticed a possible tear on the thumb of his left glove. To be safe, EVA managers decided to end the spacewalk after about 5.5 hours, and examination and photography of the glove performed during suit removal revealed the extent of the glove tear (figure 4). A similar incident occurred during the third EVA of STS-120. MMOD craters are not the only possible cause of this glove damage, but are one of the leading possible causes.

Locations of 4 of the 6 impacts on the hand rail removed from the PMIA are indicated by blue tape.
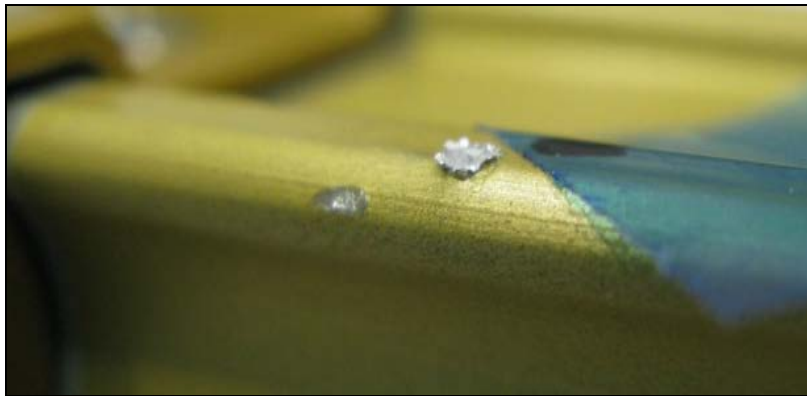
Figure 2.– The JSC HVIT group found six craters on one handrail removed
from the ISS Pump Module Integrated Assembly (PMIA) and returned
on STS-135. The largest crater found on the PMIA handrail (#38 in overview)
was 1.85-mm in diameter with 0.33-mm-high crater lips.

Detached Spall
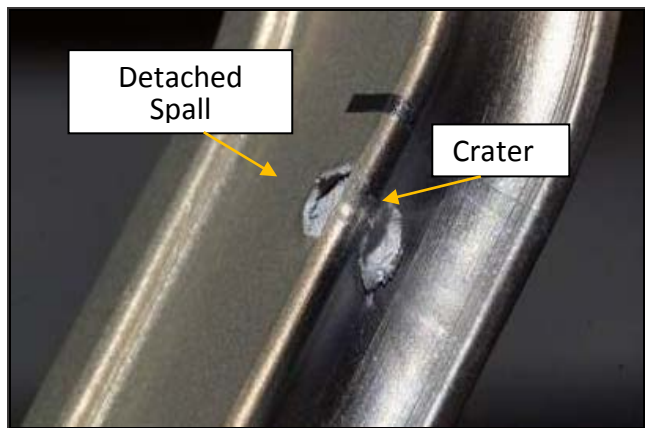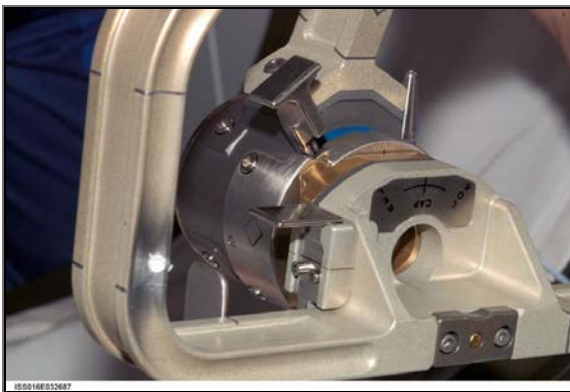
Crater

Figure 3.– Prior to STS-123 EVA, the ISS crew found a nearly 5-mm diameter crater on the
EVA D-handle tool stored externally on ISS. Note that the detached spall from the side
opposite the MMOD impact crater also has sharp edges. The D-handle is made of materials that
are similar to those used in a typical ISS dog-bone handrail.

Figure 4.– Damage to the left glove of one of the EVA crew after STS-118 EVA #3.

The ARES Directorate's HVIT group in the Human Exploration Science Office and the Engineering Directorate's Crew and Thermal Systems Division, under the leadership of the EVA Project Office, worked together from 2008 to 2012 to assess the risk of cut gloves from MMOD craters on handrails and develop methods to identify and repair craters on handrails. The HVIT provided assessments of the frequency of craters with lip heights that could result in glove damage and worked with White Sands Test Facility (WSTF) to provide samples of realistic hypervelocity impact damage to handrails to help support development of the tools and procedures used to find and repair damage to handrails. HVIT-WSTF impact tests of handrails in 2011 and 2012 were used to provide samples of impact damage that were used to certify handrail covers that EVA crew fit over impact damage discovered on orbit; the covers prevent gloves from being torn by the MMOD craters. This effort culminated in several changes to EVA hardware and procedures that minimize the risk that sharp edges will the EVA gloves, including the following:

1. Toughening the gloves by adding additional materials to areas that are sensitive to cuts.

2. Monitoring the status of MMOD impacts on the handrails via photographs and maintaining a database of potential sharp edges on handrails, referred to as the ISS Imagery Inspection Management System (IIIMS), for EVA planning purposes. HVIT and Image Science and Analysis Laboratory personnel jointly review photographs of ISS handrails and other surfaces to identify MMOD damage that is documented in the IIIMS database and used to inform EVA crews of potential sharp edges during EVA planning. Currently, the IIIMS contains more than 200 records of MMOD impacts to handrails and other areas that could be contacted during EVA.

3. Developing EVA procedures and tools to detect and repair or cover sharp edges from MMOD impacts on handrails.

Since the above changes were incorporated into EVA hardware and procedures, the incidents of cut gloves have been greatly reduced.

Toughened Thermal Blankets for Micrometeoroid and Orbital Debris Protection

Eric Christiansen, Dana Lear

Thermal blankets are used extensively on spacecraft to provide thermal protection from temperature extremes encountered in space. Typical thermal blankets are relatively thin (1/4-in. to 1/2-in. thick) and provide effective thermal protection, but they can provide only minimal protection from hypervelocity MMOD particles. As a consequence, MMOD shielding is often necessary to supplement the protection provided by thermal blankets alone to meet MMOD protection requirements. Because thermal blankets and MMOD shielding share similar physical space on the outside hull of a spacecraft, an integrated hardware design that performs as a thermal blanket and MMOD shield could yield numerous benefits, such as reduced mass and cost.

The JSC ARES Directorate's HVIT group and the Engineering Directorate's Structural Engineering Division worked together in 2011 and 2012 to integrate MMOD protection with standard thermal blankets (figure 1). These MMOD toughened thermal blankets incorporate one or more layers of materials near the exterior of the blanket that are effective at breaking up MMOD particles; other layers deeper in the blanket that resist fragment penetration; and low-mass, open-cell foam materials that separate the layers and improve MMOD protection. Typical materials used to enhance the MMOD protection of thermal blankets include fiberglass cloth, ceramic fabrics, and high-strength flexible materials. Hypervelocity impact tests were performed at White Sands Test Facility (WSTF) to demonstrate the effectiveness of the toughened blankets (figure 2), which can stop MMOD particles that are 5-mm to 6-mm in diameter, as opposed to the standard thermal blanket, which is completely penetrated by submillimeter-diameter MMOD particles (typically on order 0.5 mm). This translates roughly into a factor of 1000x decrease in MMOD risk of thermal blanket penetration and damage to underlying equipment. The means to determine the location, depth, and extent of MMOD impact damage is obtained by adding impact detection sensors at one or more locations within the blanket (figure 3). The toughened thermal blankets were tested in thermal-vacuum chambers at JSC (figure 4) to prove that the materials integrated into the thermal blanket to improve MMOD protection did not adversely affect the thermal performance of the blankets.

The toughened thermal blankets have application in a number of areas on the ISS and commercial spacecraft. For instance, the blankets are being considered for use in protecting the metal bulkheads of an inflatable module from MMOD impacts.

Figure 1.– Toughened thermal blankets.

Figure 2.– Hypervelocity impact tests were performed to demonstrate the effectiveness of the toughened thermal blankets.
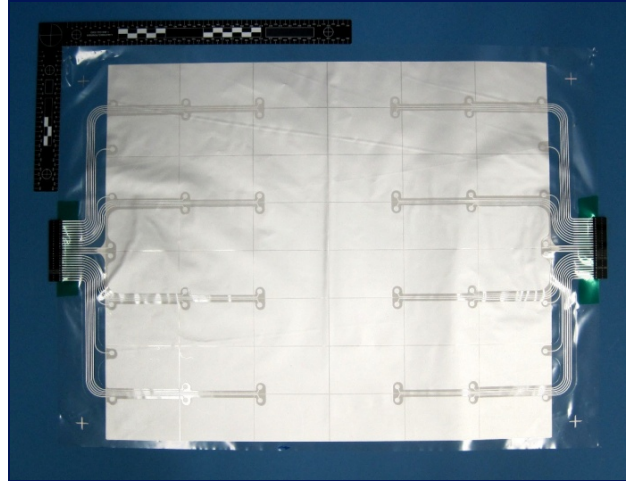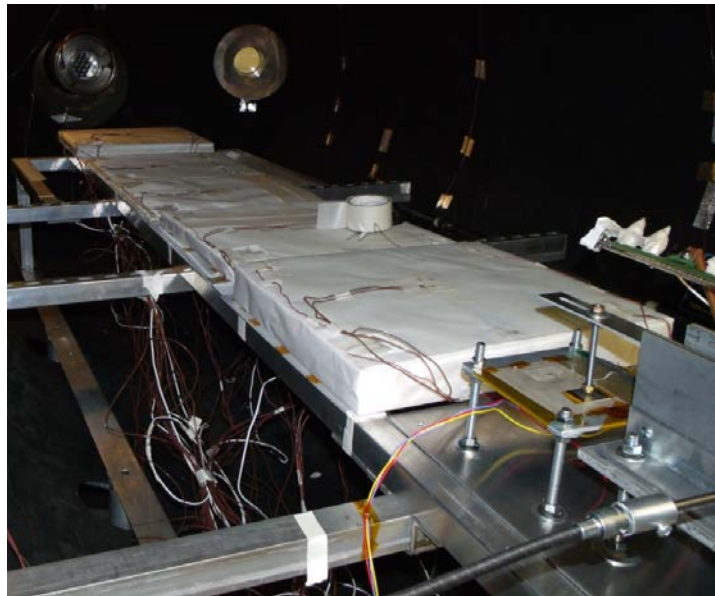
Figure 3.– Impact sensor film.

Figure 4.– Thermal-vacuum tests of toughened thermal blankets.

Shell-NASA Vibration-Based Damage Characterization

John Michael Rollins

Introduction

This article describes collaborative research between Shell International Exploration and Production (IE&P) scientists and ISAG personnel to investigate the feasibility of ultrasonic-based characterization of spacecraft tile damage for in-space inspection applications. The approach was proposed by Shell personnel in a Shell-NASA "speed-matching" session in early 2011 after ISAG personnel described challenges inherent in the inspection of MMOD damage deep within spacecraft thermal protection system (TPS) tiles. The approach leveraged Shell's relevant sensor and analytical expertise. The research addressed the difficulties associated with producing 3D models of MMOD damage cavities under the surface of a TPS tile, given that simple image-based sensing is constrained by line of sight through entry holes that have diameters considerably smaller than the underlying damage cavities. Damage cavity characterization is needed as part of a vehicle inspection and risk reduction capability for long-duration, human-flown space missions. It was hoped that cavity characterization could be accomplished through the use of ultrasonic techniques that allow for signal penetration through solid material.

Basic Approach

The project was originally planned to require up to three tests – the acquisition test, in which the basic ability to transmit an ultrasonic signal through the TPS material of interest (and acquire a response) was examined, and one or two imaging tests to convert signal response into a 3D model of the TPS cavity being studied. The imaging tests would be conducted only if the acquisition test showed that an adequate ultrasonic signal could be detected after traveling through the tile material. As it turned out, the acquisition test and following analysis showed that the acoustic transmissivity through TPS material was too poor to pursue the method into the imaging tests. The process of test planning through final report generation took place between January and December 2012, and the project is considered complete with respect to ISAG participation.

Acquisition Test

The acquisition test was performed at JSC. Shell designed the tests; provided test articles of interest, transducers, and a submersion pool for one of its test articles; and sponsored the sensing (*i.e.*, vibrometer) resources. NASA and its contractors provided the tiles, the test work area, signal-generation equipment, the lifting apparatus, drainage, and safety and technician support.

Test Implementation

Each trial consisted of attaching an ultrasonic transducer near or onto one surface of a test article and reading the response with the laser vibrometer. The test data was collected by Polytec vibrometer analysts (using their equipment) and analyzed by the project lead scientist from Shell, who had designed the test procedure.
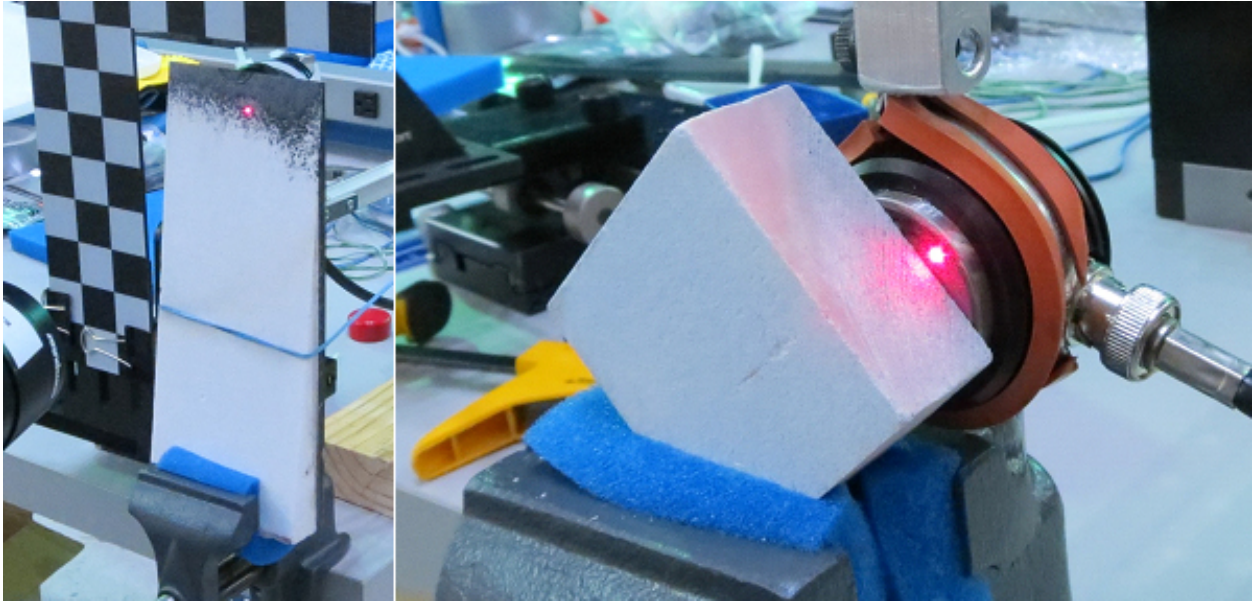
Figure 1.– (Left to right) Tile wedge and low-density tile slab with a vibrometer laser spot hitting the transducer.

Test Results

For through-transmission testing with the tile wedge, extremely large attenuation (1000x amplitude damping per inch of thickness) was observed in comparing ultrasonic excitation with response amplitudes (after propagation through tile material). Given these results, ISAG has no further plans to pursue such a method for spacecraft damage characterization. Results were more promising for at least one test article from Shell, and Shell may pursue such analysis further.
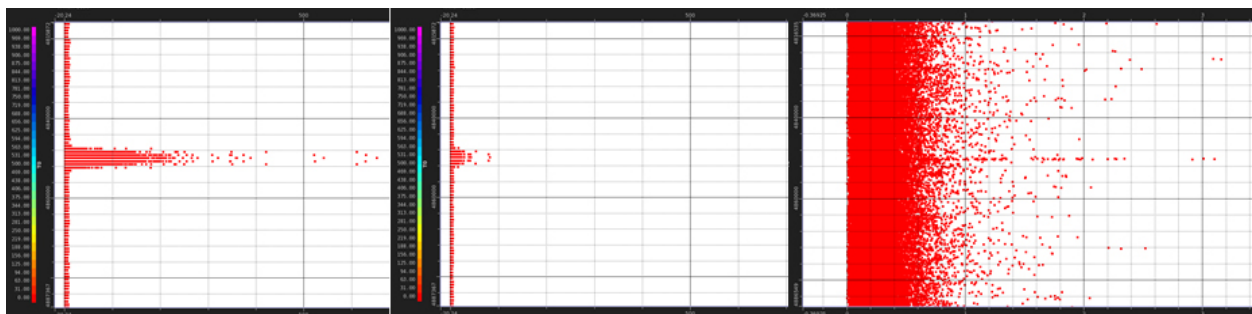
Figure 2.– Plots showing the relative amplitude of an ultrasonic signal propagating through the tile wedge, after transmission through (left to right) 0.16-in., 0.40-in., and 0.87-in. of thickness, respectively. Note that the amplitude is practically in the noise for a signal traveling through less than an inch of tile. Courtesy of Shell IE&P.

Orbital Debris Mitigation Requirements and the GRAIL Spacecraft

Nicholas Johnson and Gene Stansbery

NASA's Orbital Debris Program Office, which is part of the ARES Directorate at JSC, has been instrumental in reducing the growth of orbital debris in Earth orbits through research and development of orbital debris mitigation requirements. It has now begun a new era in which lunar orbits are also protected.

Although NASA's original orbital debris mitigation policies and safety standard during the 1990s did not address orbits beyond the Earth, NPR 8715.6, NASA Procedural Requirements for Limiting Orbital Debris, issued in 2007, for the first time addressed objects in orbits about the Moon. NPR 8715.6A, issued in 2009, states that NASA program and project managers "shall not plan to leave objects in lunar orbit unless a documented need is stated in the ODAR" (Orbital Debris Assessment Report).

Two NASA Gravity Recovery and Interior Laboratory (GRAIL) spacecraft completed their year-long mission in orbit about the Moon December 17, 2012, when they were sent to make a controlled impact into a lunar mountain. This disposal action was in compliance with recommendations in NPR 8715.6A that were designed to protect historic and scientifically valuable lunar surface sites.[1]

Affectionately known as Ebb and Flow (figure 1), the two 200-kg dry mass spacecraft entered lunar orbit on New Year's Eve 2011 and New Year's Day 2012, respectively, and worked primarily from a 55-km altitude science orbit. As their reservoirs of hydrazine propellant dwindled, plans were made to target their crash onto the lunar surface rather than let them fall randomly.

Figure 1.– Artist's view of the two GRAIL satellites flying in close formation in lunar orbit.

For the disposal of the two GRAIL spacecraft, a trajectory was selected to carry the spacecraft toward an unnamed lunar mountain near the north pole (figures 2 and 3). The final resting place for the two GRAIL spacecraft has been named for the late Sally Ride, the first U.S. woman in space and a proponent of the Moon KAM (Moon Knowledge Acquired by Middle School Students) cameras carried by the GRAIL spacecraft.

Figure 2.– The final ground track of the two GRAIL spacecraft.

Figure 3.– The two GRAIL spacecraft struck the lunar surface just 30 seconds apart at a speed of nearly 2 km per second.
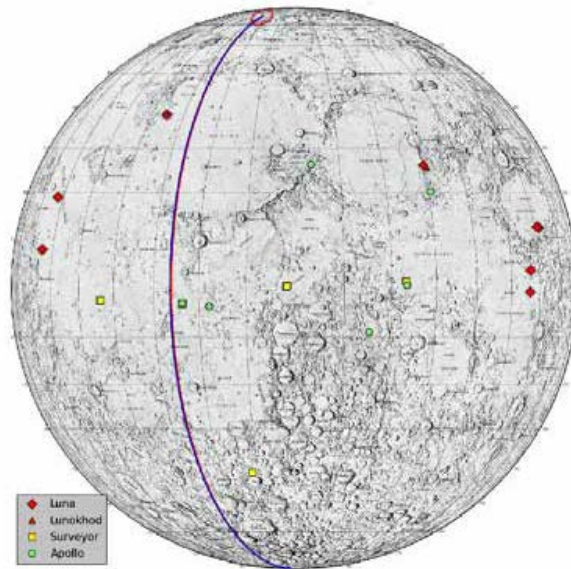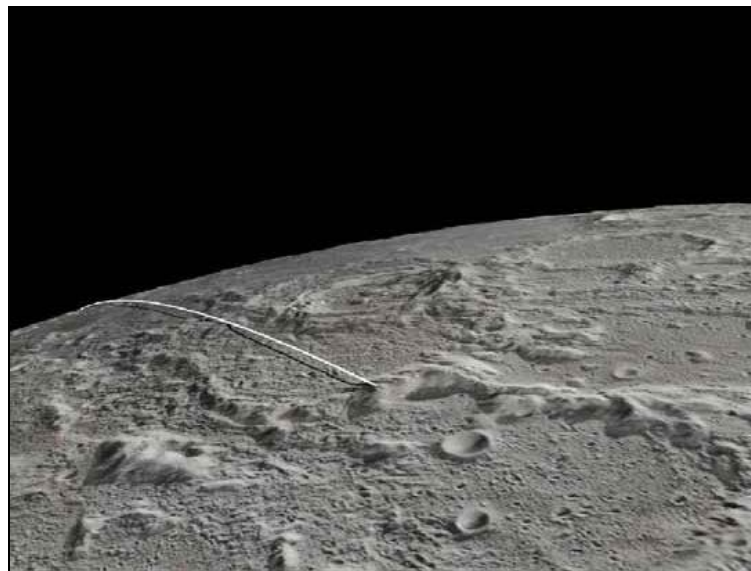
1. NASA Procedural Requirements for Limiting Orbital Debris, NPR 8715.6A, May 14, 2009, Section 3.3.3.

Origin of the Inter-Agency Space Debris Coordination Committee

Nicholas Johnson

The Inter-Agency Space Debris Coordination Committee (IADC) is recognized as the preeminent international technical organization for all issues associated with orbital debris. This august body now comprises 12 member agencies representing 11 nations and the regional European Space Agency (ESA). October 2012 marked the 25th anniversary of the first ESA-NASA orbital debris coordination meeting, which would evolve into the IADC, and the 20th anniversary of the proposal to establish a formal, multinational group of orbital debris experts.

Good things often arise from unfortunate events, and the IADC is a case in point. On November 26, 1986, an Ariane 1 second stage spontaneously exploded in low Earth orbit, creating the largest orbital debris cloud to that date. A total of 492 large pieces of debris were eventually cataloged from the fragmentation, although, fortunately, only 32 remain in orbit today. This significant space event led NASA's Orbital Debris Program Office to host an international conference on the breakup of launch vehicle upper stages the following May and led ESA to establish the Space Debris Working Group.

Following the successful conference, NASA and ESA decided to hold a bilateral orbital debris coordination meeting in Rolleboise, France, in October 1987, "to discuss the various aspects of space debris, exchange opinions, present study results and agree on contact points for policy, management, and technical experts." Due to the considerable number and breadth of topics of mutual interest, a decision was made to hold a second meeting the following year, which in turn led to additional meetings at roughly annual intervals.

In early 1989, a U.S. Government interagency report on orbital debris recommended that "the U.S. should inform other space-faring nations about the conclusions of this report and seek to evaluate the level of understanding and concern of other nations and relevant international organizations about orbital debris issues. Where appropriate, the U.S. should enter into discussions with other nations to coordinate debris minimization policies and practices." Consequently, by the end of 1989 NASA orbital debris experts had visited both the Soviet Union and Japan and established separate orbital debris working groups with the two nations.

Thus, in 1990 NASA was supporting three distinct, but very similar, bilateral orbital debris coordination meetings. This inefficient situation began to take a toll on NASA orbital debris experts in terms of time, travel, and expense. A consolidation of these efforts was the logical next step. At the sixth meeting of the ESA-NASA orbital debris coordination committee in April 1991, Japan was invited to be an active participant. Beginning with the next gathering in February 1992, the forum was officially renamed the ESA-Japan-NASA orbital debris coordination committee, but the original ESA-NASA numbering system was retained, making this the seventh official meeting. A few days after this meeting, which took place in the Netherlands, NASA orbital debris specialists extended

their journey to Moscow to meet with their Russian counterparts for the next meeting of the U.S.-USSR orbital debris coordination committee.

By the eighth meeting of the ESA-Japan-NASA committee, which was held at JSC in Houston, Texas, in October 1992, the need for a more formal and possibly more inclusive organization was apparent. A straw-man Terms of Reference for the new committee was circulated for review and comment. The scope of the proposed committee's activities was to "(1) review all ongoing cooperative debris research activities between member organizations, (2) identify, evaluate, and approve new opportunities for cooperation, and (3) serve as the primary means for exchanging information and plans concerning orbital debris research activities."

The ninth meeting of the committee, hosted by ESA at the European Space Operations Center (ESOC) at Darmstadt, Germany, in April 1993, was the first to include all four of the founding members of the IADC, although a new name for the committee had yet to be chosen. At this meeting, the concept of establishing a steering group and four working groups (measurements, environment and database, testing and shielding, and mitigation) was adopted. Each future meeting would be divided into opening and closing plenary sessions with concurrent splinter meetings of the steering group and the four working groups in between.

The name of the Inter-Agency Space Debris Coordination Committee was officially adopted in Moscow in October 1993. Here, the first formal IADC Terms of Reference was signed by the heads of the four delegations: K. Debatin for ESA, S. Toda for Japan, G. Levin for NASA, and A. Krasnov for the Russian Space Agency (RKA). Although much expanded, the current IADC Terms of Reference retains many elements of the original framework document.

The IADC grew rapidly with the addition of the space agencies of China (CNSA) in 1995; France (CNES), India (ISRO), and the United Kingdom (then BNSC, now UKSA) in 1996; Germany (then DARA, now DLR) in 1997; Italy (ASI) in 1998; the Ukraine (then NSAU, now SSAU) in 2000; and Canada (CSA) in 2010. The 12-member committee now holds its annual 4-day meeting each spring with more than 100 orbital debris specialists attending. The Steering Group, composed primarily of the heads of each member agency delegation, also meets for 1 day each fall on the sidelines of the International Astronautical Congress.

The many achievements of the IADC include the publication of the first international set of space debris mitigation guidelines, the establishment of a data exchange network for the uncontrolled reentry of satellites posing elevated risks to people and property on Earth, organized campaigns for observation of untracked debris in both low- and high-altitude orbits, and a manual on the design and effectiveness of shielding to protect spacecraft from space debris. Although it is not part of the United Nations (UN), since 1997 the IADC has normally provided a special technical presentation before the annual meeting of the Scientific and Technical Subcommittee of the UN Committee on the Peaceful Uses of Outer Space (COPUOS). The IADC space debris mitigation guidelines were used as the foundation for the development of the UN COPUOS space debris mitigation guidelines.

Additional information about the IADC and its activities can be found at www.iadc-online.org.

Effectiveness of Satellite Postmission Disposal To Limit Orbital Debris Population Growth in Low Earth Orbit

J.-C. Liou

Orbital debris mitigation measures have been developed to reduce the growth of the debris population. A major component in debris mitigation is postmission disposal (PMD). The key PMD element for low Earth orbit (LEO – the region below 2000-km altitude) satellites is the 25-year rule. It is intended to limit the long-term presence of rocket bodies (R/Bs) and spacecraft (S/C) as well as mission-related debris in the environment. The effectiveness of PMD has been demonstrated and documented since mitigation measures were developed in the 1990s. This article provides an update, based on the current environment, using the NASA orbital debris evolutionary model – LEGEND (Low Earth orbit-to-Geosynchronous orbit ENvironment Debris model). This model was developed by the NASA Orbital Debris Program Office at JSC, and the PMD study was completed in 2012.

The study focused on the ≥10 cm population in LEO. The historical simulation spanned the years 1957 through 2011 and followed the recorded launches and known breakup events. The simulation was projected 200 years into the future, with launch traffic from a span of 8 years, 2004–2011, repeated during the projection period. An 8-year mission lifetime was assumed for future S/C. No station-keeping or collision-avoidance maneuvers were implemented, and only objects 10 cm and larger were included in collision consideration. Additionally, no explosions were allowed for R/Bs and S/C launched after 2011. The 25-year PMD rule compliance rates were set at 0 percent, 10 percent, 50 percent, 75 percent, and 95 percent, respectively, for the five study scenarios.

Figure 1 shows the effective numbers of objects in LEO, including both the historical and the five future projections. Each projection curve is the average of 100 Monte Carlo (MC) LEGEND runs. As expected, the 0-percent PMD projection follows a rapid and nonlinear increase in the next 200 years. With 50-percent compliance with the 25-year rule, the population growth is reduced by approximately half. However, even with 95-percent compliance with the 25-year rule, the LEO debris population will increase by an average of more than 50 percent in 200 years.

The projected collision activities are shown in figure 2 and summarized in figure 3. A catastrophic collision occurs when the ratio of impact energy to target mass exceeds 40 J/g. The outcome of a catastrophic collision is the total fragmentation of the target, whereas a noncatastrophic collision results only in damage to the target and the generation of a small amount of debris. Even with 95 percent compliance with the 25-year rule, on average, 26 catastrophic and 19 noncatastrophic collisions are expected in the next 200 years.

Predicting the future debris environment is very difficult. The results are always sensitive to key assumptions adopted by the model, including the future launches and solar activity. Nevertheless, one can make reasonable assumptions, define nominal scenarios, and then draw conclusions from the average results for effective environment management. This updated study again illustrates the effectiveness of orbital debris mitigation. It is the first and the most cost-effective defense against future population growth. On the other hand, the study results also show that even with no future explosion and global 95-percent compliance with the 25-year rule, the LEO debris population is expected to increase slowly during the next 200 years. To stabilize the future debris population and reduce collision activities in LEO, more aggressive measures, such as active debris removal, should be considered by the international community.

LEGEND Simulations (averages of 100 Monte Carlo runs per scenario)

Legend:
- Reg launches + 0% PMD
- Reg launches + 10% PMD
- Reg launches + 50% PMD
- Reg launches + 75% PMD
- Reg launches + 95% PMD

X-axis: Year (1950 to 2210)
Y-axis: Effective Number of Objects (>10 cm) in LEO (0 to 60,000)
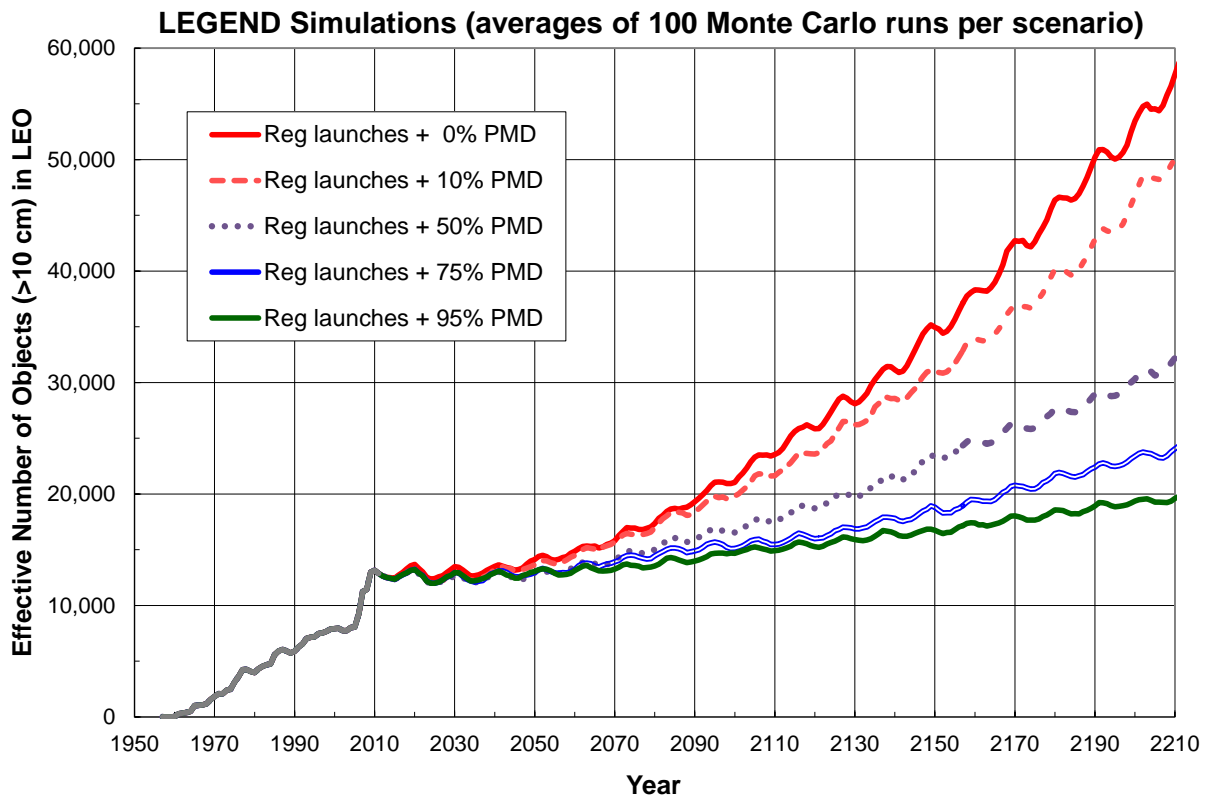
Figure 1.– Effective numbers of the 10-cm and larger objects in LEO. The effective number is defined as the fractional time, per orbital period, an object spends below 2000-km altitude. The simulations assumed no explosions for S/C and R/Bs launched after 2011.
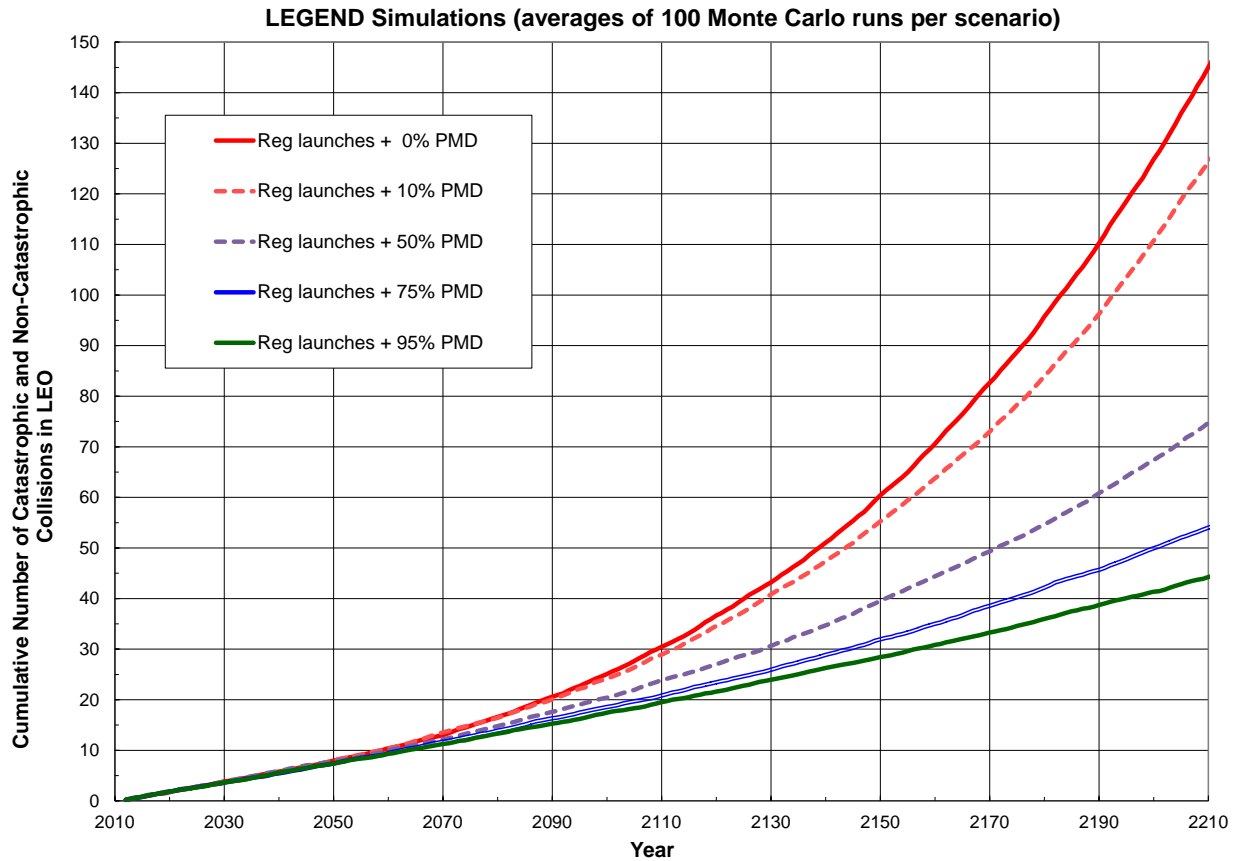
Figure 2.– Cumulative numbers of catastrophic collisions predicted by the five-projection scenario. Each curve represents the average of 100 Monte Carlo runs.

	0% PMD	10% PMD	50% PMD	75% PMD	95% PMD
Cat. Collisions	71	63	39	30	26
Non-cat. Collisions	76	65	37	24	19
Total Collisions	147	128	76	54	45

Figure 3.– Projected collision activities for the next 200 years in LEO. All collisions are for objects 10 cm and larger. The numbers are averages of 100 Monte Carlo runs.

An Analysis of the FY-1C, Iridium 33, and Cosmos 2251 Fragments

J.-C. Liou

The beginning of the year 2013 marks the sixth anniversary of the destruction of the Fengyun-1C (FY-1C) weather satellite as the result of an anti-satellite test conducted by China in January 2007 and the fourth anniversary of the accidental collision between Cosmos 2251 and the operational Iridium 33 in February 2009. These two events represent the worst satellite breakups in history. A total of 5579 fragments have been cataloged by the U.S. Space Surveillance Network (SSN), and almost 5000 of them were still in orbit in January 2013 (see figure 1). In addition to these cataloged objects, hundreds of thousands (or more) of fragments down to the millimeter size regime were also generated during the breakups. These fragments are too small to be tracked by the SSN, but are large enough to be a safety concern for human space activities and robotic missions in low Earth orbit (LEO, the region below 2000 km altitude). Like their cataloged siblings, many of them remain in orbit today.

These two breakup events dramatically changed the landscape of the orbital debris environment in LEO. The spatial density of the cataloged population in January 2013 is shown as the top blue curve in figure 2. The combined FY-1C, Iridium 33, and Cosmos 2251 fragments (black curve) account for about 50 percent of the cataloged population below an altitude of 1000 km. They are also responsible for the concentrations at 770 km and 850 km, altitudes at which the collisions occurred. The effects of the FY-1C, Iridium 33, and Cosmos 2251 fragments will continue to be felt for decades to come, as illustrated in figure 3. For example, approximately half of the generated FY-1C fragments will remain in orbit 20 years from now.

In general, the Iridium 33 and Cosmos 2251 fragments will decay faster than the FY-1C fragments because of their lower altitudes. Of the Iridium 33 and Cosmos 2251 fragments, the former have much shorter orbital lifetimes than the latter, because lightweight composite materials were heavily used in the construction of the Iridium vehicle, leading to the higher area-to-mass ratios of the fragments.

Name	Cataloged Debris	Debris Decayed	Debris in Orbit
FY-1C	**3378**	302	3076
Cosmos 2251	**1603**	261	1342
Iridium 33	**598**	119	479
Total	**5579**	682	4897

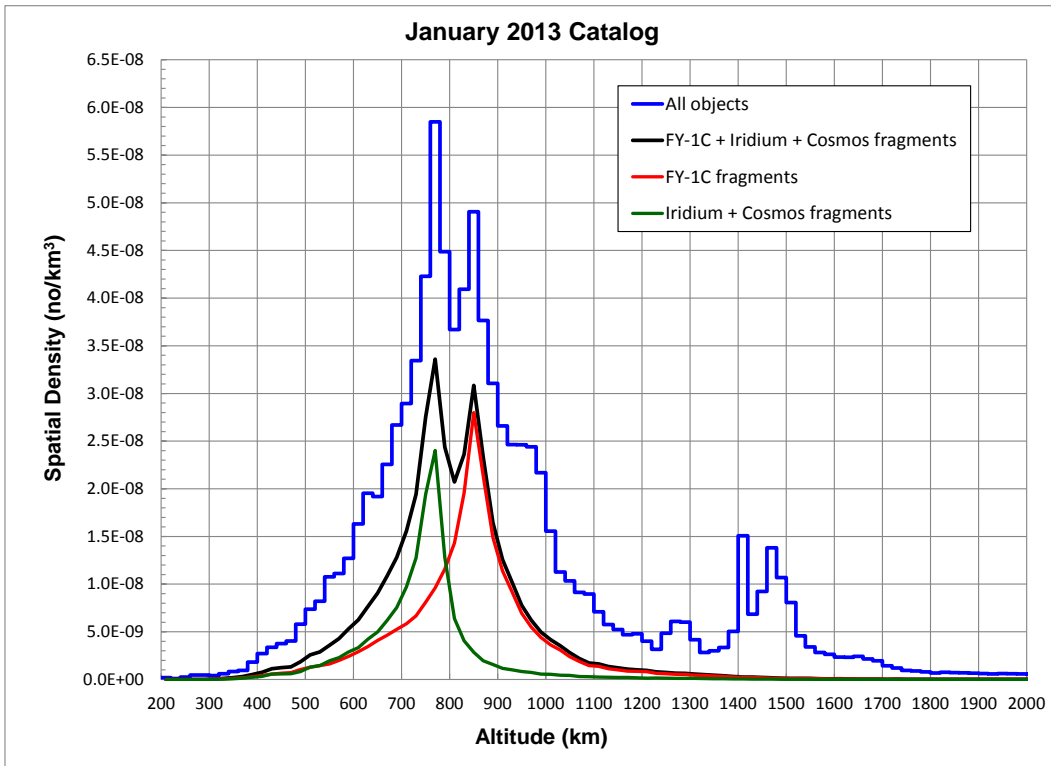*Figure 1.– A summary of the FY-1C, Cosmos 2251, and Iridium 33 breakup fragments (as of January 2013).*

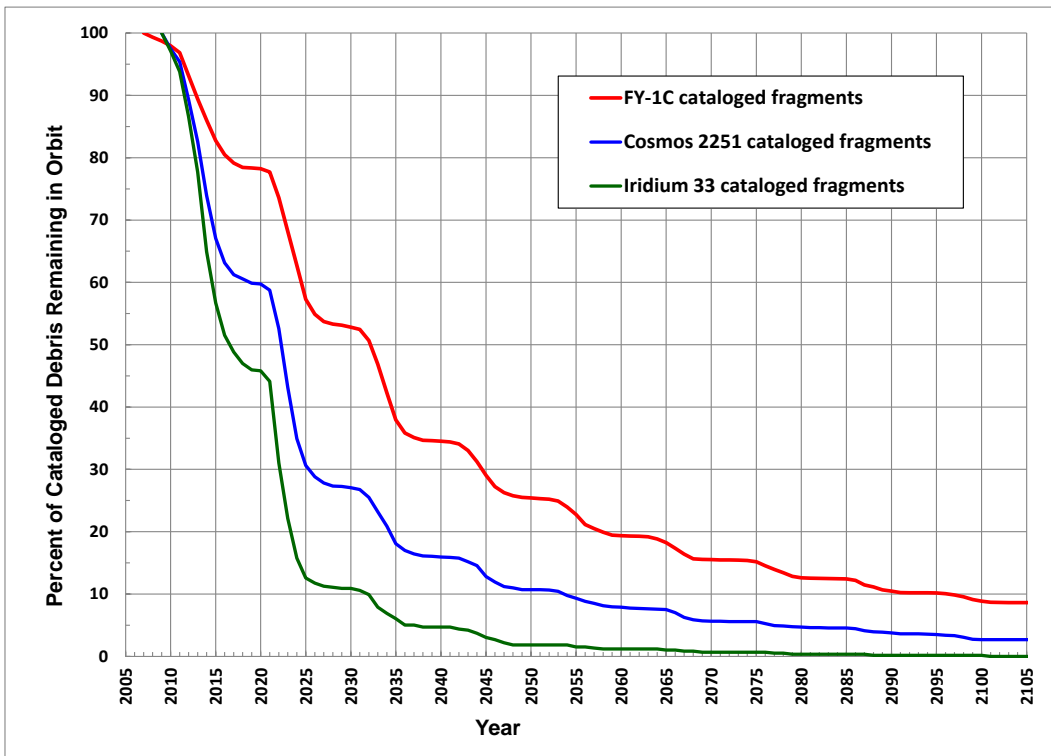*Figure 2.– Spatial density distribution of the cataloged objects as of January 2013.*

Figure 3.– Projected decay of the cataloged FY-1C, Iridium 33, and Cosmos 2251 fragments. Projection assumes a return to normal solar activity beginning in 2020.

Detection of Optically Faint GEO Debris

P. Seitzer, S. Lederer, E. Barker, H. Cowardin, K. Abercromby, J. Silha,
A. Burkhardt

There have been extensive optical surveys for debris at geosynchronous orbit (GEO) conducted with meter-class telescopes, such as those conducted with MODEST (the Michigan Orbital DEbris Survey Telescope, a 0.6-m telescope located at Cerro Tololo in Chile), and the European Space Agency's 1.0-m space debris telescope (SDT) in the Canary Islands.

These surveys have detection limits in the range of 18th or 19th magnitude, which corresponds to sizes larger than 10 cm assuming an albedo of 0.175. All of these surveys reveal a substantial population of objects fainter than R = 15th magnitude that are not in the public U.S. Satellite Catalog.

To detect objects fainter than 20th magnitude (and presumably smaller than 10 cm) in the visible requires a larger telescope and excellent imaging conditions. This combination is available in Chile. NASA's Orbital Debris Program Office has begun collecting orbital debris observations with the 6.5-m (21.3-ft diameter) "Walter Baade" Magellan telescope at Las Campanas Observatory (see figure 1). The goal is to detect objects as faint as possible from a ground-based observatory and begin to understand the brightness distribution of GEO debris fainter than R = 20th magnitude. Outstanding questions include: Does the distribution continue to increase as one reaches fainter limiting magnitudes, and therefore smaller and smaller sizes, and if so, how? How does this small size regime compare with the distribution of debris at low Earth orbit (LEO)?
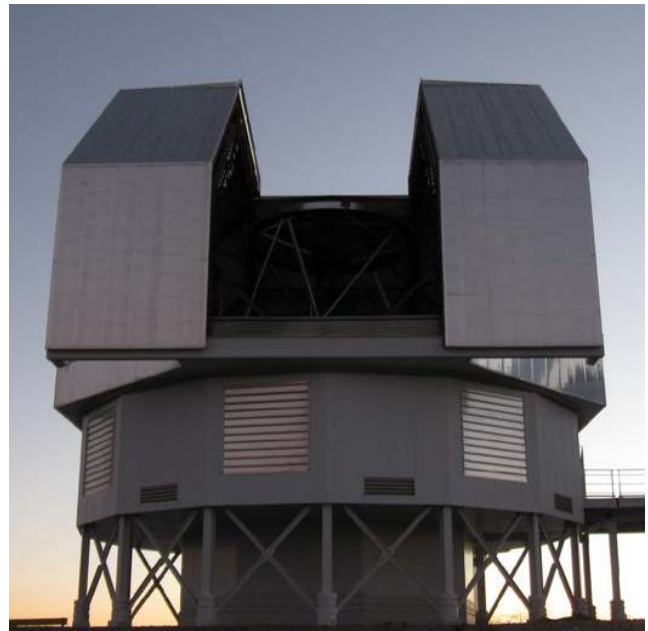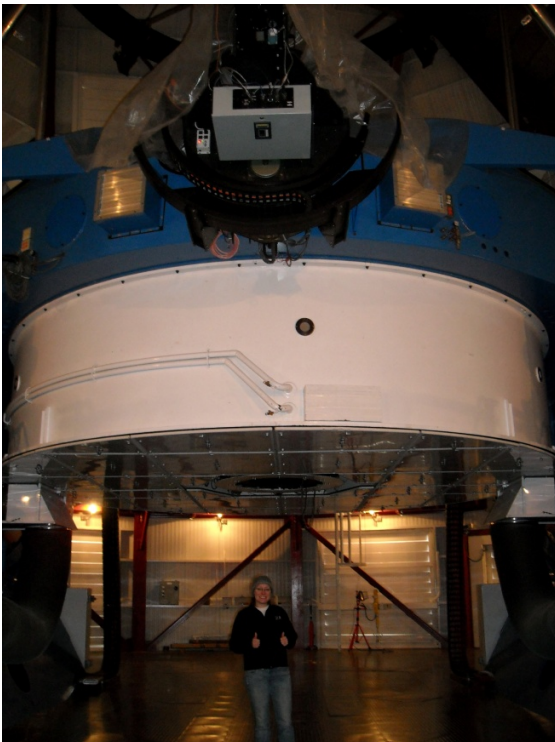
Figure 1.– The 6.5 m "Walter Baade" Magellan telescope at Las Campanas Observatory in Chile.

Preliminary results were obtained during 6 hours of observing time obtained March 25–27, 2011. The Inamori Magellan Areal Camera and Spectrograph (IMACS) instrument in f/2 imaging mode was used. It is composed of a mosaic of eight CCDs and has a field of view of 0.5 degrees in diameter (figure 2, right). This is the widest field of view of any instrument on either Magellan telescope. The image scale is 0.4 arc-seconds/pixel. The limiting magnitude for a 5-s exposure though a Sloan r′ filter is measured to be fainter than R = 21. The system saturates at R = 15th magnitude in 5 s in the typical excellent sub-arc-second image quality obtained using the Magellan telescopes.
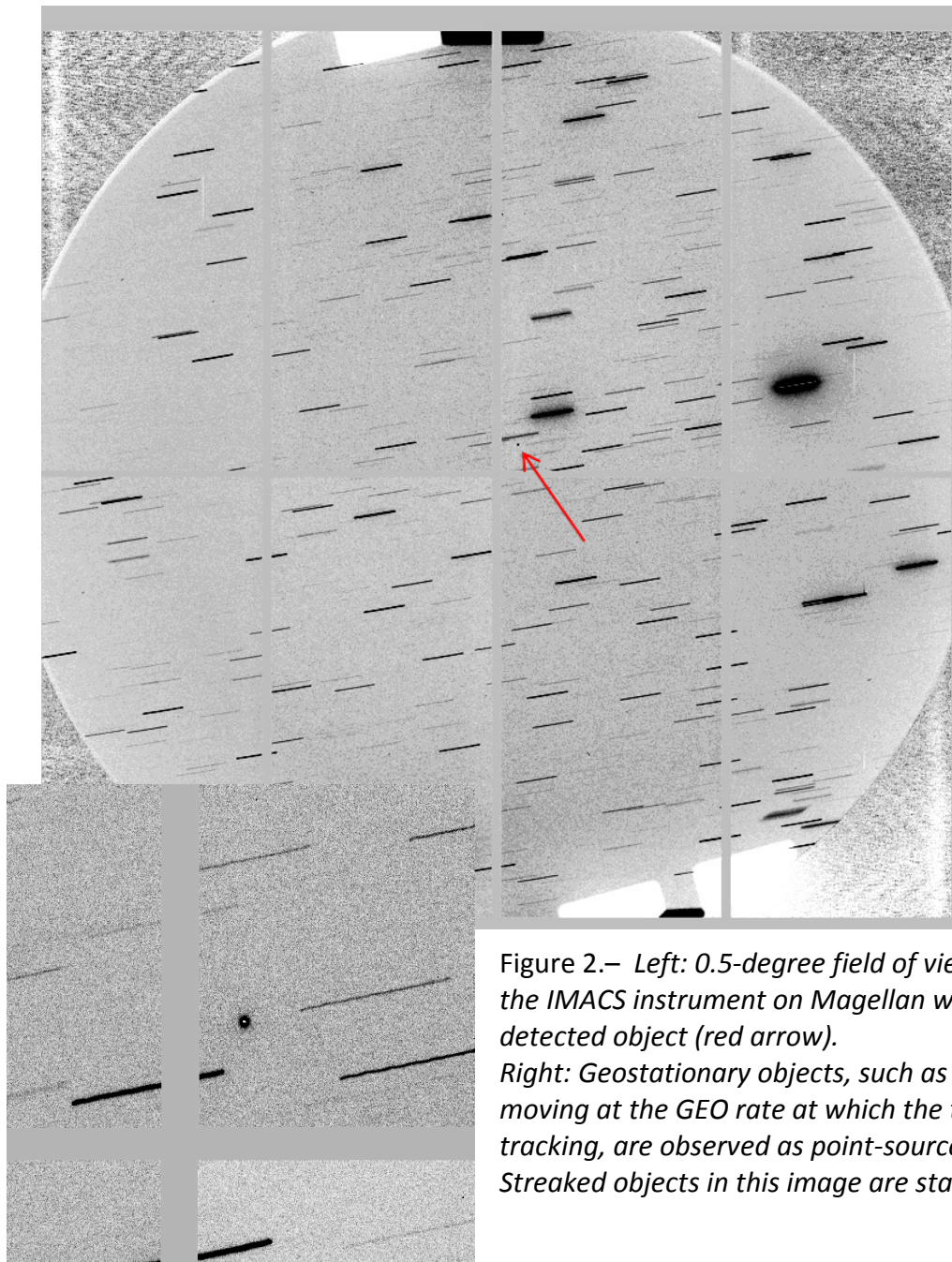
Figure 2.– *Left: 0.5-degree field of view seen by the IMACS instrument on Magellan with a detected object (red arrow).*
Right: Geostationary objects, such as satellites, moving at the GEO rate at which the telescope is tracking, are observed as point-source objects. Streaked objects in this image are stars.

The aim was to observe an area that is as close as possible to the edge of the Earth's shadow at GEO for two reasons: 1) this minimized the Sun-object-Earth phase angle (creating a "full-moon" effect), thereby maximizing the apparent brightness of the object, and 2) objects below GEO were in Earth shadow and thus not visible. This is important because the measurable quantities from this data are brightness, positions, and angular rates (at the time of the observations, calculating real-time orbits was not possible).

In 6 hours of photometric observing time, 19 individual objects were detected, as determined by manual review of all the images. Of these, 12 had rates consistent with GEO objects, appearing as point-sources instead of streaks (figure 2, left), or streaks moving in a different direction or rate than the stars (figures 3–5). For an object to be deemed real (and not a source of noise, such as cosmic-rays), it must appear in at least three images. Objects with hour angle (HA) rates within ±2 arc-seconds/s and declination (DEC) rates within ±5 arc-seconds/s were kept. These rates correspond to motions expected for GEO objects in circular orbits with inclinations ranging from 0 to 16 degrees. The detections group into three types: streaks, streaks of non-uniform brightness, and resolved and partially resolved flashes. Examples are presented in figures 3 through 5.

Figure 3.– An object detected as a uniform short streak. The primary motion is north to south.

Figure 4.– An object detected as a non-uniform streak.

Figure 5.– An object detected as a series of unequal brightness flashes. The primary motion is east to west.

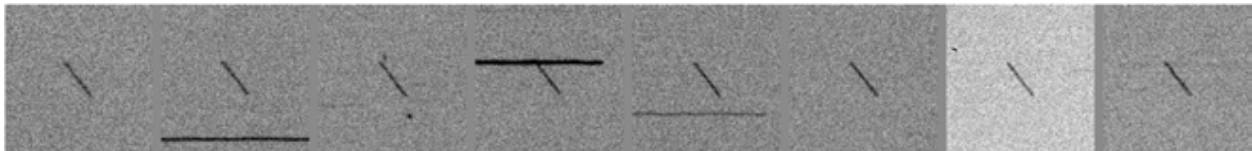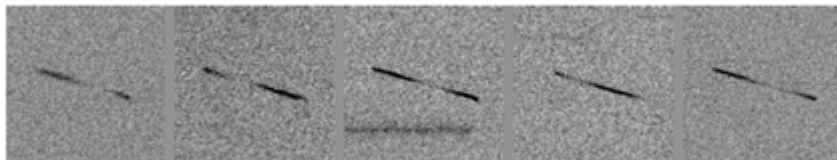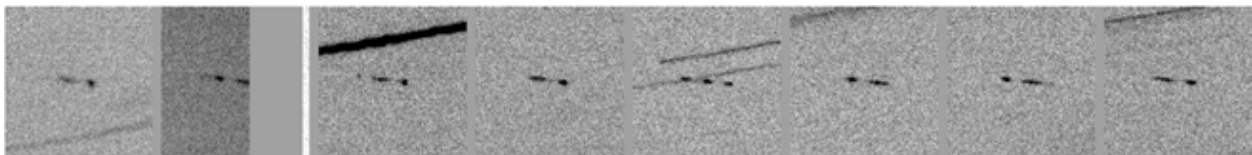Each sub-image is 51.6 x 51.6 arc-seconds in size. Horizontal lines are stars (in figure 5, the star tracks are slightly tilted to the upper right). Approximately one-third of the detections show a series of three or more flashes during each 5-s exposure. One interpretation is that the detected objects are tumbling. Objects that are non-uniform streaks are tumbling at a rate close to our 5-s exposure time; objects with flashes are tumbling faster. Approximately 25 percent of the detected objects show glints (a momentary flash).

None of the faint objects detected are in the public U.S. Satellite Catalog. The rate of detection of objects with GEO rates is approximately 10 per hour per square degree.

This can be compared with the detection rate of GEO debris on MODEST during previous observing campaigns. The CCD camera in this telescope had a field-of-view of 1.3 x 1.3 degrees, a somewhat broader filter close to the same central wavelength of the Magellan Sloan r′ filter, the same 5-s exposure time as Magellan, and a different survey technique. The average detection rate of objects with angular rates consistent with those at GEO in the range of 15th to -18th R magnitude was approximately one object per hour per square degree. Magellan's average detection rate, including objects in the 15th to 21st r′ magnitude regime, was 10 times greater. With only 6 hours of observing time using Magellan, the statistics are unfortunately small at the faint end, but more GEO objects were detected in 6 hours of observing with Magellan in a smaller field-of-view than were detected with MODEST in an 8-hour night with a camera covering an area of sky eight times larger. However, the Magellan and MODEST results are consistent with a rising population of GEO objects as one reaches fainter limiting magnitudes. Future observations with Magellan can help us begin to understand the small and faint debris population in GEO.

Coring the Wide-Field Planetary Camera 2 Radiator for Impactor Trace Residue Assessment

Phillip Anz-Meador and J.-C. Liou

After approximately 16 years in low Earth orbit aboard the Hubble Space Telescope (HST), the Wide Field Planetary Camera 2 (WFPC2) was returned to Earth in 2009 by the crew of STS-125's Servicing Mission 4. The WFPC2 radiator was exposed to the micrometeoroid (MM) and orbital debris (OD) environment and provides a unique record of the environment due to the length of time it spent in orbit as well as its relatively large 1.76 m^2 surface area. This surface was optically surveyed for impact features by a NASA and contractor team from JSC, Marshall Space Flight Center, and Goddard Space Flight Center in the summer of 2009. Approximately 700 features limited to a size of approximately 300 µm – estimated to correspond to a 100 µm OD projectile – were located and documented using a Keyence VHX-600 digital microscope.

The observed crater record will be used to bound the integrated flux, but requires a knowledge of the HST's attitude history, damage equations to correlate the crater features found on the WFPC2's surface to estimated projectile size, and a discrimination between the MM and OD components of the environment. This discrimination is required, as the two components possess quite distinct velocity, density, and directional distributions. As the damage equations depend upon these variables, they must be inferred or determined by direct measurement to implement the damage equations correctly and thereby assess the MM and OD fluence.

Project planning began in 2009 and was predicated upon prior sampling campaigns to characterize surfaces returned from space [*i.e.,* the Long Duration Exposure Facility (LDEF)]. In these campaigns, samples or cores were cut from select surfaces and analyzed using standard Scanning Electron Microscope–Energy-Dispersive X-ray spectroscopy (SEM-EDX) techniques to assess the elemental composition of the impactor. The elemental constituents revealed the impactor to be MM, OD, or an indeterminate category. However, the WFPC2 radiator presented unique challenges due to its geometry (a rectangular section from a right circular cylinder's lateral surface), thickness (approximately 4 mm), coating (YB-71 Zinc Orthotitanate [ZOT] thermal control paint), and the size and extent of many impact features. Collecting core samples from the thick surface using a core drill offered the greatest probability of success within two major constraints: 1) not contaminating the sample during collection and 2) not compromising the integrity of the clean room in which sampling would be conducted.

The Technique
A unique sampling tool was developed to perform clean room coring of the WFPC2 impact features. The annular cutter is shown in figure 1. In this case, a standard 5/8–in.-diameter cutting tool was modified with a concentric, spring-loaded, phosphor-bronze cylinder. The cylinder is tipped with a standard O-ring to protect the feature being cored. As the core drill is brought into contact with the radiator's surface, friction between the surface and the O-ring brings the cylinder to rest within the rotating annular cutter. As the cutter is advanced into the surface, the cylinder retracts, allowing the radiator's aluminum substrate to be cut while protecting the feature of interest.

Figure 1.– The coring device developed at JSC. Cores taken have a diameter (measured at the core's painted surface) of approximately 7 mm, corresponding to the inner diameter of the annular cutter.
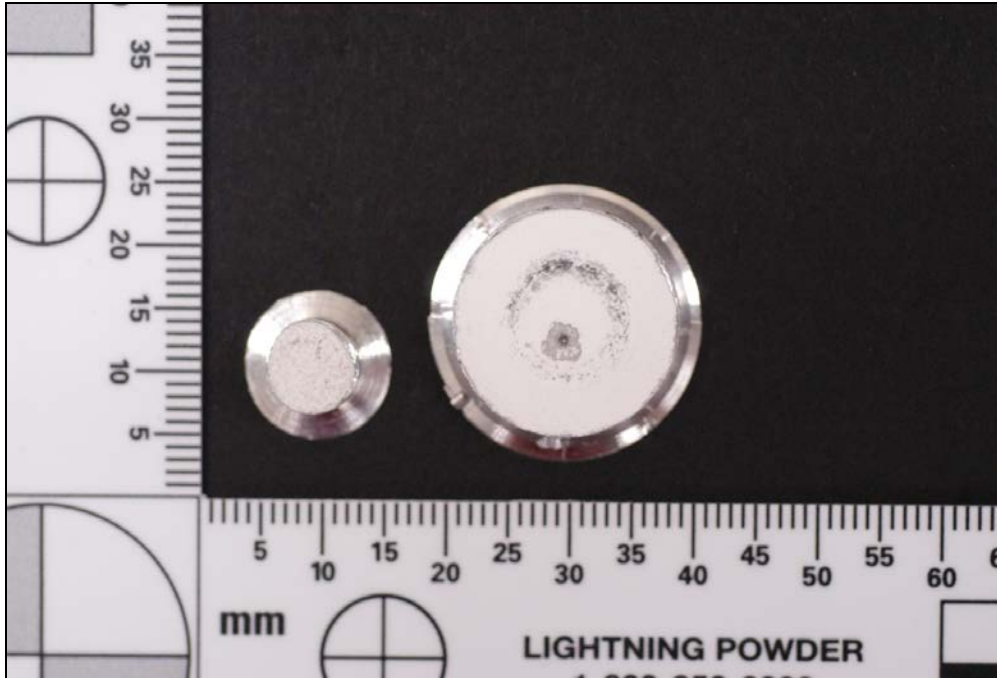
Figure 2.– Small (taken with the cutter portrayed in figure 1) and large cores collected using a larger, 1-1/16-in. diameter cutting tool. The small core is a "blank" taken as a standard reference for the YB-71 paint coating and Al substrate. Clearly visible on the surface of the large core is an impact crater displaying paint spallation. Also visible is an abrasion left by the large cutter's O-ring – this was later remedied by decreasing the cutter's spring constant.

Figures 3 and 4 illustrate the process by which cores are collected. The process begins with the identification of a feature to be cored. In figure 3, Orbital Debris Program Office team member Joe Caruana is aligning the core drill table roughly with a feature to be collected. The table allows 4 degrees of freedom in aligning the high-torque drill motor assembly with the feature. After a rough alignment, the assembly is rotated to enter the radiator's surface normally, and fine positioning is achieved with a laser alignment system.

In figure 4, the cutter is engaging the surface. As the feature is protected, so is the clean room environment – a vacuum shroud is visible around the cutter; dust generated by cutting is collected by a HEPA-filtered vacuum, while larger strands are collected by the shroud assembly itself.
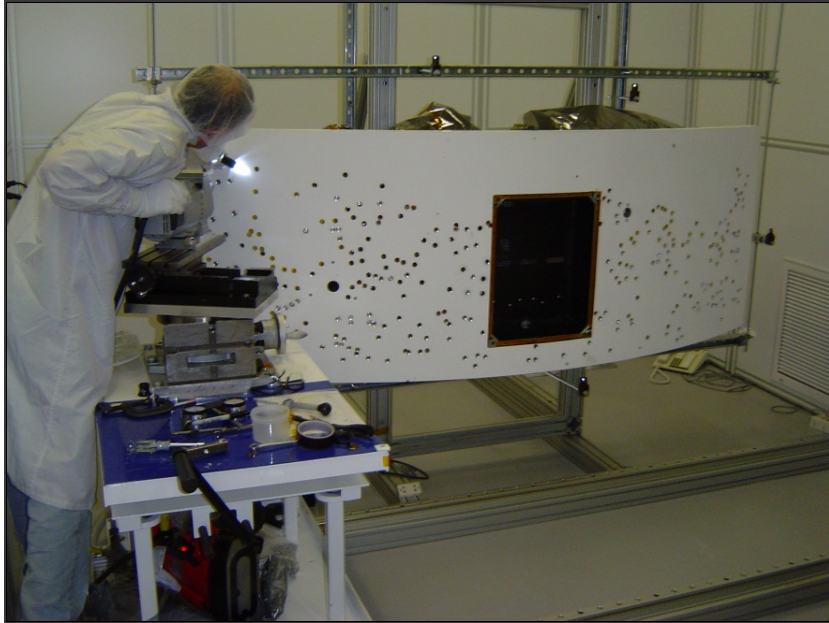
Figure 3.– Preparation for coring a feature.

Figure 4.– The system cores an impact feature.

Analysis

During project planning, it was agreed that the analysis would be shared by NASA and ESA. At JSC, the ARES SEM-EDX laboratory is charged with performing analyses to determine the elemental composition of impactors, and hence the source environment of the impactors, while the Ion Beam Center (IBC) of the United Kingdom's Natural History Museum (NHM) was chosen as ESA's agent. The cores were shared equally between NASA and ESA, becoming the laboratory sample property of each party. All core samples will be maintained in a state to allow future

analyses on the cores, should superior techniques be developed and implemented for the analysis of returned surfaces.

The ARES and NHM IBC analytical teams are currently probing core samples to identify and record traces of impactor residue materials left in and about the impact features. Impactors from the MM and OD components have been identified, but analysis has yielded indeterminate results. In this latter case, a core can yield indeterminate results because no residues were present; no residues were identified; or, in the case of craters resident only in the YB-71 paint layer, the crater geometry complicated electron beam-based instrumentation, confounding the investigation. However, a full accounting of the three categories is premature pending completion of the ARES work as well as supporting analytical activities, such as the assessment of surface attitude compared to environment directionality.

Figure 5 depicts a small, so-called "paint crater," a conical impact feature resident entirely in the paint coating. Figures 6a and 6b depict a larger impact feature. The ARES and NHM IBC teams are concentrating their analytical efforts on characterizing the elemental constituents of the residue melts in both types of features.

Figure 5.– Core sample 29, typical of the so-called "paint craters."

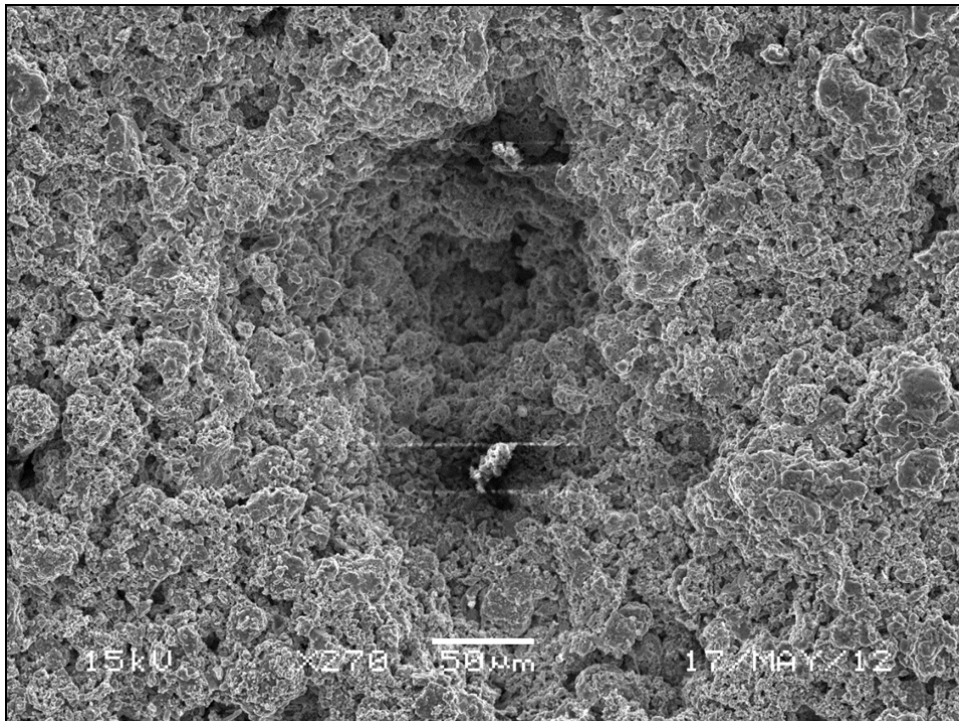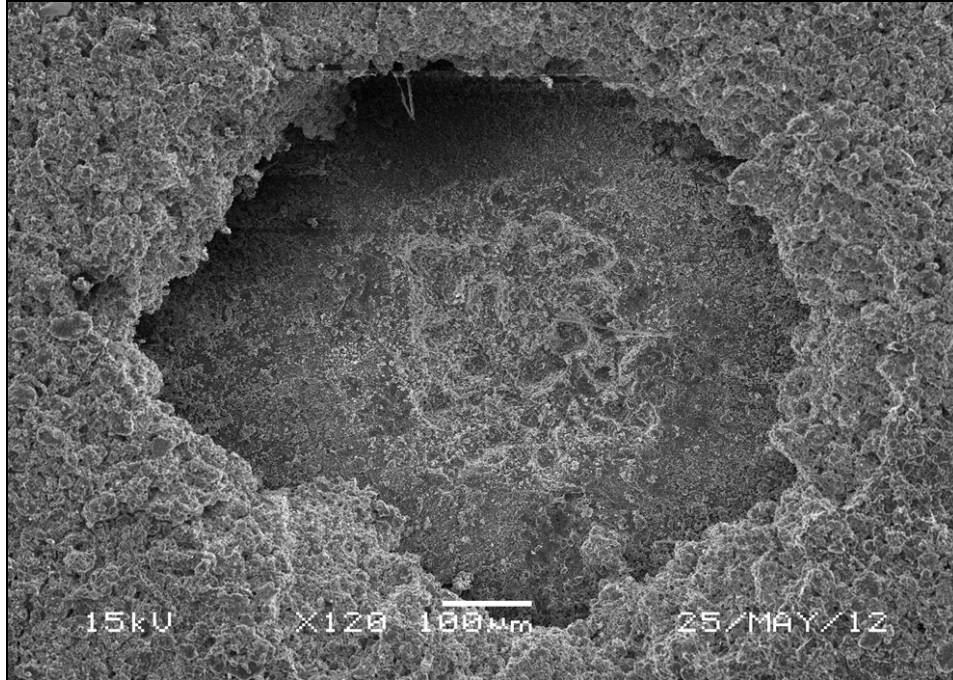*Figure 6a.– Core sample 29, typical of the larger impact features. Note the area of spalled paint and the relatively shallow impact feature on the revealed Al-6061 substrate surface.*
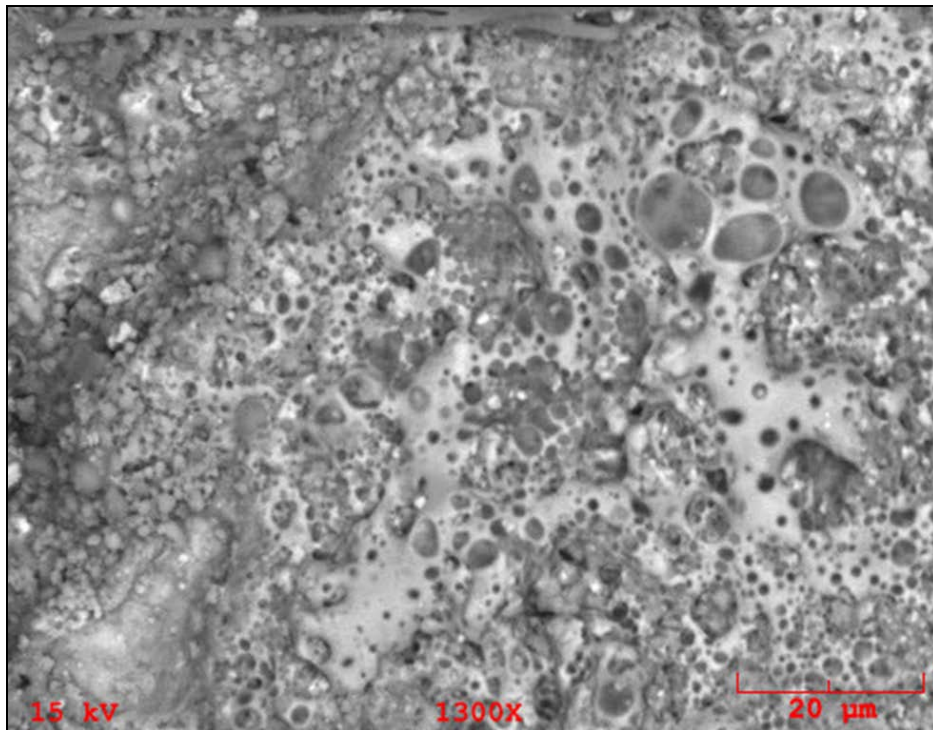

Figure 6b.– Projectile and target residue melt on the floor of the sample 29's impact feature. Note the frothy appearance and large number of vesicles in the melt.

After the two impactor populations are identified, along with the indeterminate cases, population characteristics (density, relative velocity, and directional distributions) will be used in conjunction with damage equations to estimate the impactor's characteristic size. At that point, cumulative number or flux distributions of the MM and OD components begin to serve the space environment modeling community.

Multi-Purpose Crew Vehicle Camera Asset Planning: Imagery Previsualization

K. Beaulieu

Using JSC-developed and other industry-standard off-the-shelf 3D modeling, animation, and rendering software packages, the Image Science Analysis Group (ISAG) supports Orion Project imagery planning efforts through dynamic 3D simulation and realistic previsualization of ground-, vehicle-, and air-based camera output.

A total of 11 cameras will be onboard the Multi-Purpose Crew Vehicle (MPCV) and Service Module during Exploration Flight Test 1 (EFT-1), the first test flight of Orion, scheduled to launch in September 2014. These 11 cameras will collect imagery data essential to the fulfillment of EFT-1 flight-test objectives defined by Lockheed Martin and NASA. The optimization of the onboard camera suite – the evaluation of proposed camera and lens hardware options and definition of settings, position, and orientation parameters – has been achieved using imagery previsualization techniques.

Provided simulation data for a dynamic event; camera sensor and lens specifications; and industry-standard modeling, animation, and rendering software are used to produce high-quality, accurate previsualization imagery. EFT-1 dynamic events that have been modeled using simulation data provided by Lockheed Martin include the Launch Abort System (LAS) jettison, Crew Module/Service Module separation, and the Crew Module forward bay cover (FBC) jettison.

LAS-jettison imagery will be captured by three cameras mounted inside and pointed out of Crew Module windows. Lockheed Martin and NASA require this imagery to verify a successful LAS jettison without recontact during nominal ascent. Previsualization imagery of the LAS jettison, captured by the overhead docking hatch window, is shown in figure 1.
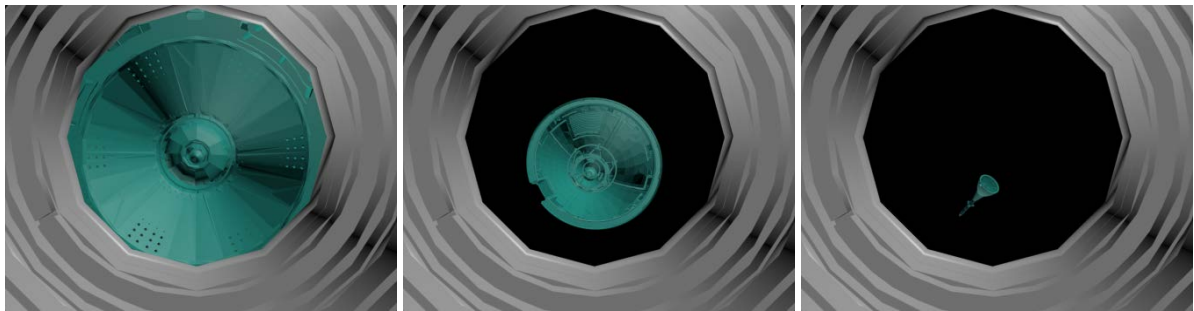
Figure 1.– Sample previsualization of EFT-1 LAS jettison.

Three high-speed cameras will be mounted in the Crew Module forward bay. These cameras will capture imagery of dynamic events during the EFT-1 descent and landing phases. The dynamic events include FBC jettison, drogue parachute deployment, main parachute deployment, and parachute steady state. Postflight ISAG analysis of the position and orientation of the FBC during jettison will be required to verify there was no recontact and validate Lockheed Martin FBC trajectory models. Custom targets defined by ISAG will be installed on the interior of the FBC. Modeling of the targets on the FBC interior, incorporating Lockheed Martin-provided FBC jettison dynamics simulation data and producing high-speed camera previsualization imagery, has been instrumental in optimizing the plan to collect this data. Sample previsualization imagery of FBC jettison as viewed from the Crew Module forward bay D camera is shown in figure 2.
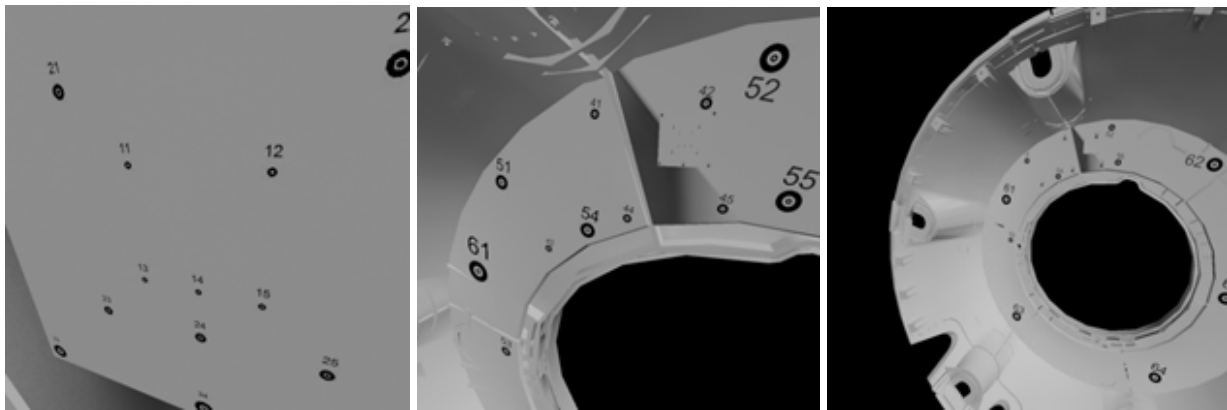
Figure 2.– Sample previsualization of EFT-1 FBC jettison.

ISAG also supports EFT-1 ground- and helicopter-based camera system optimization planning efforts. Imagery previsualization has been an instrumental tool in this process, and ISAG continues to expand this capability.

NASA Extreme Environment Mission Operations: Science Operations Development for Human Exploration

Mary Sue Bell, Ph.D.

The purpose of NASA Extreme Environment Mission Operations (NEEMO) mission 16 in 2012 was to evaluate and compare the performance of a defined series of representative near-Earth asteroid (NEA) extravehicular activity (EVA) tasks under different conditions and combinations of work systems, constraints, and assumptions considered for future human NEA exploration missions. NEEMO 16 followed NASA's 2011 Desert Research and Technology Studies (D-RATS), the primary focus of which was understanding the implications of communication latency, crew size, and work system combinations with respect to scientific data quality, data management, crew workload, and crew/mission control interactions. The 1-g environment precluded meaningful evaluation of NEA EVA translation, worksite stabilization, sampling, or instrument deployment techniques. Thus, NEEMO missions were designed to provide an opportunity to perform a preliminary evaluation of these important factors for each of the conditions being considered. NEEMO 15 also took place in 2011 and provided a first look at many of the factors, but the mission was cut short due to a hurricane threat before all objectives were completed. ARES Directorate (KX) personnel consulted with JSC engineers to ensure that high-fidelity planetary science protocols were incorporated into NEEMO mission architectures. ARES has been collaborating with NEEMO mission planners since NEEMO 9 in 2006, successively building upon previous developments to refine science operations concepts within engineering constraints; it is expected to continue the collaboration as NASA's human exploration mission plans evolve.

The Importance of Planetary Sample Returns
Planetary science has seen a tremendous growth in new knowledge as a result of recent NASA robotic missions that have detected deposits of water ice at the Moon's poles and potential conditions under which life could have flourished on Mars.

While some sophisticated data can be derived from "in-situ" measurements taken by rovers and satellites, returned planetary samples allow scientists on Earth to use the latest technologies available to maximize the scientific return. The science community has recently seen compelling sample returns, including solar wind particles (NASA's Genesis), comet particles (NASA's Stardust), asteroid particles (Japan Aerospace Exploration Agency's Hayabusa), and Antarctic meteorites, which scientists collect each Austral summer.

The National Research Council Decadal Study of 2011 recommended that NASA's chief scientific goal should be to return samples from Mars by 2023. Measurements taken by the Mars Exploration Rovers Spirit and Opportunity indicate that Mars' climate was warmer and wetter early in Mars' history – conditions in which scientists believe life could have formed. But chemical evidence of life

in materials like the rocky regolith of Mars can be quite small and difficult for robotic geologists to detect and measure.
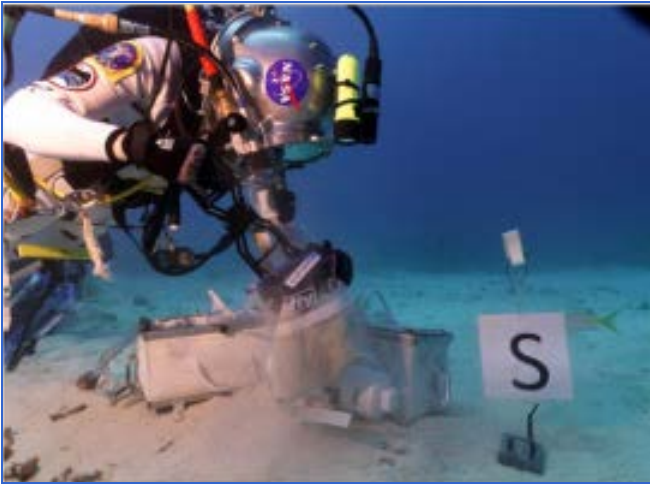
Figure 1.– *Clamshell sample collection device in use during NEEMO 16.*

Figure 2.– *NEEMO aquanauts collect and document samples.*

The ARES Directorate at JSC curates all of NASA's extraterrestrial samples. ARES' mission is to protect, preserve, and distribute samples from the Moon, Mars, and interplanetary space for scientific study. These sample collections include lunar rocks and regolith returned by the Apollo missions.

Samples from Mars will require special handling protocols from the time the sample collection site is chosen through documentation, encapsulation, and transport to Earth and to NASA's curation facility for allocation to scientists for analysis and study. Because scientists do not yet know how to differentiate an Earth-derived sample of life from a Mars-derived sample of life, scientists are eager to develop protocols that will protect Mars samples from Earth contamination. Landers, collection tools, and sample containers could all carry trace amounts of Earth biology, so they must be equipped with decontamination materials and procedures to protect the precious samples.

How do NASA's analog missions, like NEEMO, help scientists develop special sample-handling techniques for exploration programs?
Planetary environments are considered extreme for both robotic and human exploration. Apollo astronauts experienced lower gravity on the Moon and a very thin atmosphere that required them to wear a space suit with life protection and support systems. When they collected Moon rocks, the astronauts did not know if they were exposing themselves to health hazards, so they wore large bulky gloves and used special sample collection tools and containers. These protective materials and special sample devices were developed in laboratories at JSC and tested in the field by geologists. After the sampling tools and techniques were sufficiently refined, Apollo astronauts were trained to use the techniques developed by the scientists.

Figure 3.– A NEEMO 15 Aquanaut tests sample collection tools.
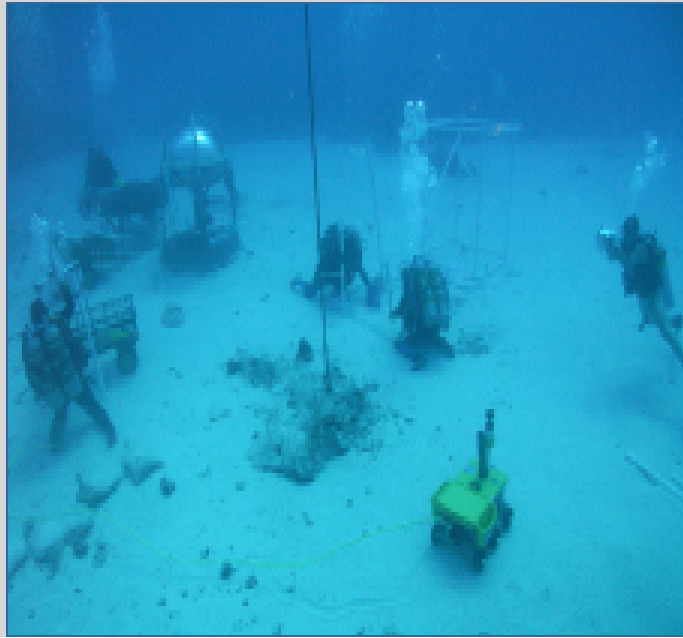
Figure 4.– Aquanauts test and develop surface operations in the reduced-gravity underwater environment.

Today, ARES scientists are developing tools and techniques for use on planets that have the same life-support requirements and gravity conditions as the Moon or Mars as well as for lower gravity environments, such as near-Earth asteroids. Low-gravity environments present special obstacles for collecting and containing geologic materials because loose material can drift away, and an astronaut can be propelled away from a planetary surface just by hitting a rock with a hammer. NEEMO is an undersea research facility that allows humans to experience reduced gravity due to the buoyancy provided by water in an environment requiring life support. During NEEMO 16, NASA refined sample collection techniques in an extreme environment and trained astronauts to use tools and procedures developed for those unique conditions.

NASA develops tools and techniques during analog missions to ensure the scientific integrity of samples returned from a variety of planetary surfaces by robots and human explorers. NASA's returned samples will help scientists understand the formation and evolution of the solar system and determine if life or the conditions for life existed on other planets. These samples will be curated for future generations, who may be able to employ advanced techniques not yet available to researchers.

How does this analog activity fit with NASA's current mission plans?
NASA is actively planning to expand the horizons of human space exploration, and with the Space Launch System and the Orion crew vehicle, humans will soon have the ability to travel beyond low Earth orbit, opening a solar system of possibilities. NASA's goal is to send humans to explore an asteroid by 2025. Other destinations may include the Moon or Mars and its moons.

Regardless of the destination, the work must start now. NASA is developing the technologies and systems to transport explorers to multiple destinations, each with its own unique – and extreme – space environment. Because sample return requirements are mission specific, the handling protocols are designed specifically for the types of questions the scientific community hopes to answer using samples from a particular planetary destination. ARES curation scientists are collaborating with mission architecture engineers to develop mission goals that are aligned with science goals. ARES scientists participate in analog missions to develop protocol and scientific operations – from mission conception to execution and sample return – to ensure that the requirements of the scientific community will be met and the scientific return to the public will be maximized.

The 2012 Moon and Mars Analog Mission

Lee Graham

The 2012 Moon and Mars Analog Mission Activities (MMAMA) scientific investigations were completed on Mauna Kea volcano in Hawaii in July 2012. The investigations were conducted on the southeast flank of the Mauna Kea volcano at an elevation of ~11,500 ft. This area is known as "Apollo Valley" and is in an adjacent valley to the Very Large Baseline Array dish antenna.

Two of the four MMAMA investigations selected were led by scientists within the ARES Directorate at JSC. These included the Increasing Robotic Science proposal, the miniature Mössbauer spectrometer (MIMOS II), and the MIMOS II combined with an X-ray fluorescence (XRF) spectrometer (MIMOS IIA). The original robotic investigation proposal called for a comparative study of human field work versus the JSC C2 rover (and potentially the C2 rover with a Robonaut torso mounted on it, often called a "Centaur"). Robonaut is a dexterous humanoid robot that was designed and built at JSC, but last-minute travel restrictions eliminated it from the field test. Working with the NASA Regolith and Environment Science and Oxygen and Lunar Volatile Extraction (RESOLVE) project, a NASA Advanced Exploration System Program project hosted at the Kennedy Space Center (KSC), the MMAMA team was able to identify a replacement rover, the JUNO II (shown in figure 1), which was provided by the Canadian Space Agency. In addition, as planning progressed for the 2012 tests on Mauna Kea, an opportunity presented itself to move the MMAMA test site to a more geologically challenging location. This did, however, also reduce the test time from the original 2 weeks to only 3 days. The primary focus of the investigation was to determine the valley formation processes.

The instruments used in the test were selected based on several considerations. The major criteria included 1) applicability to the scientific investigation of the valley, 2) mobility, 3) availability, 4) remote control capability, and 5) weatherproofing capability. The MMAMA robotic investigation involved the use of six instruments, including a ground penetrating radar (GPR), a second-generation

Mössbauer/XRF spectrometer, a panoramic video camera, a magnetic susceptibility meter, a global positioning sensor (GPS) receiver, and a 3-axis accelerometer.
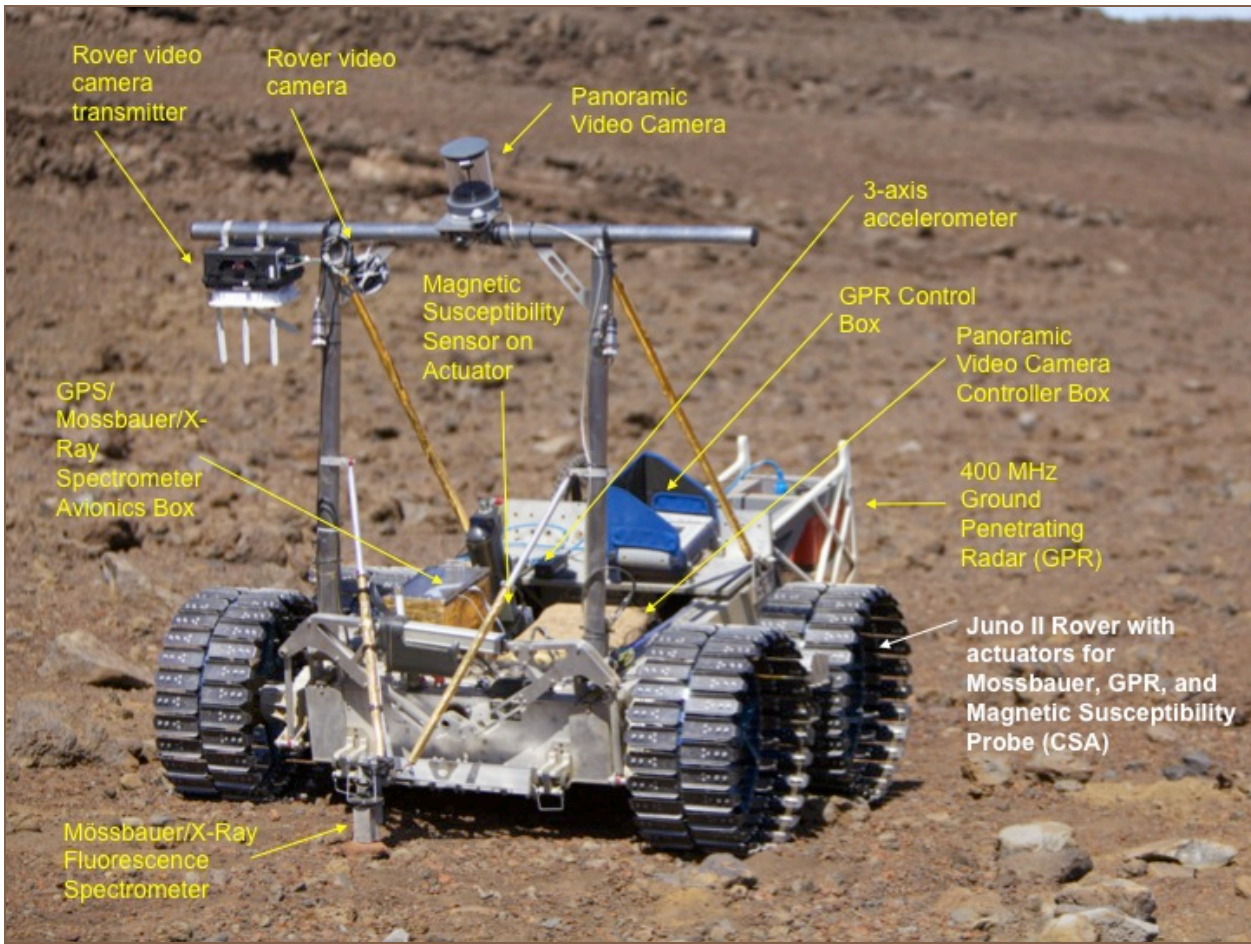
Figure 1.– Juno II Rover with actuators for Mössbauer, GPR, and magnetic susceptibility probe.

During operation in the field, a successful attempt was made to simulate a remote-controlled planetary science mission by minimizing the number of times the rover was physically touched by an operator. The only exception to this was GPR data collection, which required the operator to activate the system that was mounted on the rover each time it was used (several times each day). To accomplish the remote operation, a combination wireless and hardwired on-board instrument suite was developed. During the test, the instruments and rover were controlled by four remotely located operators (see figure 2).

Figure 2.– Rover field team on the side of the cinder cone.

Google Earth images were used as an analog to the orbital images available prior to a planetary "landing" to create notional traverses prior to the mission. Although many legs of the planned traverses could not be executed because of the rugged terrain, the effort still provided a framework from which to vary and maximized the team's efficiency in the field where rapid replanning was required (see figure 3).

The science instrumentation collected geophysical and geochemical information to provide a range of geological context about the test site. This initial evaluation of the geologic context and history of the Apollo Valley (or "landing site") was continually refined by this integrated investigation. For example, the hypothesis that a large, higher-albedo mound was part of a burst glacial dam was confirmed only by walking the formation, and though the orbital data and the video pans showed possible channels or valleys on either side of this structure, it was clear only on the ground that the west valley was the location of the glacial dam breach and the eastern portion of the valley was on a slope. This information, combined with the ability to determine the shape of the mound (the slope was steeper on the west than on the east) and the morphology to the north of it, led scientists to conjecture that the ice-dam hypothesis was possible. Further research and investigation are necessary, however, to definitively state that an ice-dam burst formed the valley.

*Figure 3.– Mauna Kea Traverse: Perspective view of Apollo Valley,
including rover traverse and science locations.*

The 2012 MMAMA science activity allowed for a small team to perform significant science over the 3 main days of testing. All personnel worked well together, even though each major instrument set began as a separate proposal (see figure 4).

Figure 4.– The MMAMA Hawaii team.

Seeing Earth Through the Eyes of an Astronaut

Melissa Dawson

The Human Exploration Science Office within the ARES Directorate has undertaken a new class of handheld camera photographic observations of the Earth as seen from the International Space Station (ISS). For years, astronauts have attempted to describe their experience in space and how they see the Earth roll by below their spacecraft. Thousands of crew photographs have documented natural features as diverse as the dramatic clay colors of the African coastline, the deep blues of the Earth's oceans, or the swirling Aurora Borealis or Australis in the upper atmosphere. Dramatic recent improvements in handheld digital single-lens reflex (DSLR) camera capabilities are now allowing a new field of crew photography: night time-lapse imagery.

During Expedition 28 in 2011, NASA astronauts Mike Fossum and Ron Garan began experimenting with the automated functions of their onboard DSLR cameras. The intent was to take low-light, long-exposure images of the dark side of the Earth not only to document the nighttime activity of our civilization, but also to provide a profound new insight into humanity's presence and its effect on our planet.

The astronauts used a bogen arm in the Cupola of the ISS to stabilize the camera, which was then set to take an image every 3 s for several minutes. The motion of the ISS allowed those still images to be assembled into dramatic movies, providing spectacular new views of the planet that have never been seen by the general public. The downlinked still images were processed by the ARES Crew Earth Observations (CEO) Office for assembly into final videos (figure 1).

As educational supplements to these videos, CEO has also created

- Annotated time-lapse videos highlighting city and place names
- Time-lapse video alongside a Google Earth tour, which plays simultaneously so the user may see both geographical and geological feature names that can be found in the video
- Narrated time-lapse videos that describe features in the video for the viewer

The videos can be accessed in varying resolutions from 640 x 426 to 1980 x 1080 high-definition within the CEO Web site at http://eol.jsc.nasa.gov/Videos/CrewEarthObservationsVideos/. Users may also download the original still images to create their own movies.

Figure 1.– Time-lapsed astronaut photograph of Western Europe (ISS030-E-185649, 03/28/2012, 28 mm), which is part of the video entitled "Aurora Borealis over Western Europe."

The public and media response to this new class of imagery has been dramatic. The videos have been highlighted by numerous publications (*i.e.,* the Chicago Tribune and USA Today); Web sites (*i.e.,* SpaceflightNow.com, Space.com, NASA.gov, and YouTube); and television broadcasts on most major networks, the Discovery Channel, and the Public Broadcasting System. The public outreach benefit to JSC and NASA as a whole is significant. This imagery has excited the public again about the power of spaceflight not only to inspire our children to study things like math and science, but also to highlight how humanity is indeed one species, populating the same planet floating in the dark, cold void of space.

As the mission of the ISS continues, many more dramatic nighttime videos will be produced, vividly illustrating our presence on the Earth like never before and reminding us of our place and obligation to protect our fragile home (figure 2).

Figure 2.– Time-lapse image of Florida and the southeastern United States at night (ISS030-E-6082, 11/24/2011, 19 mm), which is part of the video entitled "Mexico and the Eastern United States."

CEO Sites Mission Management System (SMMS)

Mike Trenchard

Late in fiscal year 2011, the Crew Earth Observations (CEO) team was tasked to upgrade its science site database management tool, which at the time was integrated with the Automated Mission Planning System (AMPS) originally developed for Earth Observations mission planning in the 1980s. Although AMPS had been adapted and was reliably used by CEO for International Space Station (ISS) payload operations support, the database structure was dated, and the compiler required for modifications would not be supported in the Windows 7 64-bit operating system scheduled for implementation the following year.

The Sites Mission Management System (SMMS) is now the tool used by CEO to manage a heritage Structured Query Language (SQL) database of more than 2,000 records for Earth science sites. SMMS is a carefully designed and crafted in-house software package with complete and detailed help files available for the user and meticulous internal documentation for future modifications. It was delivered in February 2012 for test and evaluation. Following acceptance, it was implemented for CEO mission operations support in April 2012. The database spans the period from the earliest systematic requests for astronaut photography during the shuttle era to current ISS mission support of the CEO science payload. Besides logging basic image information (site names, locations, broad application categories, and mission requests), the upgraded database management tool now tracks dates of creation, modification, and activation; imagery acquired in response to requests; the status

97

and location of ancillary site information; and affiliations with studies, their sponsors, and collaborators. SMMS was designed to facilitate overall mission planning in terms of site selection and activation and provide the necessary site parameters for the Satellite Tool Kit (STK) Integrated Message Production List Editor (SIMPLE), which is used by CEO operations to perform daily ISS mission planning.

The CEO team uses the SMMS for three general functions – database queries of content and status, individual site creation and updates, and mission planning (see figures 1 and 2).

Site	Lat1	Lon1	Lat2	Lon2	Lat3	Lon3	Lat4	Lon4	Lat5	Lon5	Lat6	Lon6	Lat7	Lon7	Lat8	Lon8	Lat9	Lon9	Created	Modified	Activate
Aalen, Germany	48.5	10.0																	20120524		
Abu Dhabi, United Arab Emirates	24.4	54.3																	20120524		
Accra, Ghana	5.6	-0.2																	20120524	20120828	
Acraman Impact, SA-AUS	-32.0	135.5																	20120524	20120820	
Ada, OK	34.8	-96.6																	20120524		
Adak, AK	51.8	-176.6																	20120524		
Addis Ababa, Ethiopia	9.0	38.7																	20120524	20120815	
Adriatic Sea	45.0	12.0	46.0	14.0	41.0	21.0	39.0	17.0											20120524		
Aegean Sea	41.0	22.0	41.0	27.0	35.0	27.0	35.0	23.0											20120524		
Aerosols, Bombay region, India	20.0	67.5	20.0	74.0	17.0	74.0	17.0	67.5											20120524		
Aerosols, Lower Yangtze Basin, China	34.0	113.0	34.0	120.0	29.0	120.0	29.0	113.0											20120524		

Figure 1.– Panel of the SMMS interface displaying site name, location, and date information. The CEO sponsors (owners) of science sites can query the database and generate reports from the database through a system of filters and report detail options (see figure 2).

Figure 2.– Panel of the SMMS interface displaying filters for site selections and report detail options.

The CEO administrator of the science site database is able to create or modify the content of sites and activate or deactivate them based on the requirements of the sponsors. The administrator supports and implements ISS mission planning by assembling, reporting, and activating mission-specific site selections for management; deactivating sites as requirements are met; and creating new sites, such as International Charter sites for disasters, as circumstances warrant. In addition to the above CEO internal uses, when site planning for a specific ISS mission is complete and approved,

the SMMS can produce and export those essential site database elements for the mission into XML format for use by onboard Earth-location systems, such as Worldmap.

The design, development, and implementation of the SMMS resulted in a superior database management system for CEO science sites by focusing on the functions and applications of the database alone instead of integrating the database with the multipurpose configuration of the AMPS. Unlike the AMPS, it can function and be modified within the existing Windows 7 environment. The functions and applications of the SMMS were expanded to accommodate more database elements, report products, and a streamlined interface for data entry and review. A particularly elegant enhancement in data entry was the integration of the Google Earth application for the visual display and definition of site coordinates for site areas defined by multiple coordinates. Transfer between the SMMS and Google Earth is accomplished with a Keyhole Markup Language (KML) expression of geographic data (see figures 3 and 4). Site coordinates may be entered into the SMMS panel directly for display in Google Earth, or the coordinates may be defined on the Google Earth display as a mouse-controlled polygonal definition and transferred back into the SMMS as KML input. This significantly reduces the possibility of errors in coordinate entries and provides visualization of the scale of the site being defined.
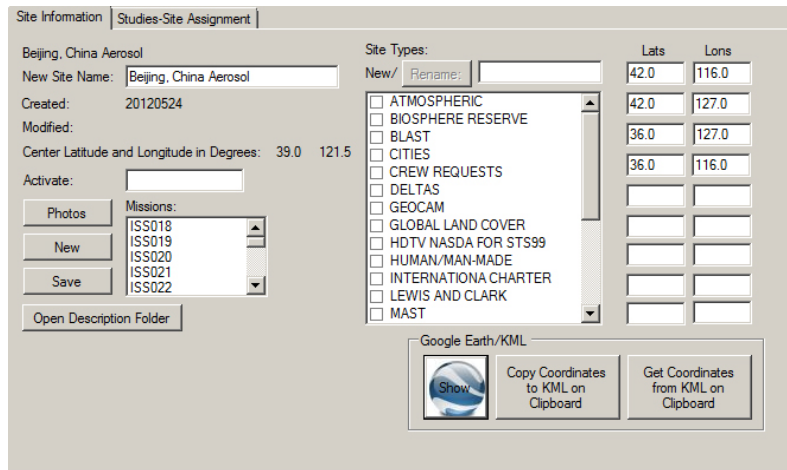

Figure 3.– Panel of the SMMS interface displaying a site's multiple coordinates and the interface with Google Earth for their definition and display via a KML expression of geographic information.
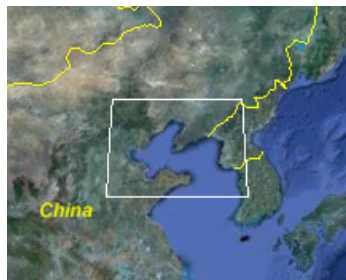

Figure 4.– Section of a Google Earth display of the Beijing, China, aerosol site coordinates.

CEO now has a powerful tool for managing and defining sites on the Earth's surface for both targets of astronaut photography or other onboard remote sensing systems. It can also record and track results by sponsor, collaborator, or type of study.

STK Integrated Message Production List Editor (SIMPLE) for CEO Operations

Mike Trenchard, James Heydorn

Late in fiscal year 2011, the Crew Earth Observations (CEO) team was tasked to upgrade and replace its mission planning and mission operations software systems, which were developed in the Space Shuttle era of the 1980s and 1990s. The impetuses for this change were the planned transition of all workstations to the Windows 7 64-bit operating system and the desire for more efficient and effective use of Satellite Tool Kit (STK) software required for reliable International Space Station (ISS) Earth location tracking. An additional requirement of this new system was the use of the same SQL database of CEO science sites from the SMMS, which was also being developed.

STK Integrated Message Production List Editor (SIMPLE) is the essential, all-in-one tool now used by CEO staff to perform daily ISS mission planning to meet its requirement to acquire astronaut photography of specific sites on Earth. The sites are part of a managed, long-term database that has been defined and developed for scientific, educational, and public interest. SIMPLE's end product is a set of basic time and location data computed for an operator-selected set of targets that the ISS crew will be asked to photograph (photography is typically planned 12 to 36 hours out).

The CEO operator uses SIMPLE to (a) specify a payload operations planning period; (b) acquire and validate the best available ephemeris data (vectors) for the ISS during the planning period; (c) ingest and display mission-specific site information from the CEO database; (d) identify and display potential current dynamic event targets as map features; (e) compute and display time and location information for each target; (f) screen and select targets based on known crew availability constraints, obliquity constraints, and real-time evaluated constraints to target visibility due to illumination (sun elevation) and atmospheric conditions (weather); and finally (g) incorporate basic, computed time and location information for each selected target into the daily CEO Target List product (message) for submission to ISS payload planning and integration teams for their review and approval prior to uplink. See figure 1.
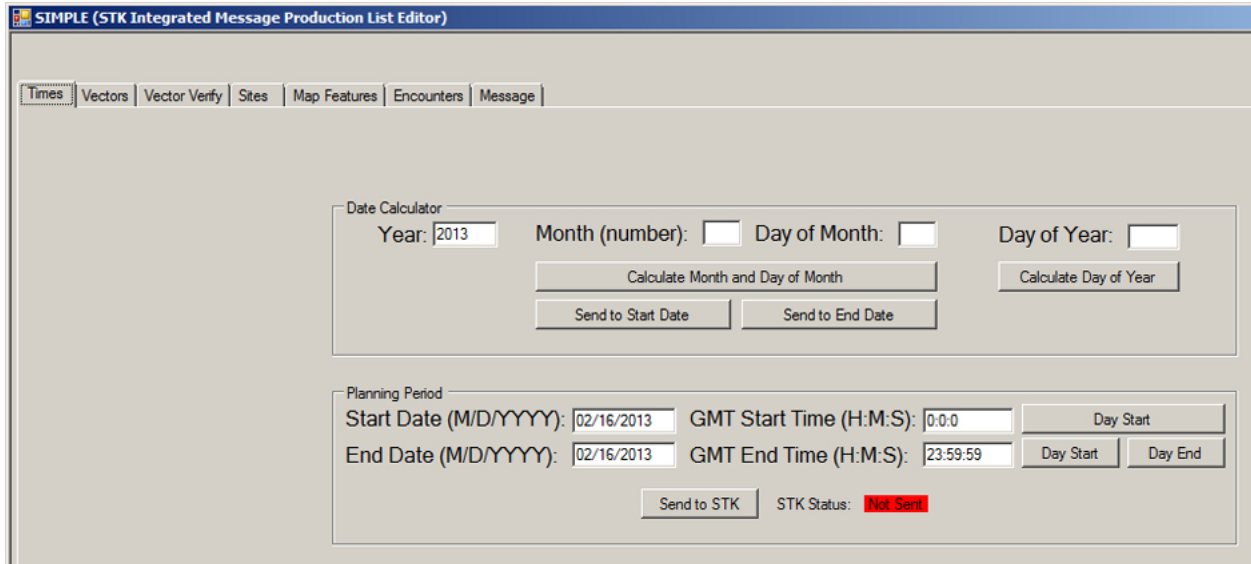
Figure 1.– Section of the SIMPLE user interface illustrating the functional tabs available to the CEO operator for daily target list production.

SIMPLE requires and uses the following resources: an ISS mission planning period Greenwich Mean Time start date/time and end date/time), the best available ISS mission ephemeris data (vectors) for that planning period, the STK software package configured for the ISS, and an ISS mission-specific subset of the CEO sites database (see figure 2).
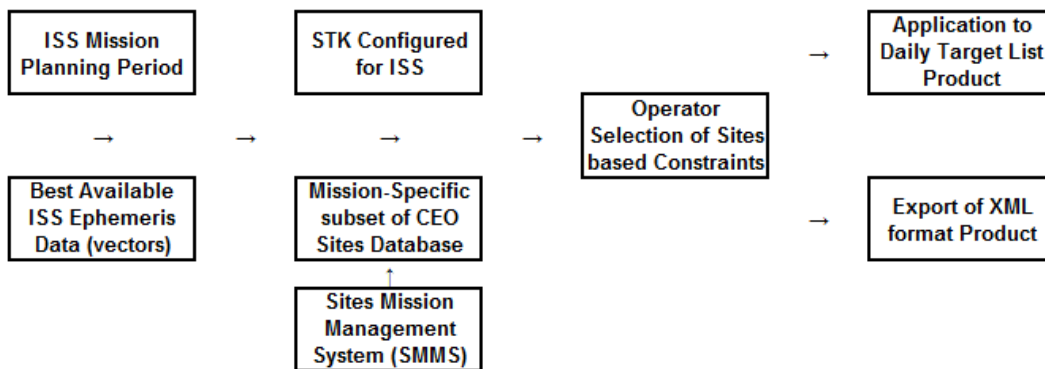
Figure 2.– Basic input and operations process flow for SIMPLE products.

The primary advantages realized by the development and implementation of SIMPLE into the CEO payload operations support activity are a smooth transition to the Windows 7 operating system upon scheduled workstation refresh; streamlining of the input and verification of the current ISS ephemeris (vector data); seamless incorporation of selected contents of the SQL database of science sites; the ability to tag and display potential dynamic event opportunities on orbit track maps; simplification of the display and selection of encountered sites based on crew availability, illumination, obliquity, and weather constraints; the incorporation of high-quality mapping of the

Earth with various satellite-based datasets for use in describing targets; and the ability to encapsulate and export the essential selected target elements in XML format for use by onboard Earth-location systems, such as Worldmap. See figure 3.
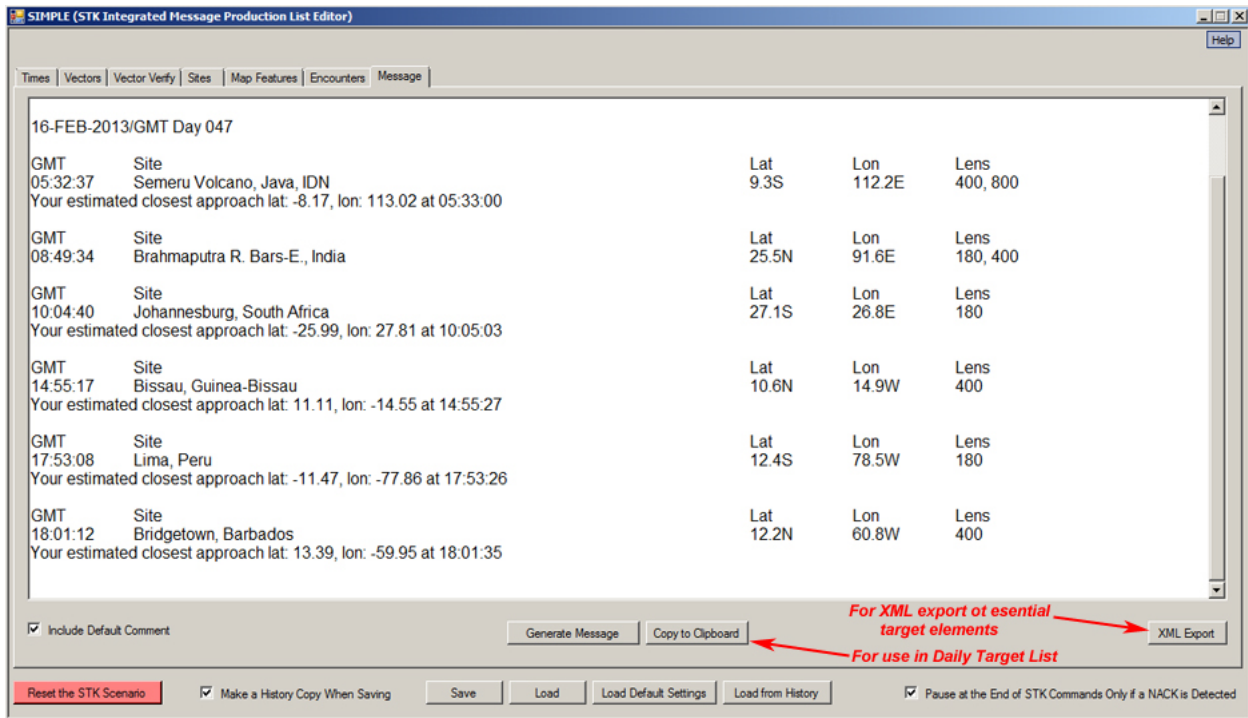
Figure 3.– Example of the SIMPLE Message tab with screened and selected target elements ready for incorporation in the daily target list product or for export as an XML-format product.

SIMPLE is a carefully designed and crafted in-house software package that includes detailed help files for the user and meticulous internal documentation for future modifications. It was delivered in February 2012 for test and evaluation. Following acceptance, it was implemented for CEO mission operations support in May 2012.

Rewriting the Landform History of One of Africa's Three Largest Basins

Justin Wilkinson

Main Perspective

The Kalahari Basin in southern Africa – one of the largest basins in Africa, along with the Congo and Chad basins – has attracted attention since David Livingstone traveled through the area in the 1840s. It is a semiarid desert with a large freshwater swampland known as the Okavango Swamp (150 km radius). This prominent megafan (a fan with radii >100 km), with its fingers of dark green forests projecting into the dun colors of the dunes of the Kalahari semi-desert, has been well photographed by astronauts over the years (figure 1). The study area in the northern Kalahari basin is centered on the Okavango megafan of northwest Botswana, whose swampland has become well known as an African wildlife preserve of importance to biology and tourism alike.
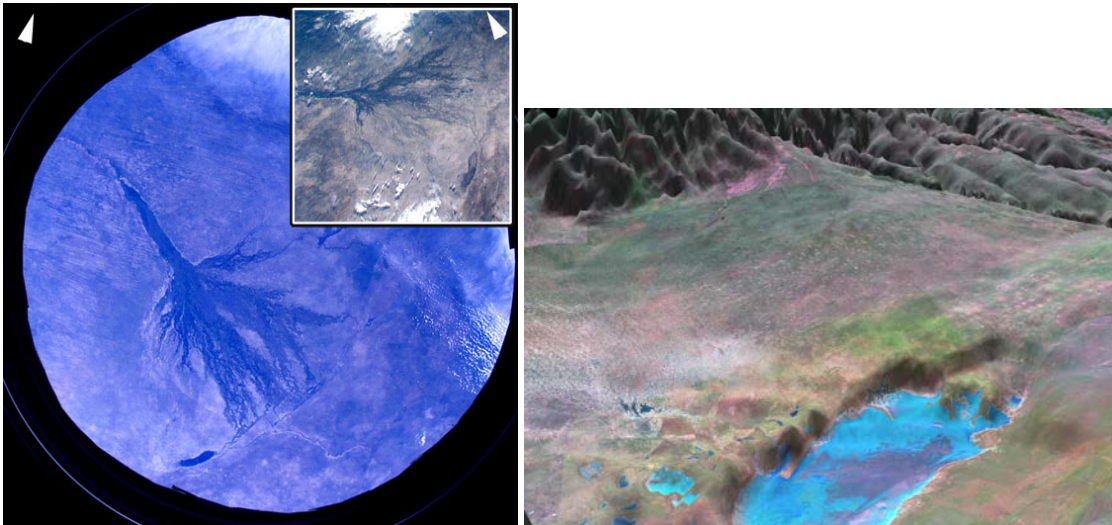
Figure 1.– Northern Kalahari Desert megafans.
(Left) Fingers of riverine forest of the Okavango megafan mark the distributaries of one of the prime megafan examples on Earth.
(Right) Vertically exaggerated Shuttle Radar Topography Mission (SRTM)-based oblique view of the Cubango megafan, the largest fan in the study area (310 km radius), with Etosha dry lake depression in the foreground.

The Okavango River is unusual because it has deposited not one but two megafans along its course: the Okavango megafan and the Cubango megafan (figure 1). The Okavango megafan is one of only three well-known megafans in Africa. Megafans on Earth were once thought to be rare, but recent research has documented 68 in Africa alone. Eleven megafans, plus three more candidates, have been documented in the area immediately surrounding the Okavango feature. These 11 megafans occupy the flattest and smoothest terrains adjacent to the neighboring upland and stand out as the

darkest areas in the roughness map of the area (figure 2). Megafan terrains occupy at least 200,000 km^2 of the study area.

The roughness map shown in figure 2 is based on an algorithm used first on Mars to quantify topographic roughness. Research of Earth's flattest terrains is just beginning with the aid of such maps, and it appears that these terrains are analogous to the flattest regions of Mars.
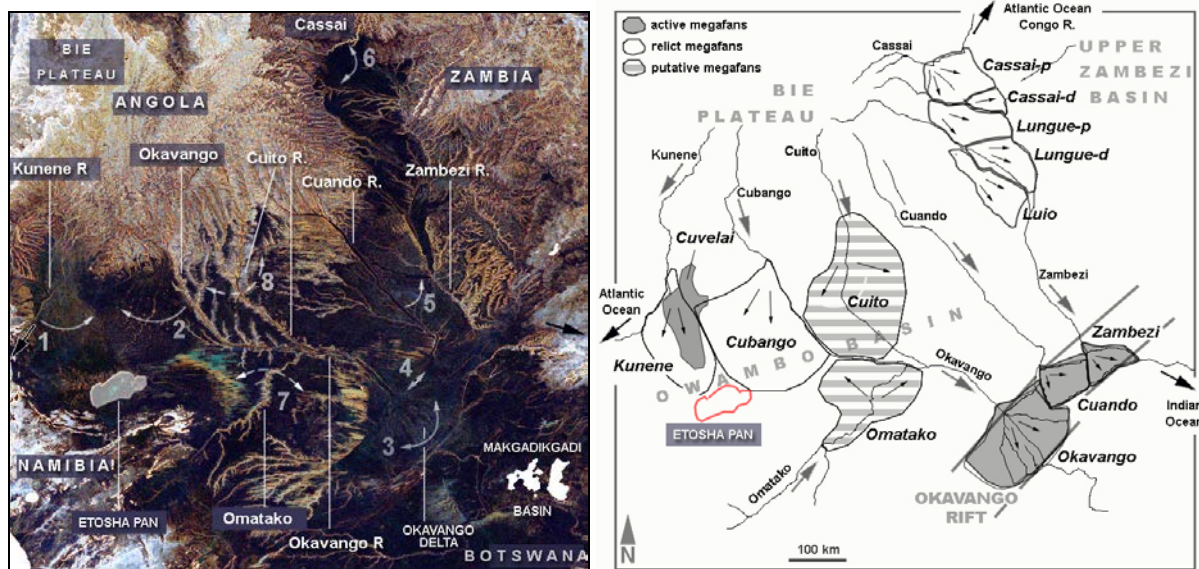

Figure 2.– Megafans as the flattest and smoothest terrains. Mars roughness map algorithms were used to construct this Kalahari Basin roughness map.
(Left) Most of the darkest zones represent large fluvial fans. Numbers refer to those fans where normal river avulsion directs discharge of major rivers into <u>separate</u> subbasins. Arrows indicate channel sweep on each megafan. Brighter tones are eroded uplands and dunefields with longer baseline roughness (see Wilkinson et al., 2006).
(Right) Megafan types (named after formative rivers). Differences in megafan type in each subbasin are striking: active in the rift, relict in the other basins, and two putative megafans. This sample probably points to likely megafan variability in African basins generally.

Implications

1. The variability in depositional style in each subbasin may apply Africa-wide: rift megafan length is dominated by rift width, whereas Owambo subbasin megafans are probably controlled by upland basin size (figure 2); Zambezi subbasin megafans appear more like foreland basin types, with the position of the trunk river controlling size.

2. These perspectives were successfully applied to identify the largest megafan in the group (Cubango, figures 1 and 2), a fan that was sufficiently overprinted by dunes and dry lakelets not to be detectable remotely. Such undertsanding can probably be applied on Mars, where Earth experience suggests megafans ought to exist.

3. Sweep angles of rivers on megafans drastically change the hydrology in some subbasins (figure 3): when the Cubango and Kunene rivers were oriented to the Etosha Pan, it was probably a permanent water body. Now that the rivers are oriented away from the basin, 93 percent of the discharge area from the pan's northerly (main) source area is gone.

4. Biotic contact between major river systems was probably controlled *by megafans situated on divides*: various fish species that originated in the Congo basin are now found in the Upper Zambezi R., and *vice versa*, apparently because of river switching behavior on the Cassai megafan (6, figure 3) that has mediated migrations both to the south and the north.

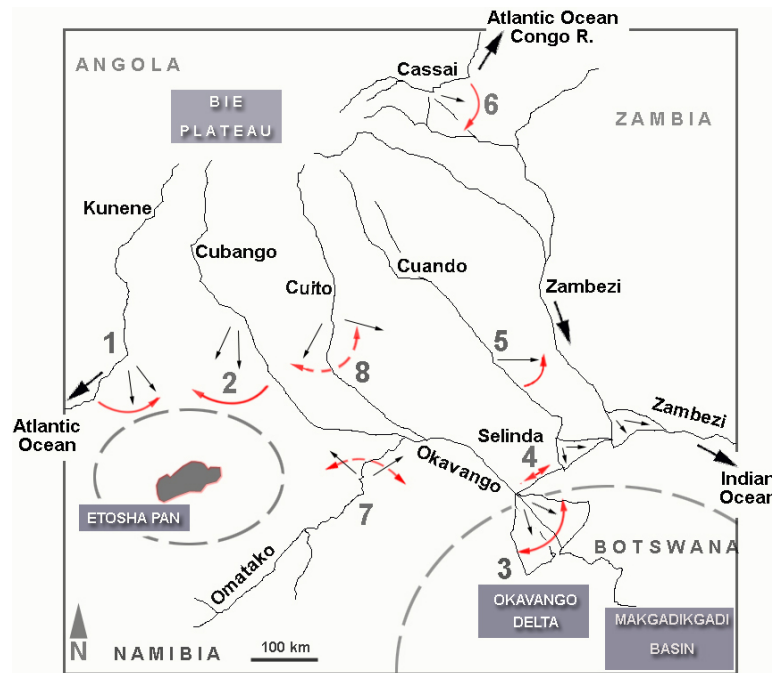

Figure 3.– Arrows indicate channel "sweep-angles" on megafans located astride basin divides. This unappreciated characteristic of megafan location appears to explain many interbasin aquatic species' distributions (Wilkinson et al., in prep.).

Megafans and Trumpeter Bird Biodiversity—Psophia Phylogeography and Landscape Evolution in Amazonia

Justin Wilkinson

Similar geographic evolution of land surfaces and bird paleogeography

Based on geomorphic character and mapped geology, geologists have interpreted the landscape surrounding the Andes Mountains as becoming progressively younger to the East. These sedimentary materials filled the late Miocene swampland that formerly occupied central and western Amazonia. Apart from the ancient landscapes of the Guiana Highlands (top right, figure 1a), Zone Ac is the oldest, followed by Zone Aw, within which megafan Jw is older than megafan Je (figure 1a).

DNA-based paleogeography of the trumpeters shows that younger clades diverge from parent lineages with increasing distance from the Andes chain. Thus, *Psophia napensis* diverges from the *P. crepitans* parent, and *P. ochroptera* diverges from *P. napensis*. The *P. ochroptera* population is confined solely to the Je megafan (figure 1a). The same trend is seen on the south side of the Amazon depression.

Since the timing of the events seems to be of exactly the same order [post-Miocene for the land surfaces and trumpeter divergence within the last 3 million years (figure 1d)], it seems reasonable to think that the megafans provided the substrate on which new bird lineages could speciate. Such physical controls of evolution are becoming more important in the understanding of biodiversity.

Major past rivers identified on the basis of bird paleogeography

In five of the seven trumpeter populations, most boundaries between the lineages are strikingly located at major modern rivers (figure 1c). However, along two of these boundaries – between *P. napensis* and *P. crepitans* and between *P. napensis* and *P. ochroptera* – no modern river exists. We examined megafan margins for the existence of past large rivers that might occupy these locations indicated by the trumpeter phylogeography.

Both locations showed prominent signs of very large rivers (*i.e.*, especially large meanders scars), on floodplains trending in directions that act as boundaries between the abovementioned clades – along two prior courses indicated by single-headed arrows in figure 1a. These paleo-rivers suggest, in effect, that the Japurá River has at different times in the past been oriented toward the Rio Negro.

This is a remarkable instance of geological understanding being advanced through interpretation of a DNA-based biogeography.
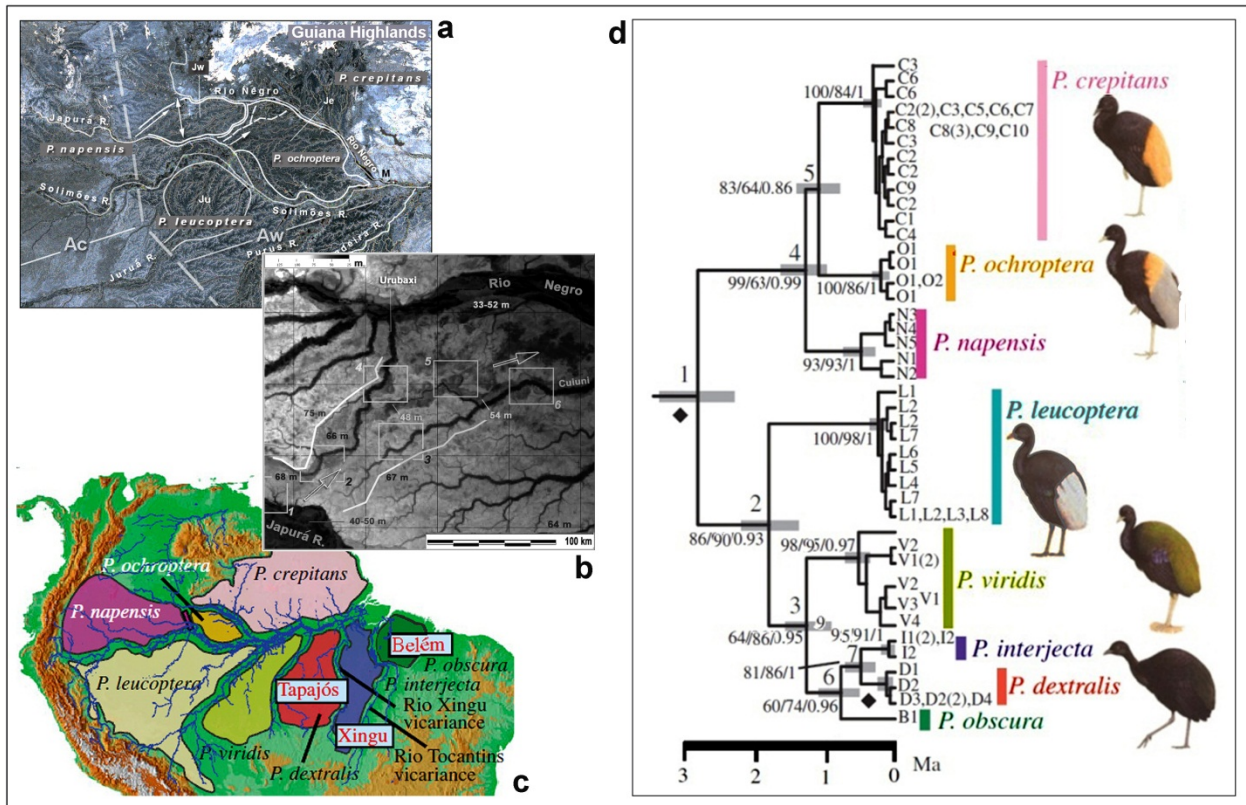
a—Topographic roughness map of South America. Roughness map (based on SRTM data and algorithms developed for Mars) shows well-developed modern megafan landscapes to the north and south of Amazonia and the preferred location of major trunk rivers located furthest from the Andes Mountains; *i.e.*, against margins of the Guiana and Brazilian shields (resulting from megafan progradation eastward). The map shows the rough and steep landscapes (*lightest tones*) and the smooth, lowest-sloped lowland landscapes, dominated by megafan plains and floodplains (*darkest tones*).

b—Newly identified paleo-river. SRTM-based topographic altitude map – lighter tones are higher surfaces, darker tones are lower surfaces. Paleo-river floodplain (between angular lines) connects the lower Japurá R. (near its confluence with the Solimões R.) to the middle Rio Negro, a distance of ~200 km. Open arrows show the direction of paleo-river flow. Spot heights show that the paleo-river floodplain lies at an altitude between that of the modern Japurá R. (40–45 m) and the upper surfaces of megafan *Jw* (75 m) due west.

c—Palaeobiogeographic model of terrestrial environments of Amazonia, showing successive clades of *Psophia*. Map shows trumpeter phylogeography at 0.8–0.3 Ma, in which *Psophia crepitans* represents the parent. Thereafter, *P. leucoptera* and *P. napensis* diverge from this parent (at 2.0-1.0 Ma and 1.3-0.8 Ma, respectively); followed by divergence of *P. ochroptera* at ~1.0-0.7. Each lineage is separated by a major river. (In other parts of Amazonia the Tapajós, Tocantins, and Xingu rivers are established, isolating three successively younger endemic trumpeter species.) From Ribas et al. (2011).

d—Phylogeny and phylogeography of *Psophia* lineages in approximately the last 3 million years. Chronogram derived from Baysian analysis of cyt b and ND2 sequences (2181 bp). Calibration derived from analysis of *RAG2* nuclear gene. Adapted from Ribas et al. (2011).

Figure 1.– Amazonia—topography and trumpeter bird DNA.

The International Space Station: A Unique Platform for Remote Sensing of Natural Disasters

William L. Stefanov, Cynthia A Evans

Assembly of the International Space Station (ISS) was completed in 2012, and the station is now fully operational as a platform for remote sensing instruments tasked with collecting scientific data about the Earth system. Remote sensing systems are mounted inside the ISS, primarily in the U.S. Destiny Module's Window Observational Research Facility (WORF), or are located on the outside of the ISS on any of several attachment points.

While NASA and other space agencies have had remote sensing systems orbiting Earth and collecting publicly available data since the early 1970s, these sensors are carried onboard free-flying, unmanned satellites. These satellites are traditionally placed into Sun-synchronous polar orbits that allow imaging of the entire surface of the Earth to be repeated with approximately the same Sun illumination (typically local solar noon) over specific areas, with set revisit times that allow uniform data to be taken over long time periods and enable straightforward analysis of change over time.

In contrast, the ISS has an inclined, Sun-asynchronous orbit (the solar illumination for data collections over any location changes as the orbit precesses) that carries it over locations on the Earth between approximately 52°north and 52° south latitudes (figure 1). The ISS is also unique among NASA orbital platforms in that it has a human crew. The presence of a crew provides options not available to robotic sensors and platforms, such as the ability to collect unscheduled data of an unfolding event using handheld digital cameras as part of the Crew Earth Observations (CEO) facility and on-the-fly assessment of environmental conditions, such as cloud cover, to determine whether conditions are favorable for data collection. The crew can also swap out internal sensor systems installed in the WORF as needed.

The ISS orbit covers more than 90 percent of the inhabited surface of the Earth, allowing the ISS to pass over the same ground locations at different times of the day and night. This is important for two reasons: 1) certain surface processes (*i.e.,* development of coastal fog banks) occur at times other than local solar noon, making it difficult to collect relevant data from traditional satellite platforms, and 2) it provides opportunities for the ISS to collect data for short-duration events, such as natural disasters, that polar-orbiting satellites may miss due to their orbital dynamics – in essence, the ISS can be "in the right place at the right time" to collect data.

An immediate application of ISS remote sensing data collection is that the data can be used to provide information for humanitarian aid after a natural disaster. This activity contributes directly to the station's Benefits to Humanity mission.

Figure 1.– Representation of polar, Sun-synchronous orbits (e.g., Landsat 7) and the inclined equatorial, Sun-asynchronous orbit of the ISS (image center).

The International Charter, Space and Major Disasters (also known as the International Disaster Charter, or IDC) is an agreement between agencies of several countries to provide – on a best-effort basis – remotely sensed data related to natural disasters to requesting countries in support of disaster response. In the United States, the lead agency for interaction with the IDC is the United States Geological Survey (USGS); when an IDC request, or activation, is received, the USGS notifies the science teams for NASA instruments with targeting information for data collection. In the case of the ISS, Earth scientists in the JSC ARES Directorate, in association with the ISS Program Science Office, coordinate targeting and data collection with the USGS. If data is collected, it is passed back to the USGS for posting on its Hazards Data Distribution System and made available for download.

The ISS was added to the USGS's list of NASA remote sensing assets that could respond to IDC activations in May 2012. Initially, the NASA ISS sensor systems available to respond to IDC activations included the ISS Agricultural Camera (ISSAC), an internal multispectral visible-near infrared wavelength system mounted in the WORF; CEO, a project that collects imagery through the ISS windows using off-the-shelf handheld digital visible-wavelength cameras; and the Hyperspectral Imager for the Coastal Oceans (HICO), a visible to near-infrared system mounted externally on the Japanese Experiment Module – Exposed Facility. Since May 2012, there have been 37 IDC activations; ISS sensor systems have collected data for 10 of these events (figure 2).
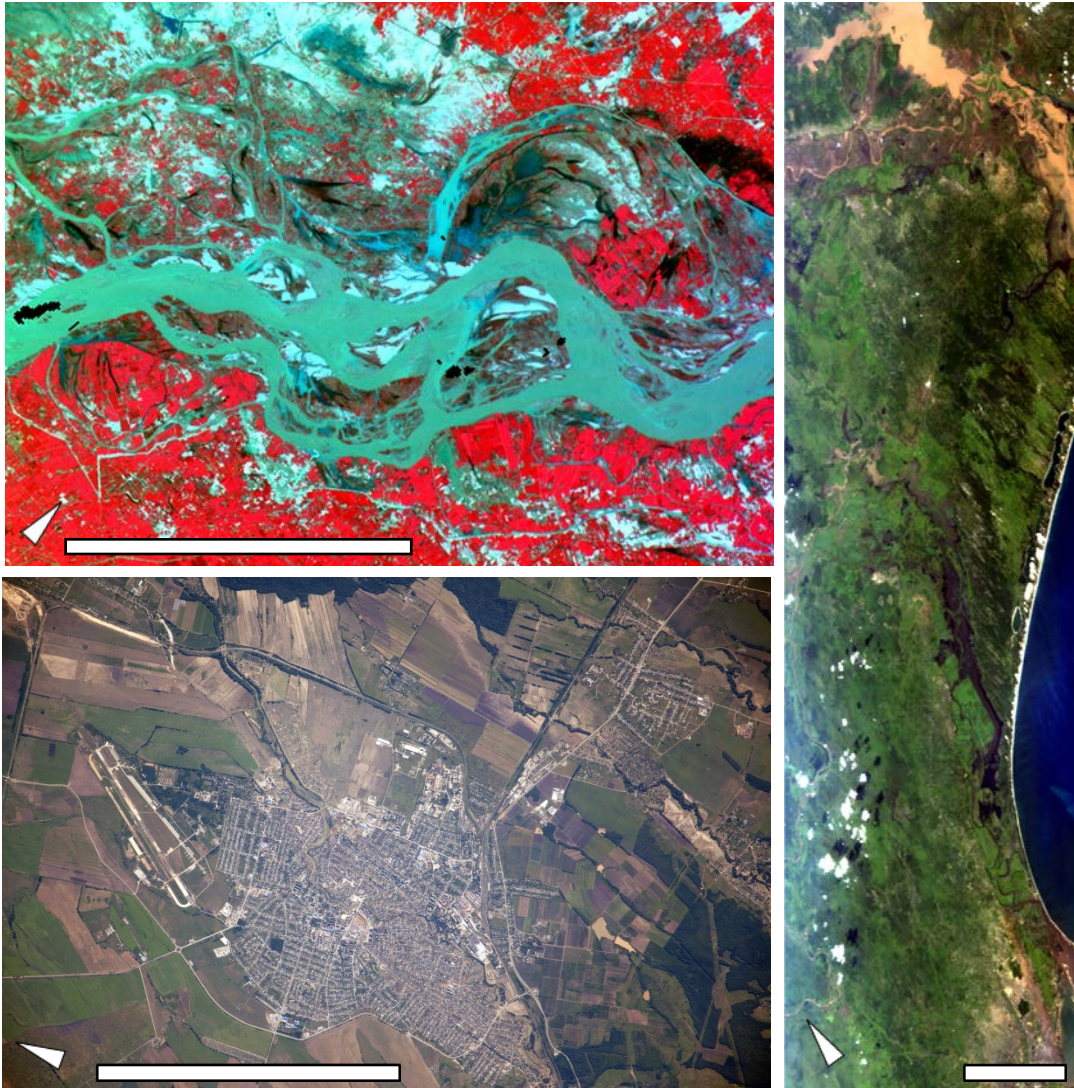
Figure 2.– Three IDC flooding events as seen from sensors on the ISS.
Top left: ISSAC, flooding in Pakistan acquired September 9, 2012, scale bar is 10 km.
Lower left: CEO, flooding in Krymsk, Russia, acquired July 10, 2012, scale bar is 5 km.
Right: HICO, flooding in Mozambique acquired February 3, 2013, scale bar is 20 km.
Pointers indicate north for each image.

The ISSAC completed its prime mission at the end of 2012 and has been replaced in the WORF with the automated ISS SERVIR Environmental Research and Visualization System, or ISERV, Pathfinder. The ISERV Pathfinder is a pointable, high spatial resolution (~3 m/pixel) camera and telescope system designed primarily as a technology demonstration. Its primary mission is to provide imagery to developing nations as part of the NASA and U.S. Agency for International Development SERVIR (Spanish for "to serve") program, but it can also respond to IDC activations.

The ISS is intended to be a test bed for multiple users over its lifetime, which means that no single remote sensing system has a permanent internal or external berth. This scheduled turnover provides

for development of new remote sensing capabilities relevant to both research and applied science – including disaster response – and represents a significant contribution to continuance and enhancement of the NASA mission to investigate changes on our home planet.

Clearance Analysis of Node 3 Aft CBM to the Stowed FGB Solar Array

Donn Liddle

In early 2011, the ISS Vehicle Configuration Office began considering the relocation of the Permanent Multipurpose Module (PMM) to the aft facing Common Berthing Mechanism (CBM) on Node 3 to open a berthing location for visiting vehicles on the Node 1 nadir CBM. In this position, computer-aided design (CAD) models indicated that the aft end of the PMM would be only a few inches from the stowed Functional Cargo Block (FGB) port solar array (see figure 1).
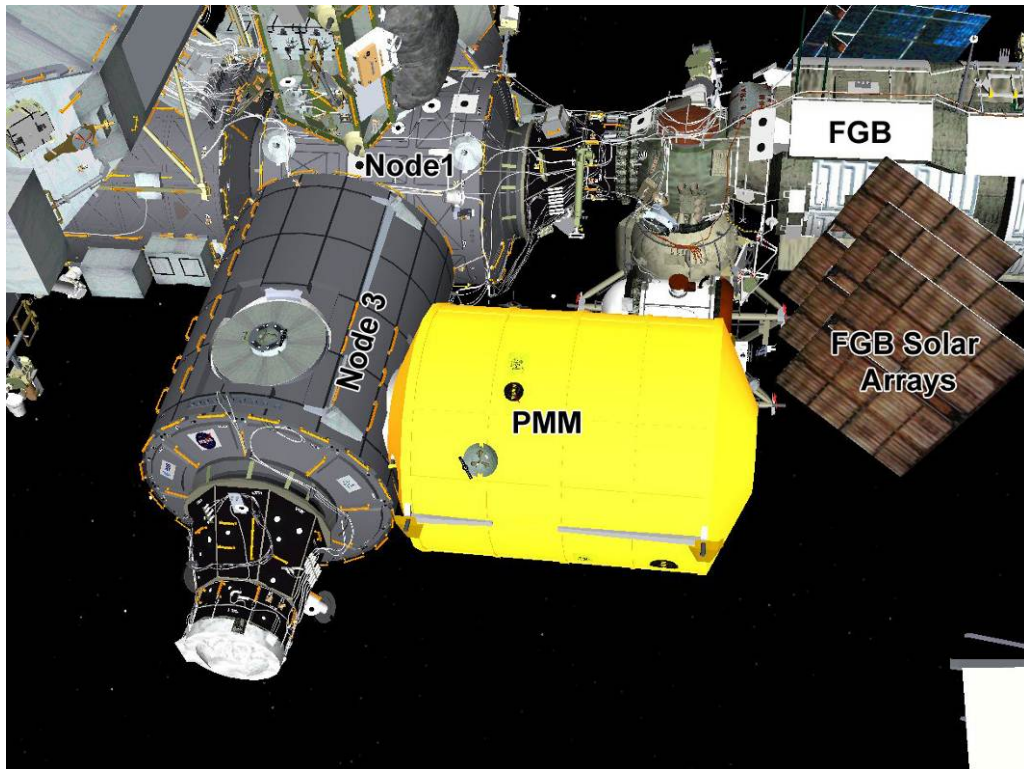

Figure 1.– Proposed relocation site for PMM with minimum clearance to FGB solar arrays.

To validate the CAD model clearance analysis, in the late summer of 2011 the Image Science and Analysis Group (ISAG) was asked to determine the true geometric relationship between the on-orbit aft facing Node 3 CBM and the FGB port solar array (see figure 2).
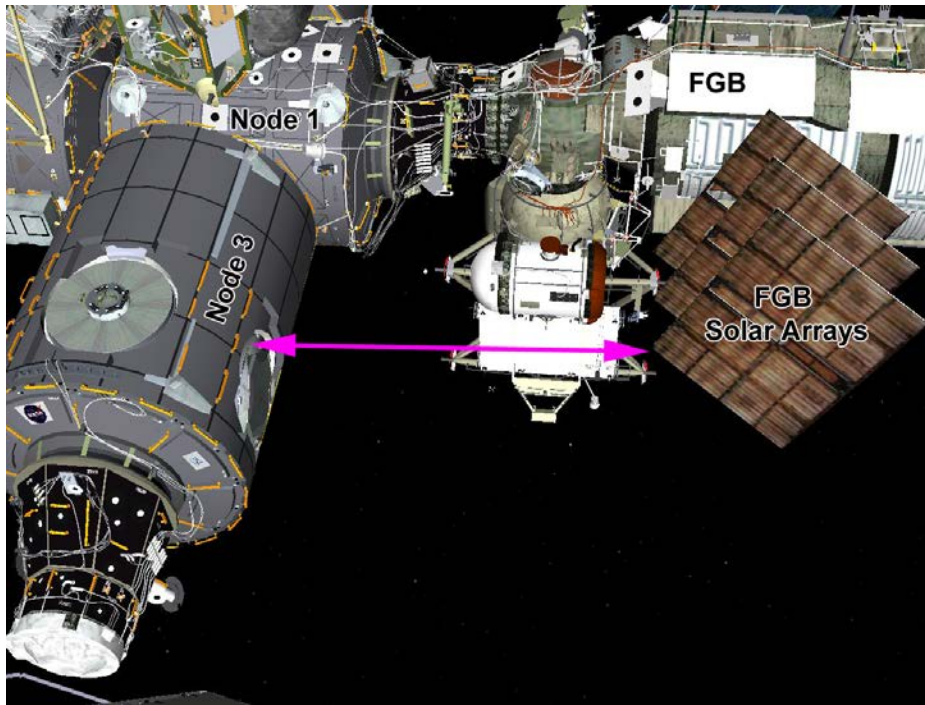
Figure 2.– Photogrammetric analysis of the aft face of Node 3, port side of Node 1, port side of pressurized mating adapter 1 (PMA1), port side of the FGB hemisphere, and port FGB solar arrays to determine the absolute location of the port FGB solar arrays relative to Node 3.

The desired measurements could be computed easily by photogrammetric analysis if current imagery of the ISS hardware were obtained. Beginning in the fall of 2011, ISAG used the Dynamic Onboard Ubiquitous Graphics (DOUG) program to design a way to acquire imagery of the aft face of Node 3, the aft end-cone of Node 1, the port side of pressurized mating adapter 1 (PMA1), and the port side of the FGB out to the tip of the port solar array using cameras on the Space Station Remote Manipulator System (SSRMS). This was complicated by the need to thread the SSRMS under the truss, past Node 3 and the Cupola, and into the space between the aft side of Node 3 and the FGB solar array to acquire more than 100 images from multiple positions.

To minimize the number of SSRMS movements, the Special Purpose Dexterous Manipulator (SPDM) would be attached to the SSRMS. This would make it possible to park the SPDM in one position and acquire multiple images by changing the viewing orientation of the SPDM body cameras using the pan/tilt units on which the cameras are mounted. Using this implementation concept, ISAG identified four SSRMS/SPDM positions from which all of the needed imagery could be acquired. Based on a photogrammetric simulation, it was estimated that the location of the FGB solar array could be measured within an accuracy of about 1 in. in each axis relative to the ISS Analysis Coordinate System (ISSACS).

In October 2011, a proposed image-acquisition plan was drafted by ISAG and released for review. The ISS Robotics flight control team (ROBO) proposed minor changes to SPDM positions 1 and 4 to meet ISS proximity requirements. The updated image acquisition plan and draft chit were

presented to and approved by the Systems Working Group (SWG) November 18 and were sent to the Vehicle Configuration Board (VCB) in early December 2011.

Working with ROBO on 3 successive days (February 21, 22, and 23), ISAG collected 161 images of the ISS. Approximately 40 images were collected from each of the four different SSRMS/SPDM positions, with each set mapping the region from the Node 3 end cone, across Node 1, along the forward port side portion of the FGB, and out the port side FGB solar arrays.

From this imagery, the best 80 images were selected for use in the analysis. The images were radiometrically enhanced to improve color and contrast and loaded into the FotoG analysis software along with the camera parameters and control data, which consisted of the coordinates for 54 handrail attachment bolts on the aft face of Node 3, in the ISSACS coordinate system.

The results of this analysis produced the measured coordinates of 116 points distributed across the face of the FGB solar array panels (see figure 3) along with propagated uncertainty estimates in each coordinate axis. These results were sent to the ISS Vehicle Configuration Office, which sent them to the Configuration Analysis Modeling and Mass Properties (CAMMP) team for comparison with the Russian-provided CAD model for the retracted FGB solar arrays.
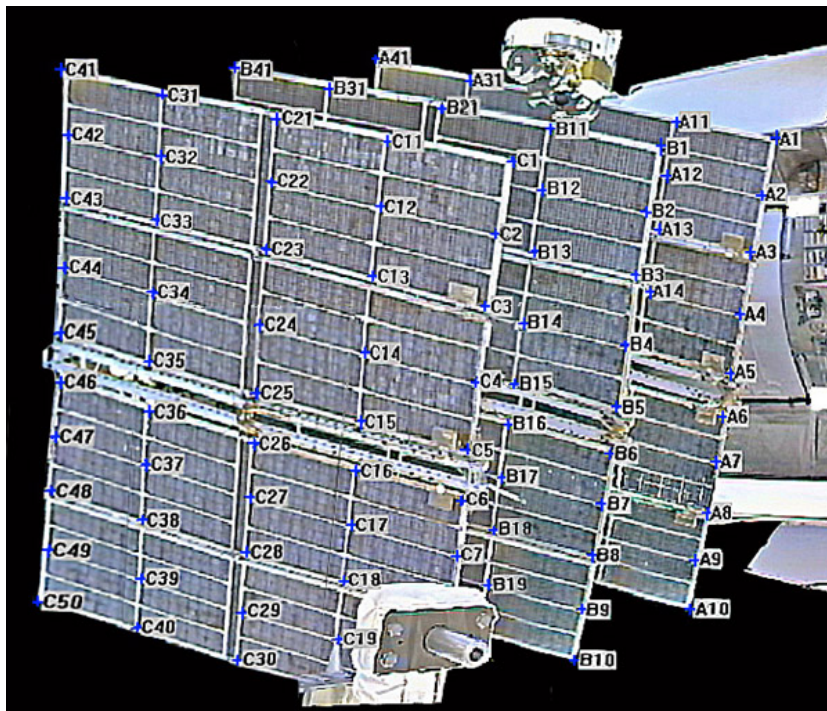

Figure 3.– Points measured on the port FGB solar array in the ISSACS coordinate system defined by Node 3

The CAMMP analysis unexpectedly showed that the measured location of the port FGB solar array was up to 41-in. further outboard than the design and was slightly twisted about its rotational axis (as shown in figures 4 and 5).
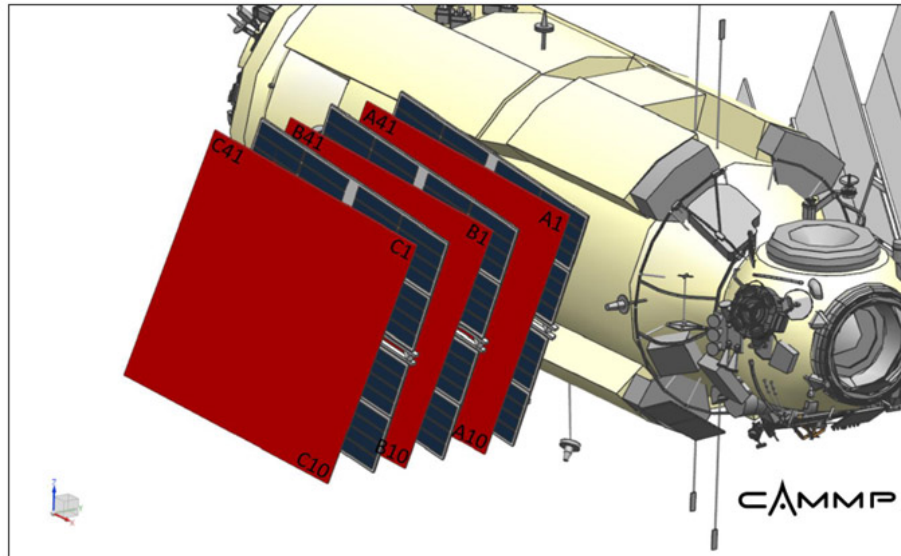
Figure 4.– Delta configuration between the measured coordinates of the
port solar array (shown in red) relative to the CAD design models (shown in blue).
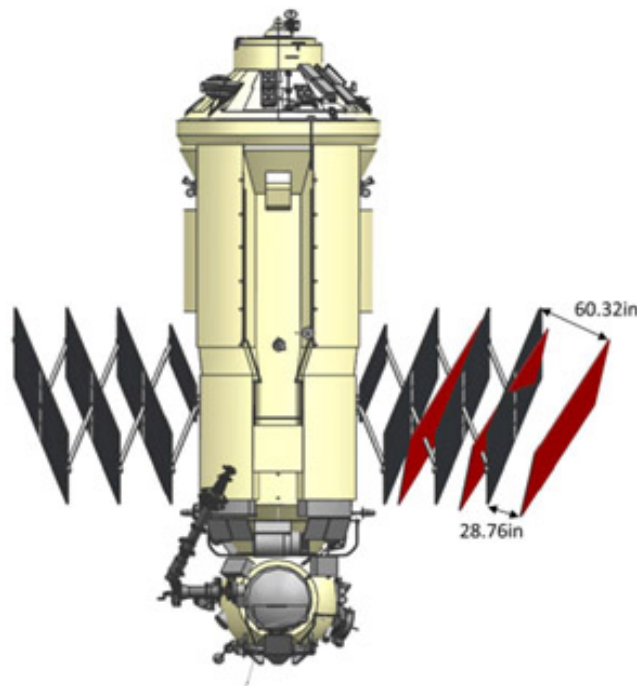
Figure 5.– Delta configuration between the measured coordinates of the
port solar array (shown in red) relative to the CAD design models (shown in gray).

The unexpected comparison results produced some initial concern regarding the accuracy of the photogrammetric measurements. To verify the measured results, ISAG personnel conducted a second analysis using just the imagery of the solar arrays in an arbitrary coordinate system defined

by the three corner points of the inboard-most panel, with the design distance between points A1 and A10 as the only scale (see figure 6).
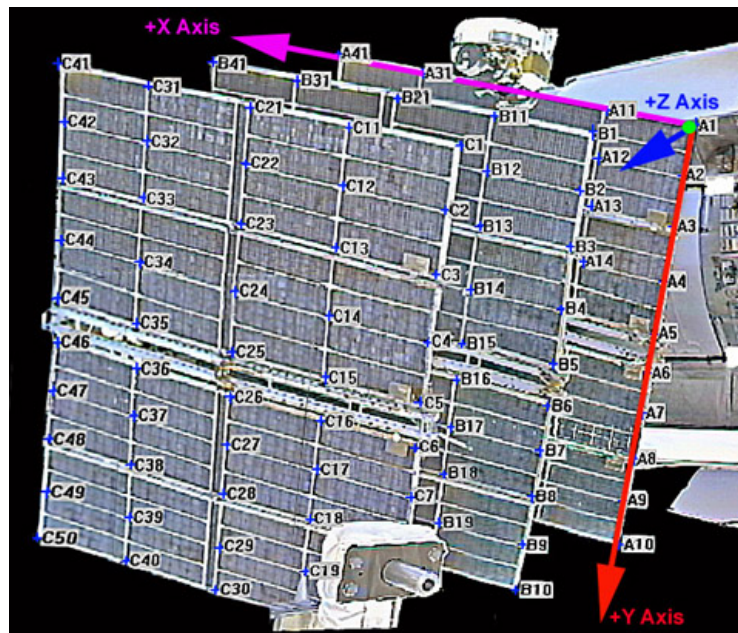

Figure 6.– Control for second analysis.

The new measurements agreed with the original results to within less than 1 in. RMS in each axis, confirming the original solar array measurements.

ISAG produced a final report for the ISS Vehicle Configuration Office documenting an apparent anomaly in the retracted configuration of the port FGB solar arrays. A copy of the measurement report was translated and sent to the Russian Space Agency. During a Vehicle Integrated Performance and Resources (VIPeR) teleconference September 24, 2012, the Russians acknowledged receipt of a translated copy of the ISAG report. The Russian representative stated that the head of the solar array design team claimed that the measured configuration was impossible unless the structure was physically broken. The Russians acknowledged that they had no expertise in photogrammetry, so the analysis technique employed was a "black box" to them, and they did not know how to use the ISAG results. They asked for a single image in which the overextension of the port solar array could be obviously seen.

On November 10, 2012, during a face-to-face meeting with their Russian counterparts at JSC, ISAG presented nadir-view imagery of the FGB acquired during Space Shuttle rendezvous. Using the known width of the pressurized portion of the FGB as a scale, this analysis clearly showed that the port FGB solar array was extended outboard further than the Russian design for the retracted solar array (see figure 7).
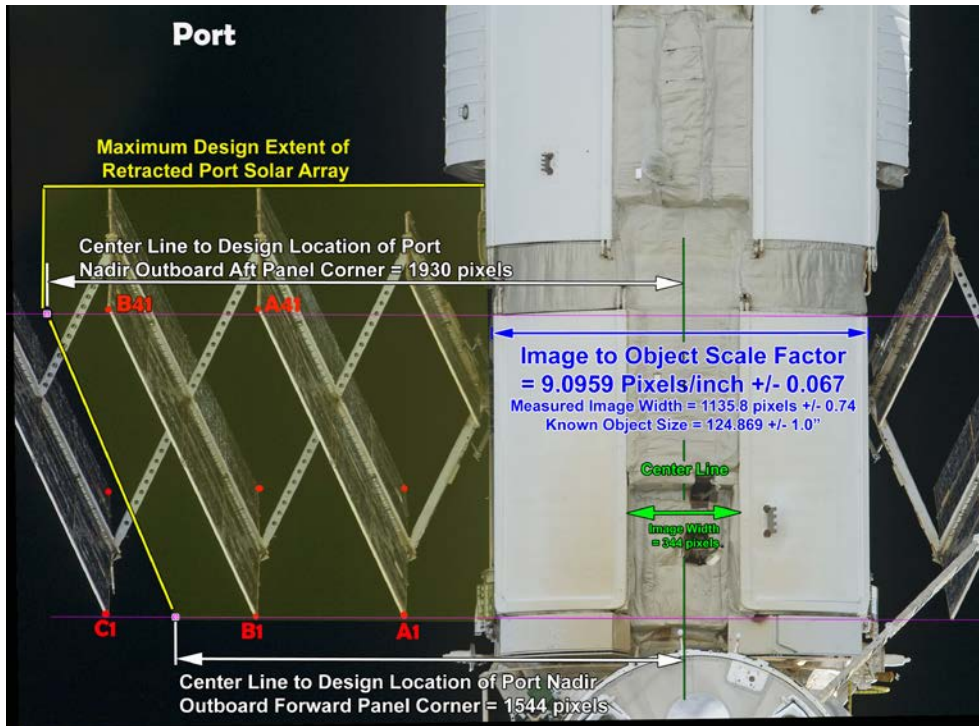
Figure 7.– Single camera measurement of the port FGB solar array.

The same photo contained the image of the starboard FGB solar array. A similar analysis revealed that it also exceeded the designed retraction state (see figure 8).
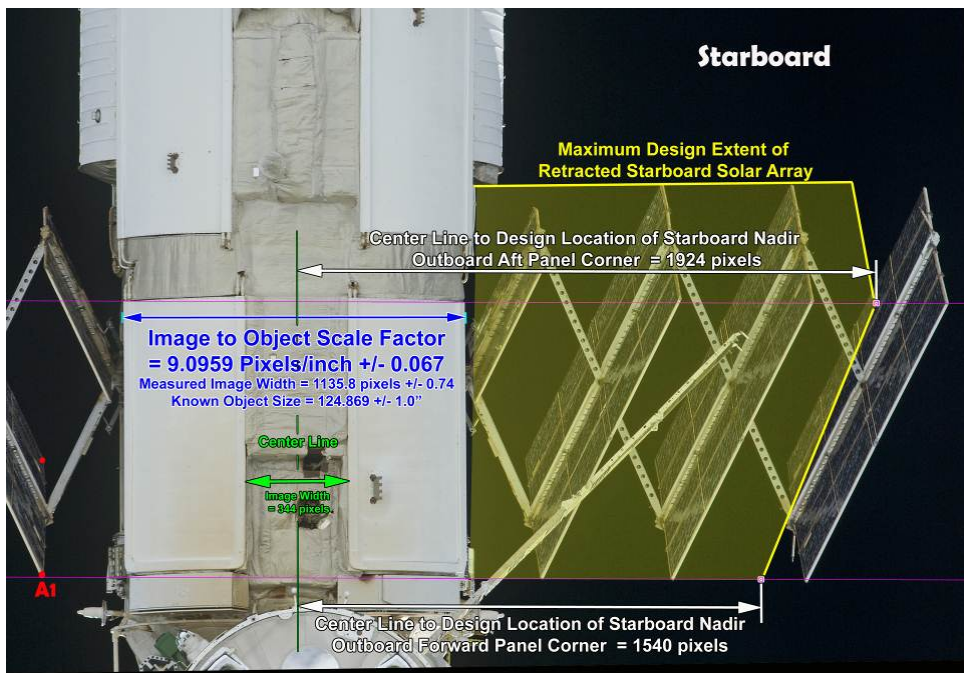

Figure 8.– Single camera measurement of the starboard FGB solar array.

ISAG presented a historical review of the port FGB solar array, showing that the retracted state of the solar array had not detectably changed between October 25, 2007, (28 days after port FGB solar array retraction) and May 18, 2011 (last available nadir image of the FGB). In response, the Russians stated that when the limit switch that controlled the solar array retraction process was tripped and power was removed from the retraction drive motor, the solar array may have rebounded outward by some small amount. They stated that this rebound would have been no more than half a meter, although no documentation or measurements were presented to support this position.

In early January 2013, ISAG located on-orbit recorded video of the port FGB solar array retraction from September 2008. The video shows that when the array reached the point of maximum retraction, it rebounded outboard and oscillated several times before finally stabilizing in a configuration that was significantly less retracted than the minimum point. A similar rebound was seen during the retraction of the starboard FGB solar array. A copy of the port and starboard solar array wing retraction video was provided to the ISS Vehicle Configuration Office and the Structures and Mechanisms Group.

In response to the discovery of the retraction anomaly, the ISS Program Office abandoned efforts to relocate the PMM to the aft Node 3 CBM and has issued a change request to relocate it to the forward Node 3 CBM. The Shuttle Engineering Change Implementation Board (SECIB) has also requested that ISAG perform a photogrammetric analysis of the starboard FGB solar array to document its current configuration.

The image-based measurement techniques employed by ISAG identified and documented a major discrepancy in the as-built configuration of the ISS. Without this capability, any attempt to relocate the PMM to the Aft Node 3 CBM would have resulted in hard contact with the port FGB solar array.

Clearance Analysis of CTC2 (on ELC4) to S-TRRJ HRS Radiator Rotation Envelope

Donn Liddle

In response to the planned retirement of the Space Shuttle Program, International Space Station (ISS) management began stockpiling spare parts on the ISS. Many of the larger orbital replacement units were stored on the Expedite the Processing of Experiments to Space Station (EXPRESS) Logistics Carriers (ELCs) mounted on the end of the S3 and P3 truss segments, immediately outboard of the Thermal Radiator Rotary Joints (TRRJs) and their attached radiators. In an August 2009 computer-aided design (CAD) assessment, it was determined that mounting the Cargo Transport Container (CTC) 2 on the inboard face of ELC4 as planned would create insufficient clearance between the CTC2 and the rotational envelope of the radiators when the TRRJs were rotated to a gamma angle of 35.0 degrees (see figure 1). The true clearance would depend on how

the Unpressurized Cargo Carrier Attachment System (UCCAS) was mounted to the S3 truss and how the ELC4 was attached to it. If the plane of the UCCAS attachment points were tilted even slightly inboard, it would significantly change the clearance between CTC2 and the Starboard TRRJ (S-TRRJ) radiators. Additionally, since CTC2 would be covered in multilayer insulation (MLI), the true outer profile of CTC2 was not captured in the CAD models used for the clearance assessment. It was possible that, even if the S-TRRJ radiators cleared CTC2, they could snag the MLI covering. In the fall of 2010, the Image Science and Analysis Group (ISAG) was asked to perform an on-orbit clearance analysis to determine the location of CTC2 on ELC4 and the S-TRRJ radiators at the angle of closest approach so that a positive clearance could be assured.
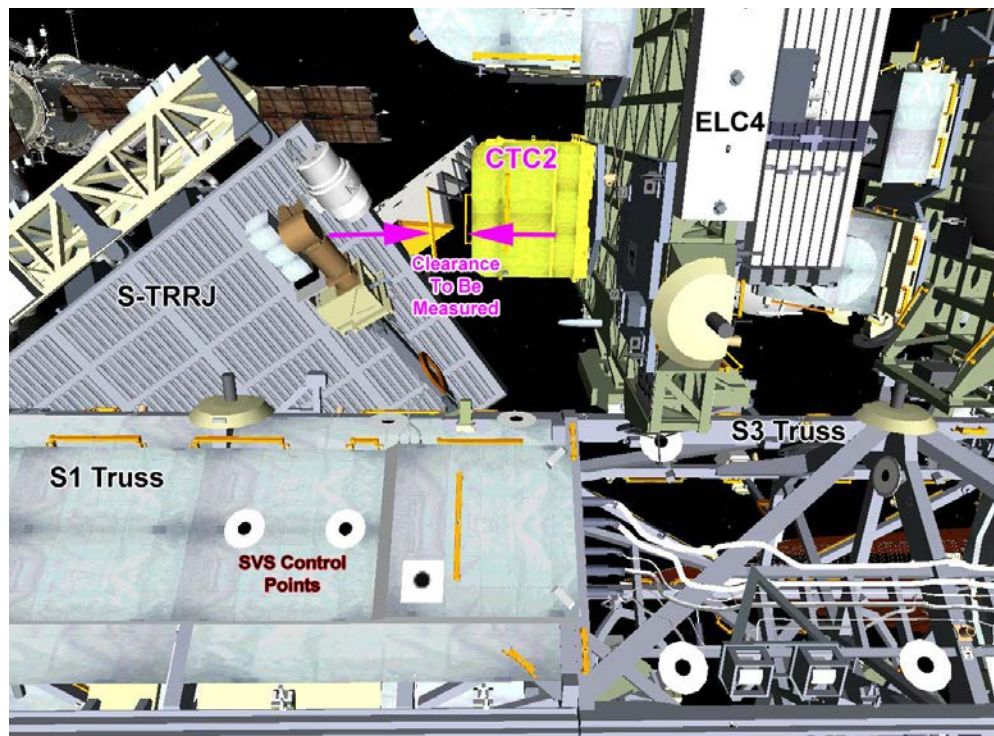
Figure 1.– CTC2 to S-TRRJ radiator clearance.

To provide the measurements as quickly as possible to aid in the assessment, it was decided that the clearance analysis would be broken into two phases.

Phase I
The location and orientation of the UCCAS fittings, which support and hold the ELC4 in place, would be measured relative to the ISS Analytical Coordinate System (ISSACS) as defined by nine preexisting Space Vision System (SVS) targets affixed to the forward/zenith side of the S1 and S3 truss segments (see figure 2). The location of the outboard edge of the S-TRRJ radiator would also be measured when positioned at the angle of closest approach to CTC2 (gamma = 35.0 degrees). This data would allow the Digital Pre-Assembly Group to predict how the ELC4 would sit on the UCCAS and how that would translate into the clearance between CTC2 and the S-TRRJ radiators.

Figure 2.– Phase I measurements.

Phase II

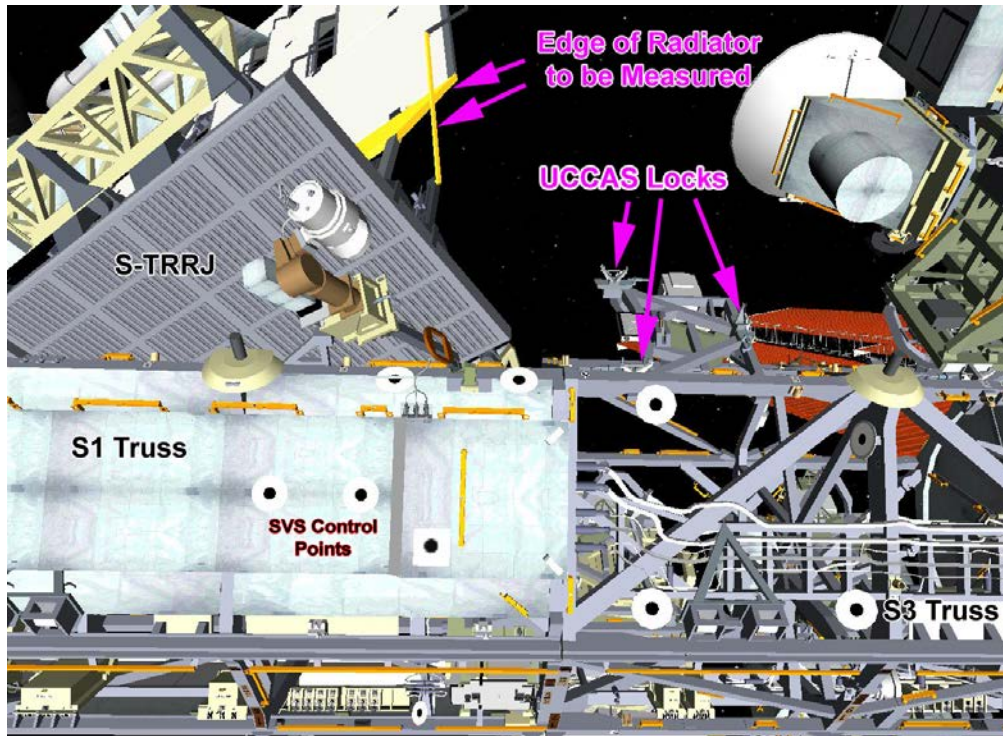After the ELC4 was delivered and installed into the UCCAS, the position of the CTC2 mounting plate on the inboard face of ELC4, would be measured in the ISSACS coordinate system relative to the SVS control points used in Phase I. Although CTC2 would not yet be mounted on ELC4, the working envelope of CTC2 could be mathematically added to the measured position of ELC4 to produce a best estimate for CTC2's mounted location. Comparing CTC2's best estimated location to the S-TRRJ radiator (measured in Phase I); relative to the ISSACS coordinate system, would provide a direct measurement of the expected clearance.

Due to the impending delivery of ELC4 (scheduled for January 2011), planning for the Phase I clearance analysis began immediately. Using the Dynamic Onboard Ubiquitous Graphics (DOUG) program, ISAG designed a way to acquire images of the SVS control points on truss segments S1 and S3, the aft facing edge of the S-TRRJ Heat Rejection Subsystem (HRS) radiator, and the three UCCAS latch mechanisms mounted on the zenith face of the S3 truss using the Space Station Remote Manipulator System (SSRMS). To minimize the number of SSRMS movements, the Special Purpose Dexterous Manipulator (SPDM) would be attached to the SSRMS. This would make it possible to park the SPDM in one position and acquire multiple images by changing the viewing orientation of the SPDM body cameras using the pan/tilt units on which they are mounted. Using this implementation concept, ISAG identified four SSRMS/SPDM positions from which the majority of the needed imagery could be acquired. Five additional images would be acquired using the CP-3 external ISS camera mounted on the S1 truss immediately inboard of ELC4. Based on a

photogrammetric simulation, it was estimated that the measured location of the HRS radiator and UCCAS latch points would be accurate to about 0.3 in. in each of the three axes relative to ISSACS.
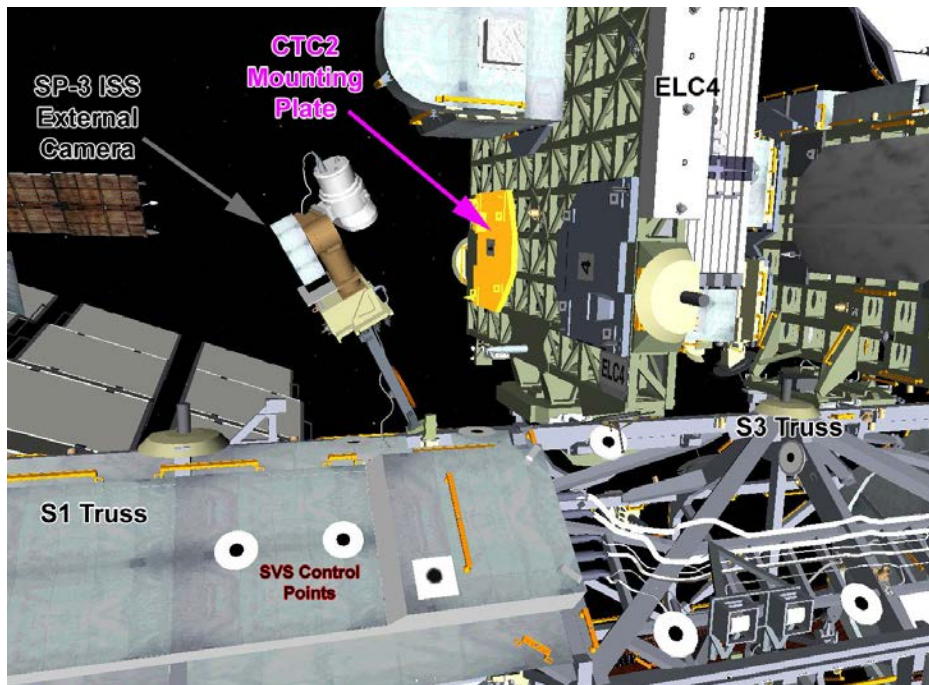

Figure 3.– Phase II measurements.

Working with ROBO, ISAG collected 78 images of the ISS December 29, 2010. From this imagery, the best 40 were selected for use in the analysis process. The images were radiometrically enhanced to improve color and contrast and loaded into the FotoG analysis software along with the camera parameters and control data, which consisted of the coordinates for the nine SVS targets on the S1 and S3 trusses in the ISSACS coordinate system.

The results of this analysis produced the coordinates of 11 points distributed across the outboard face of the S-TRRJ radiator panel and 4 points on each of the three UCCAS latch mechanisms in the ISSACS coordinate system with propagated uncertainty estimates in each coordinate axis. These results were delivered to the ISS Digital Pre-Assembly Group, which used the UCCAS latch mechanism points to estimate the installed position of ELC4/CTC2. This position was then compared to the measured location of the S-TRRJ radiator. This analysis suggested that even with the worst case dynamic scenario, there would still be at least 1.63 in. positive clearance between the S-TRRJ radiator and the CTC2. With the best available analysis showing adequate clearance, the ISS program continued to plan for the installation of CTC2 on ELC4.

The ELC4 was launched January 24 aboard STS-133, arrived at the ISS January 26, and was installed on the S3 UCCAS January 27, 2011. After installation, ROBO released the SSRMS joint locks and allowed the ELC4 to settle into its natural position. They then measured that position using the SSRMS joint angles. This showed that the ELC4 was within the tolerance bands of the predicted

location computed from ISAG's UCCAS measurements, thereby validating the structural models. With these results, ISS program management became confident that there would be a sufficient (although small) positive clearance, and in early February 2011, they dropped the requirement for the Phase II analysis. In early April 2011, ISAG was informed by Structures and Mechanisms that ISS program management now wanted to perform the Phase II measurements.

Since its arrival on H-II Transfer Vehicle #2 (HTV2) early in January 2011, CTC2 had been stored on the SPDM attached to the mobile transporter (MT). The new plan was to measure the location of the CTC2 immediately after it was installed on ELC4, which was scheduled for August 2011. ISAG developed the SSRMS joint angles to position the SPDM body cameras so that imagery of the SVS control points and the inboard face of ELC4/CTC2 could be obtained. After much negotiation with ROBO, an image acquisition plan was released July 1, 2012.

CTC2 was installed on ELC4, and the images required to support the photogrammetric clearance analysis were acquired on September 9, 2011. Additionally, an edge-on image of CTC2 and the S-TRRJ radiator at the angle of closest approach was obtained to immediately prove positive clearance (see figure 4).

Out of about 86 images collected, the best 50 were selected for use in the analysis process. These images, the camera parameters, and 9 SVS control targets were used to compute coordinates for 20 points distributed across the inboard and forward face of CTC2, as shown in figures 5 and 6.

Figure 4.– Clearance between CTC2 and
S-TRRJ Radiator

Coordinates for 50 additional points on the inboard surface of ELC4 were also computed and delivered to the ISS Digital Pre-Assembly Group along with uncertainty estimates in each axis.

The results were delivered to the ISS Structures and Mechanisms Group, which combined them with the S-TRRJ radiator measurements computed in Phase I to compute the final clearance results, as stated below:

"The combined measurement showed a clearance of 10.84" between the radiator and the CTC-2 (a bit better than expected). When we account for worst case conditions (worst possible thermal effects + worst on-orbit loads + uncertainty in our measurements & models) we still show an analyzed clearance of 7.89" (again, the best clearance we've seen)."
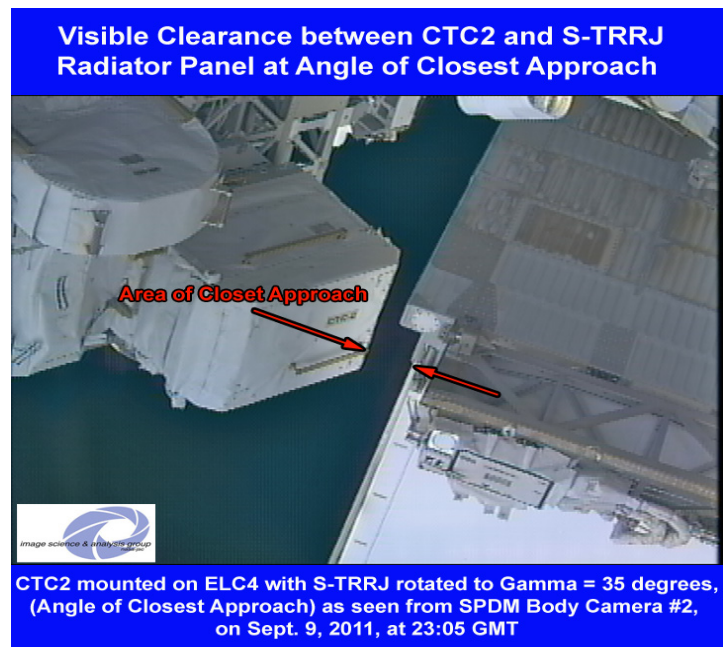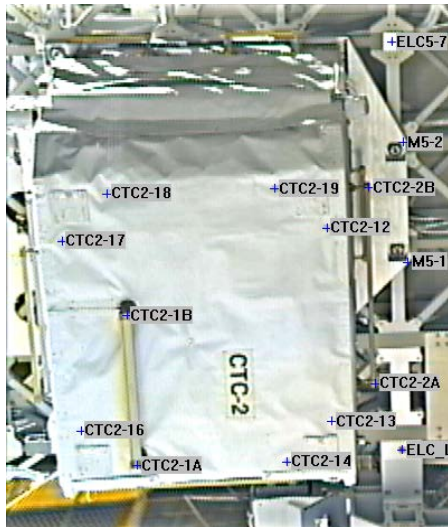
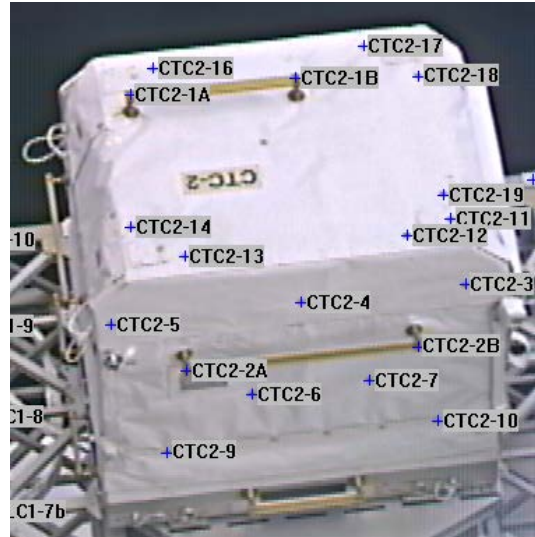*Figure 5.– Point measured on the inboard face of CTC2.*

Figure 6.– Point measured on the forward face of CTC2.

The image-based measurement techniques employed by ISAG provided measurements of the as-assembled, on-orbit hardware configuration, which verified positive clearance both in static and dynamic modes. This measurement capability reduces the overall risk of ISS operation for both NASA and its partner nations.

Analyzing an Aging ISS

R. Scharf

The ISS External Survey integrates the requirements for photographic and video imagery of the International Space Station (ISS) for the engineering, operations, and science communities. An extensive photographic survey was performed on all Space Shuttle flights to the ISS and continues to be performed daily, though on a level much reduced by the limited available imagery. The acquired video and photo imagery is used for both qualitative and quantitative assessments of external deposition and contamination, surface degradation, dynamic events, and MMOD strikes. Many of these assessments provide important information about ISS surfaces and structural integrity as the ISS ages. The imagery is also used to assess and verify the physical configuration of ISS structure, appendages, and components.

During the Space Shuttle Program, a general survey of the ISS with shuttle imagery assets could be performed during approach, while docked, and during the departure Shuttle fly-around. Shuttle images of the ISS comprised most of the imagery used to observe the condition of the ISS exterior. With the retirement of the Space Shuttle, many external surfaces of ISS became blind spots that cannot be easily viewed with ISS imaging assets alone. ISS assets include external video cameras

that can be ground controlled and crew handheld imagery taken from ISS windows or during extravehicular activity (EVA).

The Image Science and Analysis Group has mapped the areas of ISS that can be imaged with external fixed video cameras and crew handheld imagery taken from ISS windows. The images in figure 1 show the ISS external surfaces with imagery coverage in white, while areas in maroon cannot be imaged from external or crew handheld cameras.
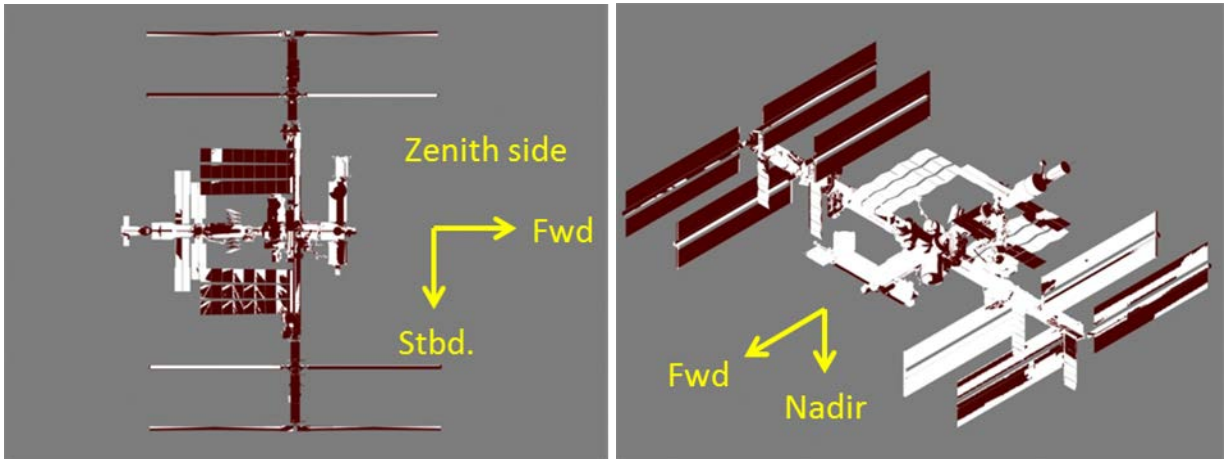
Figure 1 – Areas in white on the zenith and nadir/port/aft views are visible with external fixed video cameras and/or crew handheld imagery.

To track ISS surfaces as they age, the ISAG developed the ISS Imagery Inspection Management System (IIIMS) as a Web page based database for the ISS community. In addition to tracking external deposition, contamination, and surface degradation, the IIIMS database tracks potential sharp edge sources on the ISS truss and elements in response to the risk identified by the ISS Program. Most of the potential sharp edge risks are believed to be caused by MMOD strikes.

The IIIMS database uses an expanded view of the ISS as a visual drill down to search database findings. The home page for IIIMS is shown in figure 2, below. After clicking on an ISS component, a page for that component is shown with a CAD view of it along with a list of all the findings for that component. Alternate screens provide a table of all database findings and tables that show potential sharp edge risks by specific planned EVAs.

Figure 2.– IIIMS homepage with expanded view of the ISS for visual drill down to ISS surface findings.
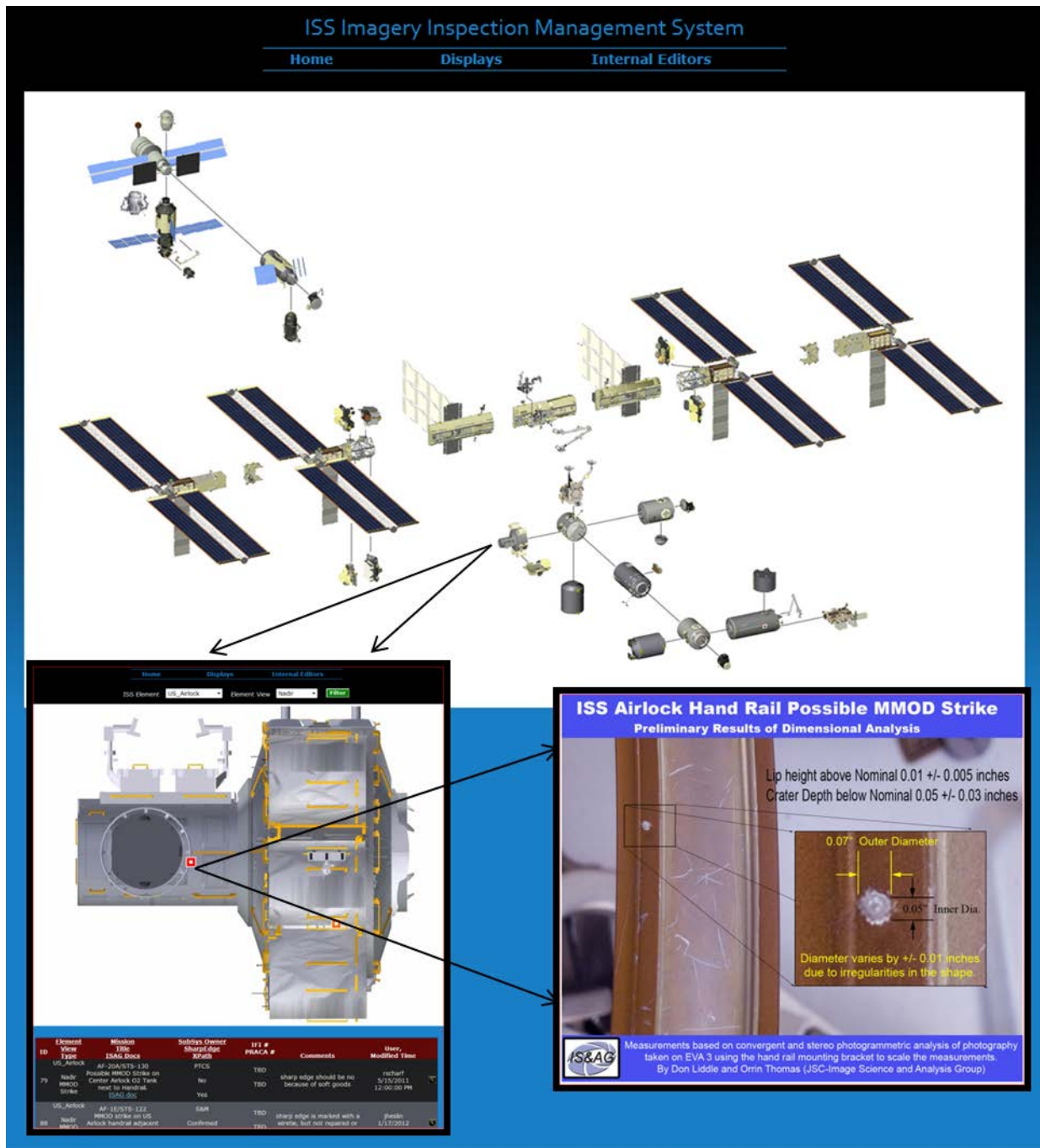
Jaclyn Allen, Charles Galindo, Paige Graff, and Kim Willis
http://ares.jsc.nasa.gov/ares/education/index.cfm

Local Education and Outreach

The ARES Directorate education team is charged with translating the work of ARES scientists into content that can be used in formal and informal K-12 education settings and assisting with public outreach. This is accomplished through local efforts and national partnerships. Local efforts include partnerships with universities, school districts, museums, and the Lunar and Planetary Institute (LPI) to share the content and excitement of space science research. Sharing astromaterials and exploration science with the public is an essential part of the Directorate's work. As a small enclave of physical scientists at a NASA Center that otherwise emphasizes human space operations and engineering, the ARES staff is frequently called upon by the JSC Public Affairs and Education offices to provide presentations and interviews. Scientists and staff actively volunteer with the JSC Speaker's Bureau, Digital Learning Network, and National Engineers Week programs as well as at Space Center Houston activities and events. The education team also participates in many JSC educator and student workshops, including the Pre-Service Teacher Institute and the Texas Aerospace Scholars program, with workshop presentations, speakers, and printed materials.

ARES scientists and staff attend local science fairs and give presentations at many schools, often bringing lunar and meteorite displays and images of Earth from space. Scientists mentor university faculty and students in programs sponsored by the NASA education and equal opportunity offices as well as LPI. The staff frequently provides tours of ARES research and curatorial laboratories to JSC personnel and visitors.

The ARES education team has strong partnerships with other institutions and participates in a variety of solar system educator workshops, staff presentations, and the Science Mission Directorate (SMD) Planetary Education and Public Outreach Forum. ARES education staff also present workshops for the Texas Space Grant Consortium (figure 1).

National Partnerships

Programs with a national reach are an important vehicle for ARES education efforts. With funding from the NASA Discovery and New Frontiers Mission Program, the Lunar and Meteorite Sample Education Disk Program, and SMD Education, the ARES education team is an active member of the NASA space science education community. The team is involved in the following national efforts to reach formal and informal educators:

- Providing content for NASA's Earth Observatory Web site

- Affiliation with Girl Scouts USA and the NASA Girl Scout Core Trainers

- Participation in educator workshops in conjunction with the Discovery and New Frontiers Program

- Organization of NASA Space Science Day Events

- Organization of classroom connection webinars and educator workshops offered through the Expedition Earth and Beyond Program

Figure 1.– Educators experience hands-on activities to share in their classrooms.

ARES continues to have a presence at state and national venues to provide science educators and after-school educators with workshops focused on ARES Directorate solar system exploration and research on topics including asteroids, the Moon, and Mars.

ARES Continuing Education Projects
ARES has five continuing education projects that reach a national audience – Earth Observations Education and Public Outreach, the Lunar and Meteorite Sample Education Disk Program, Expedition Earth and Beyond, NASA Discovery Program Education, and NASA Space Science Day continue to serve a large national audience.

Earth Observations Education and Public Outreach
Astronaut photography of Earth is extremely popular with students, teachers, and the general public, and this excitement is used to leverage interest in science and exploration. The ARES Directorate provides at least one annotated human spaceflight image per week to Earth Observatory, NASA's

flagship Earth science education Web site, at http://earthobservatory.nasa.gov. More than 1 million astronaut photographs of Earth are downloaded by educators and the public each month from the Gateway to Astronaut Photography of Earth, http://eol.jsc.nasa.gov. The photographs have proven to be popular with students, teachers, and the general public, and the site has received numerous educational citations.

Lunar and Meteorite Sample Education Disk Program

The Lunar and Meteorite Sample Education Disk Program is a long-standing program for the entire country. The program, which is available to schools, museums, planetariums, and libraries throughout the country, offers the loan of six lunar or meteorite samples encapsulated in a 6-in. diameter, clear Lucite disk to educators certified in the use of the samples. Distribution of the disks has made it possible for millions of people to examine the Apollo lunar and meteorite samples. The educational sample disks are accompanied by educational materials, including a teachers' guide and image support.

Certification and training of educators are an integral part of the program to borrow the disks. The ARES education team serves as trainers, delivering scientific background information, hands-on activities, and security information to NASA Aerospace Education Services Project (AESP) specialists and NASA Education Resource Center (ERC) educators, who prepare educators to use the disks. The nationwide Lunar and Meteorite Sample Education Disk Program is currently managed by the ARES Directorate.

Expedition Earth and Beyond

Expedition Earth and Beyond (EEAB) is an inquiry-based student geosciences program developed and led by the ARES Education Program. The program facilitates student-led, authentic research investigations that promote the study of Earth and planetary body comparisons.

EEAB uses astronaut photographs of the Earth collected during Space Shuttle missions as part of the ARES International Space Station (ISS) Crew Earth Observations (CEO) payload; the photographs are available online at the Gateway to Astronaut Photography of Earth Web site, http://eol.jsc.nasa.gov. The program provides a classroom-friendly structure that allows teachers in grades 5–12 to use these stunning images of Earth as part of research conducted in the classroom (figure 2). Student teams can also request that astronauts on the ISS acquire new CEO imagery that supports their research (figure 3). Students not only obtain and use current NASA data but actively participate in current NASA exploration.

ARES scientists also communicate directly with student teams to mentor them throughout their research, helping students as they conduct their research and providing a great motivational tool. Students share and present their research "live" to ARES and other participating scientists using distance-learning technologies. Experiences provided through EEAB allow students to model the process of science and help prepare them to become NASA's next generation of scientists and explorers.

Figure 2.– Students work on a research investigation.

CHARLESTON MIDDLE SCHOOL TEAM IMAGE
Juan de Nova Island and Reef, Mozambique Channel
Image ID: ISS027-E-11429 Acquired 4/19/11
Image courtesy of Crew Earth Observations and Image Science & Analysis Laboratory,
NASA Johnson Space Center

Figure 3.– CEO image acquired for a student research team.

Educator professional development workshops train hundreds of teachers to use inquiry-based, standards-aligned curricular materials designed to help students model the scientific process (figure 4). These materials enable teachers to replace previously used classroom curricula with more engaging, relevant, and inspiring activities that use the excitement of current exploration as the hook. Activities are designed to help students model the skills and practices used by Science, Technology Engineering, and Math (STEM) professionals.

Figure 4.– Teachers build a planetary comparison feature wall at the EEAB educator workshop.

Through EEAB, classrooms across the nation can connect with ARES scientists in several ways. Classroom connection webinars enable ARES scientists to conduct interactive presentations that allow participants to increase their knowledge of Earth, planetary comparisons, and science being conducted within the ARES Directorate. Webinars have focused on such topics as using Earth to make planetary comparisons, studying volcanos on Earth and in the solar system, viewing aurora from space, and more. To highlight ARES participation in the Mars Science Laboratory (MSL) mission, numerous webinars connected ARES with thousands of students across the nation (figure 5).
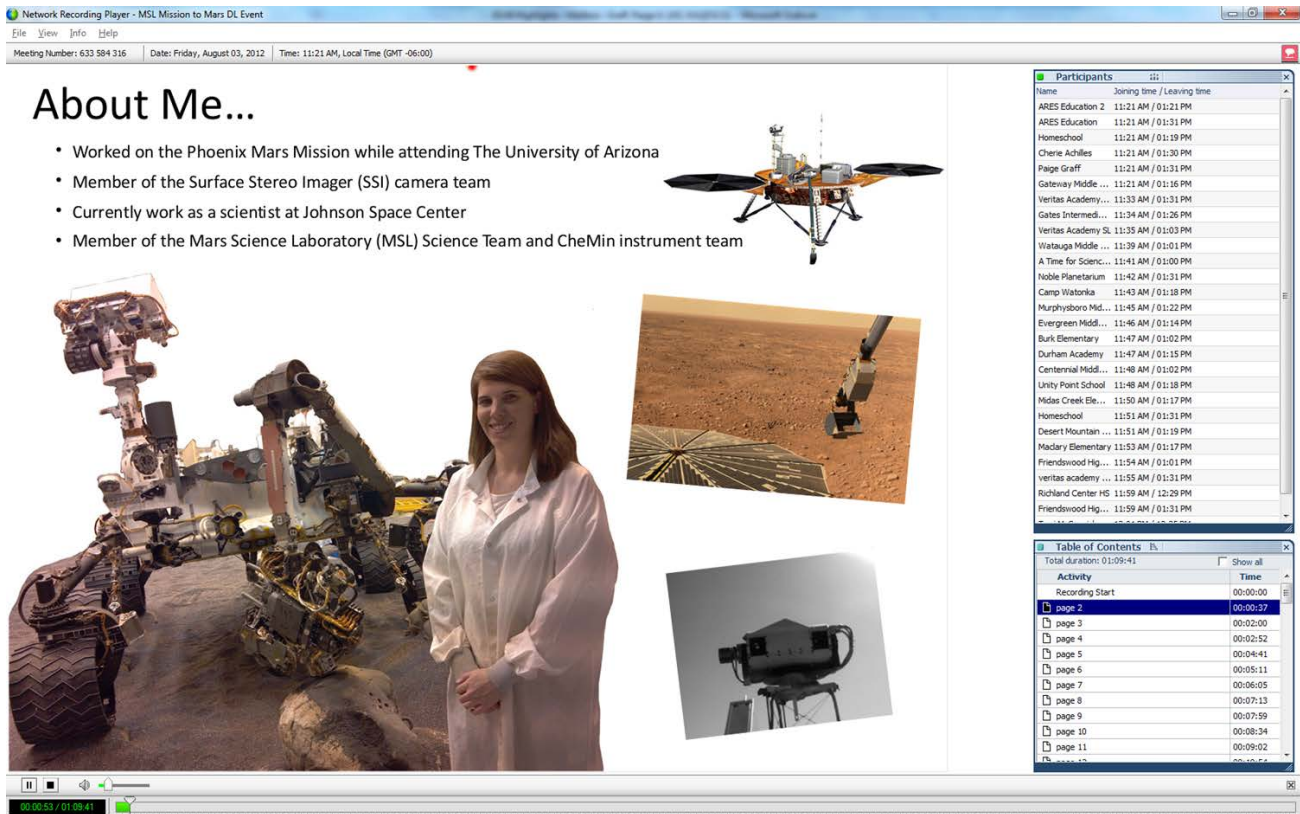
Figure 5.– Connecting scientists with classrooms.

NASA Discovery Program Education

Through educator workshops and student events, ARES staff shares the excitement and challenge of NASA's robotic exploration with teachers, students, and the public. The workshops and events endeavor to showcase ARES scientists and engineers working on exploration missions.

NASA Space Science Days

NASA Space Science Days (NSSD) are undergraduate-mentor-led educational outreach programs that expose middle school students to STEM-related SMD educational products based on an upcoming science mission such as a current Discovery mission. ARES' partners in this endeavor are

- The University of Texas at Brownsville and Texas Southmost College (UTB/TSC) – South Texas Engineering Math and Science Program

- Society of Hispanic Professional Engineers (SHPE) – Foundation

- International Ultraviolet Association (IUVA)

To accomplish this, the following five rotating components occur each year:

- **Mini-information training sessions at SHPE's National Institute for Leadership Advancement (NILA) conference held in August.** These sessions are held to recruit new SHPE student and professional chapters. SHPE requires all chapter officers to attend its annual 3-day

intensive leadership training, and NSSD has taken advantage of the event to expose all SHPE chapters to NSSD goals. NSSD also solicits proposals from chapters interested in having NSSD host an event in their communities.

Figure 6.– SHPE student leaders at NILA describing lunar and Martian soil simulants.

- **Science content mentor training.** Mentor training is held at JSC every year in December; two students from each past and future NSSD site attend a 2-day workshop conducted by ARES. Mentors attend lectures and tour laboratories to learn about ARES and prepare them to give presentations using a thematic approach to the content and related hands-on activities.

Figure 7.– Mentor science content training at JSC.

- **The original NSSD event at UTB/TSC.** The original NSSD event is held at the UTB/TSC campus in Brownsville, Texas, each January. The event, now in its 10th year, allows new mentors to see how the program works and actively participate in the mentoring process. About 700 fifth and eighth graders from the Texas Rio Grande Valley school districts attend the event.

Figure 8.– Local fifth graders use remote imaging data to show NSSD mentors where they would land on Mars.

- **Teacher-mentor training workshops at all NSSD sites are selected from proposals submitted by candidate host sites.** Upon selection of the NSSD host site, which is typically a local university, a teacher-mentor training workshop is held approximately 2 months prior to the NSSD event. SMD products are distributed to local middle school teachers, and the teachers are trained to participate in the event. Mentors from a local university and some upper-level high school students are also trained to lead hands-on activities.

Figure 9.– Teachers compare planet sizes using various fruits and spices as models.

- **National NSSD events.** NSSD host sites are awarded through a proposal-review process after NILA. Currently, there are six NSSD sites nationwide, with two sites celebrating their third annual NSSD event at their university.

Figure 10.– Students from Cache County, Utah, eagerly wait to view lunar and meteorite educational disks through a microscope.

Publications

The following activities and education packages have been developed and published by the ARES Directorate in collaboration with classroom educators. The presentation of accurate science through hands-on learning experiences is a hallmark of the ARES education team.

- Blue Marble Matches
  http://ares.jsc.nasa.gov/ares/eeab/BMM.cfm

- Destination: Mars!
  http://ares.jsc.nasa.gov/education/activities/destmars/destmars.htm

- Expedition Earth and Beyond Student Scientist Guidebook
  http://ares.jsc.nasa.gov/ares/eeab/SSG.cfm

- Exploring Meteorite Mysteries
  http://ares.jsc.nasa.gov/education/activities/expmetmys/expmetmys.htm

- Mars Soil Sleuths
  http://ares.jsc.nasa.gov/education/index.cfm

- Modeling the Solar System
  http://ares.jsc.nasa.gov/Education/pdf_files/ModelingSolarSystem.pdf

- Oh, What A Pane!
  http://ares.jsc.nasa.gov/ares/eeab/WAP.cfm

- Spheres of Earth
  http://ares.jsc.nasa.gov/ares/eeab/SOE.cfm

ARES Directorate Contacts

Name	Position	Phone	E-mail	Mail code
Eileen K. Stansbery, Ph.D.	Director, ARES	281-483-5540	eileen.k.stansbery@nasa.gov	KA
Gregory J. Byrne, Ph.D.	Deputy Director, ARES	281-483-0500	gregory.j.byrne@nasa.gov	KA
Joni W. Homol	Secretary	281-483-7337	joni.w.homol@nasa.gov	KA
Carlton C. Allen, Ph.D.	Manager, Astromaterials Curation	281-483-5126	carlton.c.allen@nasa.gov	KT
Cindy A. Evans, Ph.D.	Deputy Manager, Astromaterials Curation	281-483-0519	cindy.evans-1@nasa.gov	KT
Suzanne Summers	Secretary	281-483-5033	suzanne.summers-1@nasa.gov	KT
David S. Draper, Ph.D.	Manager, Astromaterials Research	281-483-9486	david.draper@nasa.gov	KR
Lindsay P. Keller, Ph.D.	Deputy Manager, Astromaterials Research	281-483-6090	lindsay.p.keller@nasa.gov	KR
Beverly C. Haygood	Secretary	281-483-7316	beverly.c.haygood@nasa.gov	KR
Tracy A. Calhoun	Manager, Human Exploration Science	281-483-5839	tracy.a.calhoun@nasa.gov	KX
Susan K. Runco, Ph.D.	Deputy Manager, Human Exploration Science	281-244-8848	susan.k.runco@nasa.gov	KX
Douglas W. Ming, Ph.D.	Lead, ARES Exploration	281-483-5839	douglas.w.ming@nasa.gov	KA
Wendell W. Mendell, Ph.D.	Assistant Director for Exploration	281-483-5064	wendell.w.mendell@nasa.gov	KA
Nicholas L. Johnson	Chief Scientist for Orbital Debris	281-483-5313	nicholas.l.johnson@nasa.gov	KX
Eugene G. Stansbery	Manager, Orbital Debris Program	281-483-8417	eugene.g.stansbery@nasa.gov	KX